



Conrad Piasecki, Dipl.-Ing.

# **Evaluation of Mobile Emission Measurement Technology in the Motorcycle Segment: A novel Approach in the Field of Emission Simulation with Inventory Models**

## **DOCTORAL THESIS**

to achieve the university degree of

Doktor der technischen Wissenschaften

submitted to

**Graz University of Technology**

Supervisor

Ao. Univ.-Prof. Dipl.-Ing. Dr. techn. Stefan Hausberger  
Institute of Internal Combustion Engines and Thermodynamics

Assoc. Prof. Mech. Eng. PhD Leonidas Ntziachristos  
Laboratory of Applied Thermodynamics, Aristotle University of Thessaloniki

Graz, August 2019

## AFFIDAVIT

I declare that I have authored this thesis independently, that I have not used other than the declared sources/resources, and that I have explicitly indicated all material which has been quoted either literally or by content from the sources used. The text document uploaded to TUGRAZonline is identical to the present doctoral thesis.

22/08/2019

Date



Signature

## Foreword

The study at hand was elaborated during my time as a scientific researcher at the Federal Highway Research Institute (BAST), where I have been working on calculation- and simulation issues of road traffic related emissions in Germany. The idea for this work arose from a joint research project in cooperation with Graz University of Technology - Institute of Internal Combustion Engines and Thermodynamics, Research Area Emissions - that focused on the investigation of motorcycle emissions under real driving conditions.

First, I would like to thank the head of the Institute of Internal Combustion Engines and Thermodynamics at Graz University of Technology, Univ.-Prof. Dipl.-Ing. Dr. techn. Helmut Eichlseder for the chance to carry out this work at the Institute. My extraordinary thanks at TU Graz go to Ao. Univ.-Prof. Dipl.-Ing. Dr. techn. Stefan Hausberger for the supervision and the support of this work, the numerous open discussions and the valuable suggestions during the preparation of this thesis. Furthermore, I would like to thank the whole team of the Research Area Emissions for the great cooperation of the joint research project and the outstanding support over the entire time of processing this work.

In addition, my special thanks go to Assoc. Prof. Mech. Eng. PhD Leonidas Ntziachristos at the Laboratory of Applied Thermodynamics - Aristotle University of Thessaloniki - for the co-supervision of this dissertation.

At the Federal Highway Research Institute I would like to thank the head of the division of automotive engineering Dipl.-Ing. Andre Seeck for the continuous promotion of scientific activities and the possibility of carrying out such a work in this department. My special thanks at BAST go to my former- and current heads of units, under whom I have been active in the recent years: Dr. rer. nat. Dipl.-Phys. Jost Gail for his support to find a topic like this and helping me to start this project, as well as Dipl.-Phys. Uwe Ellmers for his ongoing support - especially in the final phase of this work – and his continuous, open-minded way to find constructive solutions in whatever complicated matters. I would also like to thank Dr.-Ing. Dipl.-Ing. Bernd Bugsel for many helpful discussions and advices, not just in the context of this work.

Many thanks to my parents for their continuous support they have given me, especially during my time at school and during my studies. Finally, gratefulness to whom gratefulness is due, I really want to thank Hannah Sell for her great support and her patience she has given me during this whole project.

**Table of Contents**

I	Abstract.....	3
II	Kurzfassung.....	4
III	List of Abbreviations.....	5
1.	Introduction.....	9
2.	Powered Two-wheelers Emissions – Formation Mechanism and Components.....	14
2.1.	Powered Two-wheelers Exhaust Gas Emissions.....	15
2.1.1.	Formation Mechanism.....	15
2.1.2.	Exhaust Gas Emission Components.....	17
2.2.	Evaporative Emissions.....	20
2.2.1.	Diurnal / Breathing losses.....	22
2.2.2.	Hot Soak Emissions.....	22
2.2.3.	Permeation.....	23
2.2.4.	Running Losses.....	23
2.2.5.	Refuelling Losses.....	23
2.3.	Non-Exhaust Emissions.....	23
3.	Emission Legislation of Powered Two-wheelers – Vehicle Classification and Test Procedures.....	25
3.1.	Classification of Powered Two-wheelers according to EU-Legislation.....	25
3.2.	Hot Emission Test Procedure and Tailpipe Emission Limits.....	26
3.3.	Evaporative Emission Test Procedure.....	28
3.3.1.	Diurnal Losses and Hot Soak Emission Test Procedure.....	28
3.3.2.	Permeation Test Procedure.....	29
4.	Emission Calculation and Simulation in the European Union – Background and Models.....	30
4.1.	Background.....	30
4.2.	Emission Calculation Models.....	31
4.2.1.	PHEM (Passenger Car and Heavy Duty Emission Model).....	33
4.2.1.1.	Emission Map Creation.....	34
4.2.1.2.	Emission Simulation.....	39
4.2.2.	HBEFA (Handbook Emission Factors of Road Transport).....	40
4.2.3.	TREMOT (Transport Emission Model).....	42
4.2.3.1.	Vehicle Fleet Data.....	43
4.2.3.2.	Traffic Data.....	44
4.2.4.	COPERT.....	45

---

---

5.	Emission Measurement Program – Approach.....	47
5.1.	On-board Emission Measurement Program.....	48
5.1.1.	Test Vehicle.....	48
5.1.2.	On-board Emission Measurement Equipment – Specifications.....	49
5.1.3.	Test Routes.....	50
5.1.4.	On-board Trip Dynamic Evaluation.....	52
5.1.4.1.	Relevant Dynamic Parameters.....	53
5.1.4.2.	Basic Trip / Cycle Parameters.....	54
5.1.4.3.	Driving Dynamics Results.....	56
5.2.	On-board Emission Measurement Results.....	61
5.2.1.	Uncertainties in the On-board Emission Measurement Program.....	64
5.3.	Chassis Dynamometer Emission Measurement Program.....	64
5.3.1.	Two-Wheeler Test Bench Facilities.....	65
5.3.2.	Test Cycles.....	66
5.3.3.	Dynamometer Emission Measurement Results and Evaluation.....	66
6.	PHEM Simulation.....	70
6.1.	Motorcycle Emission Map Creation.....	70
6.1.1.	Emission Map Results.....	71
6.2.	Validation of the Emission Simulation.....	73
6.2.1.	Engine Speed Simulation.....	73
6.2.2.	Re-simulation of the Dynamometer Tests.....	75
6.2.3.	Re-simulation of the On-board Trips.....	78
6.2.4.	Driving Resistance Parameter Variation.....	80
6.3.	Vehicle Configuration for the TREMOD / HBEFA Emission Factor Simulation – Approach.....	83
6.4.	TREMOD Motorcycle Emission Factor Simulation.....	87
7.	TREMOD Motorcycle Emission Trend Scenario Calculation.....	93
7.1.	CO <sub>2</sub> and Regulated Emission Trend Scenario Results.....	93
7.2.	Non-regulated Emission Trend Scenario Results.....	97
7.3.	Cold-start Surcharges – Baseline Trend Scenario Results.....	100
7.4.	Hydrocarbon Trend Scenario including Cold-start- and Evaporative Emission Data.....	103
8.	Summary and Outlook.....	105
IV	Literature.....	109
V	List of Figures.....	119
VI	List of Tables.....	123

---

## I Abstract

The increasing demand for mobility leads to a variety of environmental- and climate-related impacts. Air pollution, particularly in urban areas, can be assigned to a large extent to the combustion of fossil fuels, predominately in the road transport sector. Here, powered two-wheelers play a considerable role, since their emission behavior is deemed to be disproportionately high contrasted with the entire vehicle fleet in Germany. In consequence the share of pollutant emissions in this vehicle category contrasted with total road traffic emissions is considered to be rather important, even though the annual traffic in this vehicle category is comparatively low.

In this context reliable information on the real-world emission behavior from all road users is essential in order to establish political measures to mitigate traffic-related impacts. Such emission information is implemented in emission calculation- and simulation models. Emission models are applied on national- and international level by national governments and authorities as a basis for the preparation of legislative actions such as, among other things, emission limits, traffic bans or environmental zones. Finally, the effectiveness of legislative enactments can be validated and the necessity of possible further actions can be evaluated.

The emission database in the German emission- and calculation model TREMOD (Transport Emission Model) in the motorcycle segment is partly outdated. Current data sets on pollutant- and greenhouse gas emissions are based on measurement programs that were carried out on exhaust-gas test benches under laboratory conditions. However, on the road motorcycles show partly higher dynamic driving conditions than test bench cycles reflect. Consequently, relevant operating conditions are not reflected adequately resulting in partly no representative emission data sets for emission simulation- and calculation purposes. Contrary to other vehicle categories – e. g. passenger cars and light duty-vehicles - that are already measured by means of portable emission measurement systems (PEMS) on the road for the generation of emission datasets in emission calculation models, there are no intentions to adapt such measurements procedures in the field of motorcycles yet.

This work investigates in how far on-board emission measurement systems are suitable for the recording of motorcycles exhaust gas emissions under real driving conditions on the road. For this purpose, a representative motorcycle was equipped with a mobile emission measurement system and test drives were carried out. Relevant exhaust gas components were recorded and the test results were evaluated. In this context, the influence of a mobile emission measurement device on the vehicle driving dynamics was investigated in order to evaluate the suitability of such measurement methods for future measurement programs. Moreover, relevant non-regulated emission components were measured on a two-wheeler chassis dynamometer test bench in order to gain a better understanding of these partly harmful emission components. Subsequently, the emission model PHEM (Passenger Car and Heavy Duty Emission Model) was supplemented with emission data obtained in the measurement program and vehicle specific emission maps were created. The emission maps were used to simulate emission factors in the classification of TREMOD. Finally, motorcycle emission trend-scenarios were calculated with TREMOD by using datasets gained from the on-board- and the chassis dynamometer measurements carried out in this study.

**Keywords:** Motorcycle emissions, PHEM, TREMOD, on-board measurement, PEMS

---

## **II Kurzfassung**

Die Zunahme von Mobilität führt zu einer Vielzahl von umwelt- und klimarelevanten Auswirkungen. Luftverschmutzung, insbesondere in städtischen Gebieten, kann zu einem großen Teil der Verbrennung fossiler Kraftstoffe vor allem im Straßenverkehr zugerechnet werden. In diesem Zusammenhang spielen motorisierte Zweiräder eine bedeutende Rolle, da ihr Emissionsverhalten im Vergleich zu anderen Fahrzeugkategorien als überproportional eingestuft wird. Infolgedessen fällt der Anteil der Schadstoffemissionen in dieser Fahrzeugkategorie im Vergleich zu den gesamten straßenverkehrsbedingten Emissionen entsprechend hoch aus, obwohl die jährliche zurückgelegte Fahrleistung in dieser Fahrzeugkategorie vergleichsweise gering ist.

In diesem Zusammenhang sind zuverlässige Information über das reale Emissionsverhalten sämtlicher Verkehrsteilnehmer notwendig, um politische Maßnahmen zur Minderung verkehrsbedingter Auswirkungen auf Mensch und Umwelt einzuleiten. Solche Informationen sind in Emissionsberechnungs- und Simulationsmodellen implementiert. Emissionsmodelle werden u. a. von Regierungsinstitutionen auf nationaler- und internationaler Ebene als Grundlage für die Vorbereitung von gesetzgeberischen Maßnahmen herangezogen. Schließlich kann die Wirksamkeit ebensolcher Maßnahmen validiert und die Notwendigkeit möglicher weiterer legislativer Schritte bewertet werden.

Die emissionsrelevanten Berechnungsparameter im deutschen Emissionsrechenmodell TREMOD (Transport Emission Model) im Motorradsegment sind teilweise stark veraltet. Aktuelle Datensätze zu Schadstoff- und Treibhausgasemissionen basieren auf Messprogrammen, die überwiegend auf Abgasrollenprüfständen durchgeführt wurden. Im realen Fahrbetrieb auf öffentlichen Straßen weisen Motorräder jedoch teilweise eine deutlich höhere Fahrdynamik auf, als Fahrzyklen auf Abgasrollenprüfständen widerspiegeln. Folglich werden relevante Fahrzustände im Rahmen der Emissionsdatengenerierung nicht angemessen abgebildet, was teilweise zu unzureichend repräsentativen Emissionsdatensätzen für die Emissionssimulation führt. Im Gegensatz zu anderen Fahrzeugkategorien – z. B. Personenkraftwagen, welche für die Erstellung von Emissionsdatensätzen bereits mit mobilen Abgasmesssystemen auf öffentlichen Straßen vermessen werden – kommen solche Messverfahren im Motorradsegment bislang nicht zum Einsatz.

Im Rahmen dieser Doktorarbeit wird untersucht, inwieweit sich mobile Abgasmesssysteme zur Erfassung von Emissionen von motorisierten Zweirädern unter realen Fahrbedingungen auf öffentlichen Straßen für die Generierung von Emissionsdatensätzen für Emissionsrechenmodelle wie TREMOD eignen. Zudem wird der Einfluss eines mobilen Emissionsmessgeräts auf die Fahrdynamik von Motorrädern untersucht, um den Einsatz solcher Messmethoden für zukünftige Messprogramme zu bewerten. Emissionsdaten aus entsprechenden Real-world-Emissionsmessungen werden in das Emissionssimulationsmodell PHEM (Passenger Car and Heavy Duty Emission Model) implementiert und fahrzeugspezifische Emissionskennfelder erstellt. Anhand der Emissionskennfelder werden Emissionsfaktoren in der Systematik von TREMOD simuliert und diese in TREMOD implementiert. Schließlich werden mit TREMOD Emissionstrendszenarien für Motorräder auf Basis von mobilen Abgasmessungen im realen Straßenverkehr für verschiedene Abgaskomponenten berechnet.

**Schlüsselwörter:** Motorrademissionen, PHEM, TREMOD, On-Board-Messung, PEMS

---

**III List of Abbreviations**

$\lambda$	Fuel-/air Ratio Lambda
°C	Temperature in Degrees Celsius
2S	2-Stroke Combustion Principle
4S	4-Stroke Combustion Principle
A <sub>f</sub>	Vehicle's frontal Area
AG	Aktiengesellschaft (joint-stock Company)
Approx.	Approximately
Ave.	Average
AVL	Anstalt für Verbrennungskraftmaschinen, Prof. Dr. Hans List GmbH
BAG	Bundesamt für Güterverkehr (German Federal Office for Freight Transport)
BAST	Bundesanstalt für Straßenwesen (German Federal Highway Research Institute)
C <sub>2</sub> H <sub>2</sub>	Acetylene, Ethyne
C <sub>2</sub> H <sub>6</sub>	Ethane
C <sub>4</sub> H <sub>6</sub>	Butadiene
C <sub>6</sub> H <sub>6</sub>	Benzene
CADC	Common Artemis Driving Cycle
CAN	Controller Area Network
ccm	Cubic Centimeters
CH <sub>4</sub>	Methane
CI	Compressed Ignition
CLD	Chemi-luminescence Detector
CO	Carbon Monoxide
CO <sub>2</sub>	Carbon Dioxide
COPERT	Computer Programme to calculate Emissions from Road Transport
CVS	Constant Volume Sampling
C <sub>d</sub>	Drag Coefficient
DG	Directorate General
DIW	Deutsches Institut für Wirtschaftsforschung (German Institute of Economic Research)
DVPE	Dry Vapor Pressure Equivalent

---

---

EC	European Commission
EEA	European Environment Agency
EF	Emission Factor
EFM	Exhaust Flow Meter
ERMES	European Research on Mobile Emission Sources
ETC / ACM	European Topic Center on Air Pollution and Climate Change Mitigation
EU	European Union
FID	Flame Ionization Detector
FTIR	Fourier Transform Infrared Spectroscopy
g	Grams
GmbH	Gesellschaft mit beschränkter Haftung (German limited liability company)
GPS	Global Positioning System
GTR	Global Technical Regulation
GWP	Global Warming Potential
H <sub>2</sub> O	Water
HBEFA	Handbook Emission Factors for Road Transport
HC	Hydrocarbons
HCHO	Formaldehyde, Methanal
HDV	Heavy-Duty Vehicle
Hz	Hertz
IFEU	Institut für Energie- und Umweltforschung (Institute for Energy and Environmental Research)
IVT	Institute of Internal Combustion Engines and Thermodynamics (Graz University of Technology)
JRC	Joint Research Centre (European Commission)
KBA	Kraftfahrt-Bundesamt (German Federal Motor Transport Authority)
km	Kilometer
kW	Kilowatt
LAT	Laboratory of Applied Thermodynamics (Aristotle University of Thessaloniki)
LCV	Light Commercial Vehicle
LIPASTO	Calculation System for Traffic Exhaust Gas Emissions and Energy Use in Finland
LRTAP	Convention on Long-range Transboundary Air Pollution

---

---

m a. s. l.	Meters above Sea Level
MC	Motorcycle
mg	Milligrams
Mio.	Million
n_norm	Normalized Engine Speed
NDIR	Non-dispersive Infrared Analyzer
NDUV	Non-dispersive Ultraviolet Analyzer
NEC	National Emission Ceiling
NEMO	Network Emission Model
NH <sub>3</sub>	Ammonia
NMHC	Non-methane Hydrocarbons
NO	Nitrogen Monoxide
No	Number
NO <sub>2</sub>	Nitrogen Dioxide
NO <sub>x</sub>	Nitrogen Oxides
∅	Diameter
OBD	On-board Diagnostic
Pe_norm	Normalized Engine Power
PEMS	Portable Emission Measurement System
PHEM	Passenger Car and Heavy Duty Emission Model
PI	Positive Ignition
PM	Particulate Matter
PMD	Paramagnetic Detector
PMP	Particulate Measurement Program
PN	Particulate Number
ppm	Parts per Million
QLC	Quantum Cascade Laser Analyzer
RDC1, RDC2	Real-world Driving Cycles for Motorcycles
RDE	Real Driving Emission Legislation (according to Regulation (EU) 2016/646)
Reg	Regulation
RPA	Relative Positive Acceleration
rpm	Revolutions per Minute
RVP	Reid Vapor Pressure

---

---

S	Sulphur
SHED	Sealed Housing for Evaporative Emission Determination
SI	Spark Ignition
SMC	Small Motorcycle
SO <sub>2</sub>	Sulfur Dioxide
t	Ton
THC	Total Hydrocarbons
TREMOD	Transport Emission Model
TS	Traffic Situation
UBA	Umweltbundesamt (German Federal Environment Agency)
UN	United Nations
UNFCCC	United Nation Framework Convention on Climate Change
v.	Version
VDA	Verband der Deutschen Automobilindustrie (German Car Manufacturer Association)
VEH	Vehicle
Versit +	Dutch Emission Model to Generate National Emission Factors
VOC	Volatile Organic Compounds
W	Watt
WMTC	Worldwide harmonized Motorcycle Emission Test Cycle
$\rho$	Density

---

## 1. Introduction and Motivation

The combustion of hydrocarbon-containing fuels leads to the formation of partly harmful pollutant components and climate-change related greenhouse gas emissions. Due to the growing demand for mobility, the share of transport-related emissions to the total anthropogenic emissions is of substantial meaning [1.1]. In addition, socioeconomic processes such as the advancing urbanization lead to shifting effects of traffic performance into urban areas that aggravate air quality problems in there. In terms of road transport, passenger cars and heavy-duty vehicles are the main sources for exhaust gas emissions and air pollution in Germany [1.2]. However, powered two-wheelers partly contribute to disproportionately high emissions as well, particularly in urban areas, since the eminent share of traffic performance in this vehicle class is carried out there [1.2]. Figure 1.1 shows the proportionate distribution of annual road traffic in Germany in 2017 differentiated by relevant vehicle categories and according to local area calculated with the German Transport Emission Model TREMOD, version 5.63 [1.2].

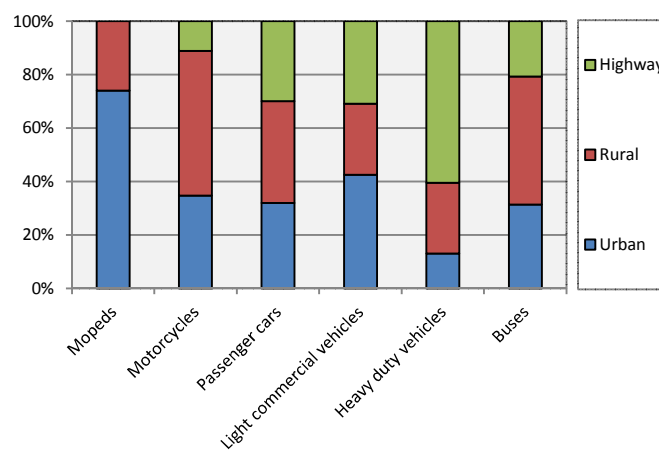


**Figure 1.1:** Annual traffic shares of relevant road vehicle categories in Germany according to local area in 2017 according to TREMOD [1.2].

Figure 1.1 indicates that about 74 % of mopeds- and 34 % of motorcycles annual traffic takes place within residential areas. Powered two-wheelers facilitate individual mobility since they have advantages with regard to practicability and agility and are not affected by difficult parking situations in congested city centers to the extent that other vehicle categories have. Not least, economic benefits like relatively low purchase- and maintenance costs and the perceived driving experiences lead to a high popularity of motorcycles and mopeds. The demand for powered 2-wheeled vehicles remains rather strong, particularly in Asia, but also within the European Union [1.3]. Figure 1.2 shows the development of the total powered two-wheeler fleet within the EU and its most relevant sales markets.

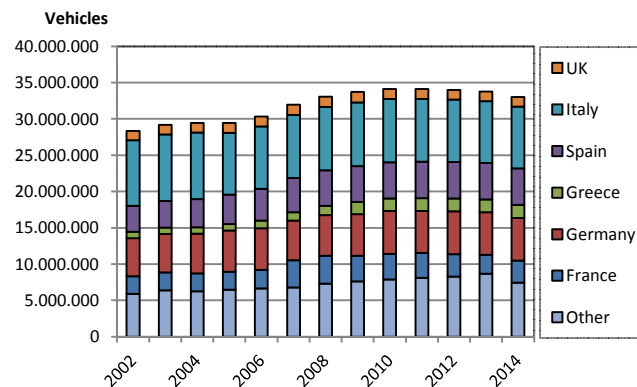


**Figure 1.2:** European powered two-wheelers market – vehicle fleet development within the EU and its most relevant sales markets, 2002 – 2014 [1.3].

The conversion of hydro-carbon-containing fuels into rotational energy inside an internal combustion engines leads to various chemical components in the exhaust gas. As a result of a complete combustion process, only carbon dioxide ( $\text{CO}_2$ ) and water-steam ( $\text{H}_2\text{O}$ ) are formed. However, substances such as carbon monoxide (CO), hydrocarbon fractions (HC) and particle emissions (here, a distinction is made between particulate matter (PM) and particulate number (PN)) result in partially incomplete combustion processes. Nitrogen-based emissions ( $\text{NO}_x$ ), mainly nitrogen oxide (NO) and nitrogen dioxide ( $\text{NO}_2$ ), are formed as a consequence of chemical reactions with nitrogen ( $\text{N}_2$ ) from the ambient air. Pollutant components like sulfur- (S) or heavy-metal-based emissions (lead, cadmium) may occur due to the combustion of low-quality fuels or oil fractions. Due to the partly simple constructional design of powered two-wheelers, in particular in the case of mopeds with two-stroke engines, several vehicle concepts often have partially bad emission characteristics [1.4]. In addition, mopeds are frequently used only for short distances, so the engine is often not operating in thermally favorable operating ranges. However, moped engines are heated up rather quickly due to a high power/mass ratio. In a consequence, mopeds show higher shares of cold-start emissions compared to other vehicle categories. Besides exhaust gas emissions, powered two-wheelers are high-emitters of evaporative emissions that consist essentially of hydrocarbon vapors [1.5]. These can be attributable to different formation mechanisms that in turn depend on factors like, among others, the ambient temperature distribution or the fuel composition. Not least, emission fractions from brakes, tires and clutches occur that are classified as non-exhaust emissions.

The above-mentioned components lead to partly different effects on human health and the environment. The pollutants in the ambient air enter the human organism through the respiratory tract and potentially also the blood circulation via the lungs. There, they can lead to a series of cardiovascular and respiratory diseases [1.6]. Some of the exhaust gas components from powered two-wheelers like volatile organic compounds (VOC) and particulate matter are classified as toxicologically effective and suspected of having carcinogenic effects on the human organism [1.7][1.8]. Some of the exhaust gas components are also suspected of interacting with each other and of affecting the climate sustainably [1.9]. The emission formation mechanisms from powered two-wheelers and the impacts on human health and the environment are discussed in chapter 2.

Opposed to the emission legislation in the passenger car- or heavy-duty vehicle sector, motorcycle- and moped emission legislation has remained unchanged for many years until 2016. Subsequently, the share of exhaust gas- and evaporative emissions from powered two-wheelers is, in some cases,

significantly worse compared to other motor vehicles of the German vehicle fleet, as demonstrated in figure 1.3.

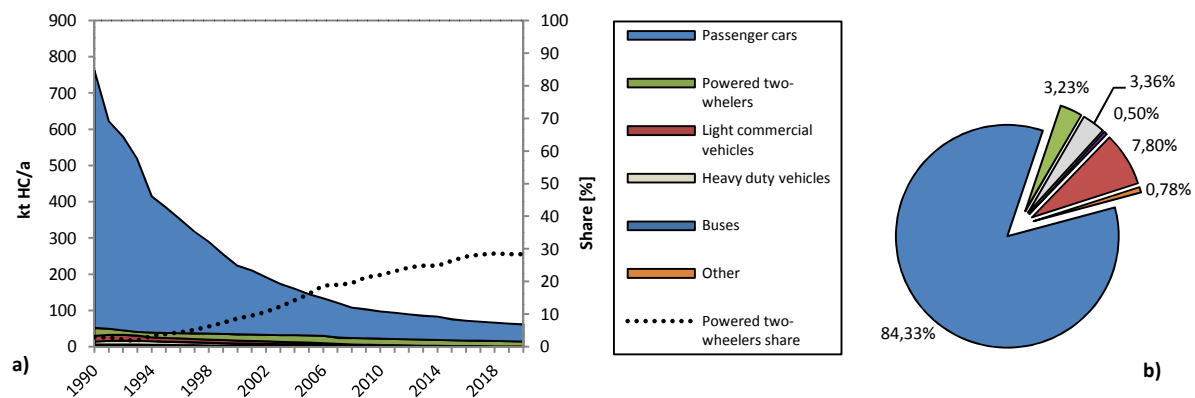


**Figure 1.3:** a) Development of the total urban hydrocarbon emissions from the road traffic sector in Germany differentiated according to vehicle category and powered-two-wheelers hydrocarbon emissions share b): Proportionate urban annual traffic by vehicle categories in 2017 [1.2].

While, for example, the HC emissions in the passenger car sector declined over the last two decades, these emission fractions stagnated in the motorcycle sector for years (figure 1.3 a). It comes out that the share of hydrocarbon emissions from powered two-wheelers in the total urban hydrocarbon emissions from road traffic in Germany is steadily rising and it is almost 27 % in 2017. However, the annual urban traffic caused by motorcycles and mopeds in the total urban annual road traffic is comparatively low with about 3,2 % in the same year (figure 1.3 b). From 2016 onwards the new regulation (EU) No 168/2013 was applicable to the light-vehicle category (L-category). Herein, the introduction of new tailpipe emission standards Euro 4 (2016) and Euro 5 (2020) is regulated. Besides the pollutant components  $\text{NO}_x$ , CO, and HC - already limited within former emission levels - tailpipe emission limit values for particulate matter PM (Euro 4) and non-methane hydrocarbons NMHC (Euro 5) are fixed for the first time. All emission values up to- and including Euro 5 are verified under reproducible conditions in defined driving cycles on exhaust gas test benches. This is to ensure a reliable, justifiable test method for all vehicle types within the same vehicle category. Besides new tailpipe emission limits, there is a restriction for evaporative emissions for powered two-wheelers for the first time from 2016 onwards. Evaporative emissions are determined in the context of the vehicle type approval procedure by measuring vehicles in gas-tight test chambers for the escape of hydrocarbon-fumes. In addition, requirements concerning the durability of emission-reducing systems as well as the on-board diagnostic interface function are defined in this regulation. The current and future emission legislation for powered two-wheelers is presented in chapter 3.

The assessment and verification of emission-related policies and regulations requires the use of emission calculation models that reflect real-world emissions, annual traffic data and the vehicle fleet development- and composition of all relevant vehicle categories to a high degree of differentiation. Besides the preparation of legislative actions, national states are obliged to inventory sector-specific data on pollutant- and climate gas emissions within the framework of national and international agreements (e. g. Kyoto protocol, NEC directive), which are also calculated on the basis of such emission models [1.10] [1.11]. For this purpose, several models have been developed within the European Union in the last decades, which partly differ in structure and function. Starting with

microscopic models that simulate the emission behavior of individual vehicles (PHEM – Passenger Car and Heavy Duty Emission Model), up to macroscopic models, which represent entire vehicle fleets in certain areas (TREMOT, COPERT – Computer Programme to calculate Emissions from Road Transport) [1.12] [1.13] [1.14]. The emission factor database of such models is based on emission measurements that are primarily carried out on exhaust-gas test benches in so-called real-world driving cycles (up to emission standard Euro 5/V), in order to reflect the emission behavior of real driving conditions as accurately as possible. The emission data are implemented into emission models according to different methodologies. An Overview of common emission simulation- and calculation models in the European Union – with the focus on the powered two-wheeler situation - including the underlying structure and database is given in chapter 4.

In the course of the development of real driving emission regulations (RDE) for the passenger car- and light-duty vehicle certification procedure within type approval - applying from 2017 onwards -, on-board emission measurement procedures have been developed, which allow analyzing and recording the tailpipe emissions of individual vehicles under real driving conditions on the road. This procedure is intended to ensure that information on vehicle emissions of individual vehicle types will be reflected in a sufficient and accurate manner. The measurement data thus obtained are also suitable as a basis for above mentioned emission models and initial research projects are already ongoing [1.15]. Due to legislative provisions and limitations with respect to measurement technology, the on-board emission measurement procedure is intended to be used only for the passenger car- and the commercial vehicle sector so far. In the field of powered two-wheelers, there are no legislative intentions to adapt on-board emission measurement procedures comparable to the RDE legislation in future. However, it is assumed that the emissions under real driving conditions in this vehicle category might exceed the emission results of laboratory measurements in some cases clearly, as engine-map sections are passed on the road that are not driven in the usual chassis dynamometer tests. This refers particularly to high-capacity, powerful motorcycles.

The above-mentioned aspects have encouraged the motivation for this doctoral thesis. The question is addressed, whether, and to what extent on-board emission measurement devices in the motorcycle segment are applicable for valid emission recordings and are such datasets suitable for emission calculation- and simulation models like TREMOD. Hence, a representative motorcycle was equipped with mobile exhaust gas measurement technology and test drives were carried out in Graz-city and surroundings see chapter 5. This method is intended to make initial statements regarding the robustness of on-board emission measurement devices in this vehicle category and to gain a better understanding of the emission behavior under real driving conditions. Additionally, the same test vehicle was investigated on an exhaust gas test bench in order to assess the validity of the on-board emission measurements. Within a chassis dynamometer measurement program, a detailed analysis of several non-regulated exhaust gas components by means of a FTIR-analyzer (Fourier Transform Infrared Spectroscopy) was carried out. This procedure is intended to provide a deeper understanding of the composition of motorcycles exhaust gases. All emission results are differentiated according to hot- and cold-start emissions and a further distinction of the emission results according to local area, namely urban, rural and motorway traffic is made. Finally, evaluations of the on-board test drives with regard to driving dynamics are carried out and contrasted with the motorcycle driving cycles in HBEFA that are adopted in TREMOD and reflect representative motorcycle driving in Germany.

---

The emission data sets gained from the measurement program - both, the on-board- and the dynamometer measurement data - are used to generate emission maps with the PHEM model developed by the Institute of Internal Combustion Engines and Thermodynamics (IVT) at Graz University of Technology. On this basis, the on-board measurement trips and the dynamometer driving cycles, which are used for the emission map generation, are simulated with PHEM and contrasted with the measurement results in order to assess the reliability and accuracy of the simulation procedure. Subsequently, the relevant TREMOD motorcycle driving cycles are simulated with PHEM and emission factors in the structure of TREMOD for the vehicle segment of the test vehicle are generated. A detailed description of the emission map generation and the PHEM simulation procedure is given in chapter 6.

The emission factors derived from the PHEM simulations are implemented in TREMOD and emission trend scenarios for regulated- and non-regulated emission components in Germany for the vehicle segment of the test vehicle are calculated see chapter 7. The results of the emission trend scenarios are differentiated according to local area, namely urban, rural and motorway traffic. In a detailed CO and HC emission trend scenario, cold-start emission surcharges are added to the hot emission scenario results in order to assess the total tailpipe emission behavior of the test vehicle concerned. Finally, emission fractions that are attributable to fuel evaporation are taken into account in these scenario calculations in order to represent all relevant emission types in the motorcycle segment.

---

## 2. Powered Two-Wheelers Emissions – Formation Mechanism and Components

There are about 5,6 million registered powered two-wheelers in 2017 in Germany, of which approx. one-third can be related to small motorcycles and mopeds with engine capacities less than 50 cm<sup>3</sup> and two-third can be assigned to the motorcycle segment characterized by engine capacities greater than 50 cm<sup>3</sup> [1.2]. There are numerous vehicle concepts available within this vehicle category, ranging from city scooters up to racing machines as well as motorcycles developed for usage in off-road terrain [2.1]. Powered two-wheelers engines frequently demonstrate high performance characteristics with regard to power output and engine speed linked with comparatively low engine weights. Compared to other road users, the performance data are in some cases above average, particularly in the field of acceleration characteristics. Different constructional engine designs are fabricated in motorcycle applications depending on the specific use-cases of the vehicle - single-cylinder engines in small and light motorcycles and mopeds; V-type engines, multi-cylinder in-line engines and boxer-motors in motorcycles of medium- and high performance classes like choppers, touring-machines, enduros- or racing bikes [2.2]. The wide range of applications make powered two-wheelers popular in the field of locomotion, both, for recreational purposes as well as for daily commuting to the place of work.

Powered two-wheelers represent a relevant source of pollutant emissions in the road traffic sector in Germany [1.2]. It is assumed that - despite to comparable low annual traffic performance - the share of emissions in this vehicle category compared to total road traffic emissions is in some cases disproportionately high [2.1]. Taking into account that powered two-wheelers annual traffic is primarily carried out in urban areas this vehicle category becomes a non-negligible source of air quality impairment. This finding also includes evaporative emissions that are predominately attributable to motorcycles and mopeds according to TREMOD [1.2].

Powered two-wheelers emissions can be divided into two main groups, depending on the underlying formation mechanisms and sources. Due to the combustion of fossil carbon-containing fuels, powered two-wheelers contribute to the formation of partly harmful exhaust gas fractions and climate-relevant emissions that escape into the environment via the exhaust gas system. These emissions are classified as exhaust gas emissions, respectively tailpipe emissions. Besides exhaust gas emissions, powered two-wheelers generate emission fractions that cannot be attributed to the combustion process itself – these emission shares are related to evaporative processes of fuel- and lubricant fractions. Furthermore, additional emission fractions result in a series of wear- and abrasion processes e. g. from tires, brakes, clutches and the road surface [2.3]. The latter emission types are attributed to non-exhaust emissions. Particle emissions that are already present in the environment and that are re-suspended in the air by turbulence effects are also classified as non-exhaust emissions. Finally, powered two wheelers are high emitters of noise emissions in the road traffic sector – as a consequence, there have been political discussions at national- and international level in this field to regulate the noise emission behavior of relevant road users [2.4]. However, noise emissions do also not have relevance in the context of this work and they are excluded from further investigations here.

---

In the field of powered two-wheelers almost all vehicle types and concepts are equipped with petrol engines - only a few motorcycle concepts equipped with diesel engines are available in the market, which have been developed predominantly within small series or individual productions [2.5]. Not least, due to partly lower power densities of diesel engines compared to petrol engines - linked with higher engine weights and motor vibrations - the development of diesel drive solutions in this vehicle category still represents a niche research area. In the framework of this work, diesel-driven vehicle concepts are excluded from further investigations, not least, because the share of diesel motorcycle emissions in the total motorcycle emissions is negligibly small - the German emission calculation- and inventorying model TREMOD does not even list diesel motorcycles as an individual vehicle sub-segment [1.2]. Other concepts not considered are powered two-wheeler designs that are driven via an electric- or hybrid propulsion system. Opposed to other relevant markets – e. g. Asia – electric motorcycles and mopeds represent an exception within the powered two-wheelers vehicle fleet in Germany [1.2] [2.6].

Within the framework of this chapter powered two-wheelers exhaust gas emissions including their formation mechanisms and health- and environmental impacts are presented within chapter 2.1. Powered two-wheelers non-exhaust emissions - particularly evaporative emissions and their underlying formation mechanisms – are discussed briefly in chapters 2.2 and 2.3. The information given in the following chapters provide a brief technical overview of relevant emission components and formation processes with reference to the further work in this study. In-depth information on the reaction chemistry is omitted in this study.

## **2.1 Powered Two-wheelers Exhaust Gas Emissions**

Exhaust gas emissions from powered two-wheelers consist of a large variety of different substances. The formation mechanisms are initiated due to the combustion of hydrocarbon-based petrol fuel in conjunction with oxygen from the ambient air inside the combustion chamber of the engine. Here, chemical energy bound in the fuel is converted into rotational energy as a result of chemical reaction processes and a reciprocating piston-crankshaft system. In chapter 2.1.1 the formation mechanisms of the relevant exhaust gas emission components are described. In particular, the main inner-engine processes resulting in the generation of emission components are presented. Chapter 2.1.2 provides an overview of powered two-wheelers most relevant exhaust gas emission components and indicates information on environmental- and toxicological impacts.

### **2.1.1. Formation Mechanism**

In the case of a complete combustion process inside an internal combustion engine (petrol) fuel fractions react with oxygen ( $O_2$ ) from the ambient air and carbon dioxide ( $CO_2$ ) emissions and water vapour ( $H_2O$ ) are formed [2.2]. The nitrogen ( $N_2$ ) and further gases contained in the ambient air (e. g. noble gases) remain unaffected in the case of an ideal combustion process and exit the engine via the exhaust gas system. However, the chemical reactions inside internal combustion engines remain partially uncompleted, resulting in the formation of additional emission fractions and pollutant components. Due to high combustion temperatures, nitrogen oxides ( $NO_x$ ) are formed based on nitrogen in conjunction with oxygen ( $O_2$ ) from the ambient air. Moreover, certain fuel fractions are

---

not converted completely, which leads to the generation of carbon monoxide (CO) and hydrocarbon (HC) emission and optionally to particle emissions. The following illustration 2.1 shows the approximate exhaust gas composition of a gasoline engine with intake manifold injection.

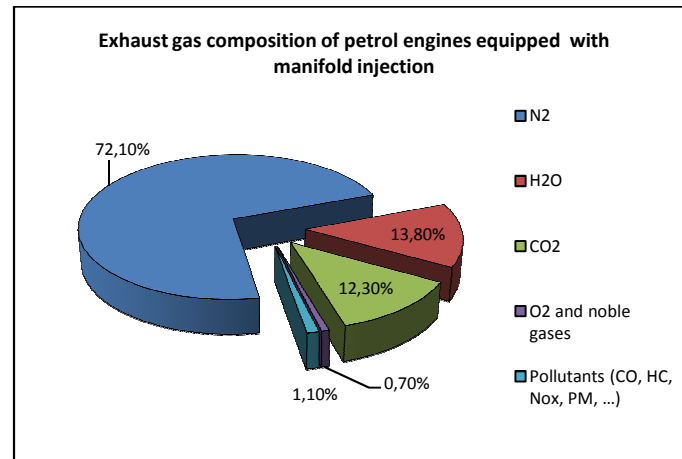


**Figure 2.1:** Exhaust gas composition of modern petrol engines equipped with manifold injection [2.7].

The emission behavior of internal combustion engines is affected by a variety of engine parameters and process variables. The combustion process itself – implemented either as a 2-stroke or 4-stroke process - and the type of the fuel injection, e. g. manifold injection, direct fuel injection or fuel preparation and -supply according to the carburettor principle - as applied predominately in older vehicles and small motorcycles - affects the exhaust gas behavior of motor vehicles and the tailpipe emission composition. Geometrical parameters such as the combustion chamber design plays a significant role as well as the gas exchange cycle via the valve train since they have direct influence on the fuel-air mixture distribution and -quality and finally on the efficiency of the combustion. Not least, the use of exhaust gas after-treatment systems, varying ambient conditions, different fuel compositions- and qualities (e. g. admixtures of Ethanol) and the individual driving style affect the composition and quantity of powered two-wheelers emission considerably [2.8].

Basically, a distinction is made between the emissions that are emitted in the warm engine operation phase and those emission fractions that occur when the vehicle is started with a cold engine (cold-start emissions). The cold-start emission behavior is sometimes significantly worse compared to the vehicle running at its ideal "hot" operating temperature. In particular, the amount of hydrocarbon-containing components and carbon monoxide during the cold-start phase is partly significantly higher in relation to the hot emission behavior. Reasons for this are, among other things, flame creeping mechanisms on cold combustion chamber components, as well as partly non-optimal operation temperatures of emission reducing systems such as the three-way catalytic converter [2.9]. Details can be found in corresponding literature sources; however, this context will not be further discussed in the framework of this study.

Petrol engines as commonly used in motorcycle applications based on the principle of spark ignition (SI), in which a fuel-air mixture is ignited inside the combustion chamber of the engine by means of an external energy source, usually a spark plug. An important parameter in this context is the air-/fuel mixture ratio  $\lambda$  which relates the air quantity inside the combustion chamber to the air quantity required for the complete combustion of the air-/fuel mixture. In the case of manifold

injection engines the ignitable mixture usually burns stoichiometrically in the range of  $\lambda = 1$  with certain bandwidths depending on the operating points and the engine load. Deviations from the stoichiometric  $\lambda$ -value to leaner- or richer fuel-air mixtures lead to increasing formation processes of pollutant emission components in the exhaust gas. In high engine load phases, for instance, it is more likely to operate the engine with rich air-/fuel mixture values ( $\lambda < 1$ ) in order to protect the engine from overheating effects and to provide the required power output. However, in this case the fuel is partially not converted completely, resulting in increased carbon monoxide (CO) and hydrocarbon (HC) emissions. In contrast to that, a shifting of  $\lambda$ -values to leaner ranges ( $\lambda > 1$ ) leads to higher combustion temperatures linked with increasing nitrogen oxide emissions in a consequence of oxygen excess during and after the combustion process. In this operating range, however, the amount of unburnt fuel fractions and carbon monoxide decreases significantly. The general relation of the  $\lambda$ -value setting to relative emission rates in internal combustion engines is shown in the following figure 2.2.

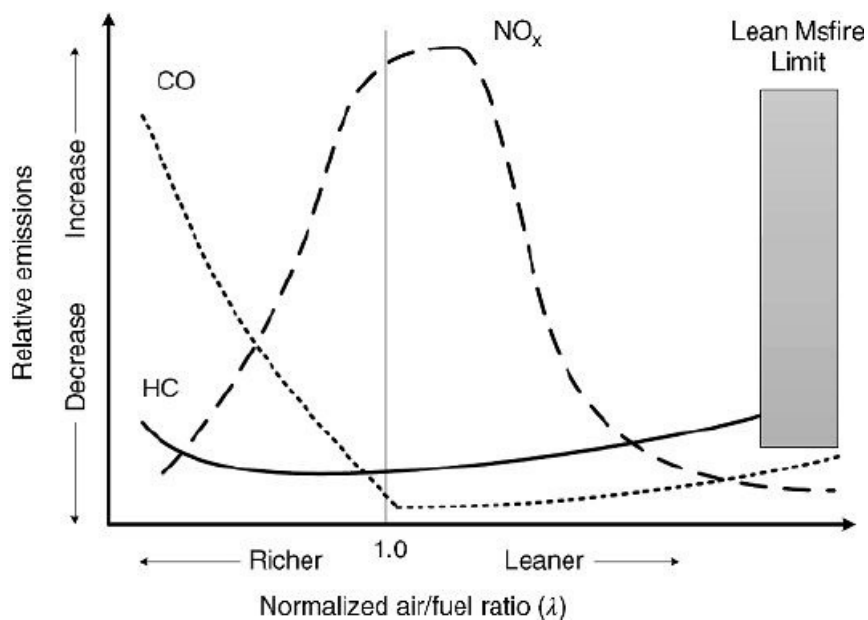


**Figure 2.2:** Effects of air-/fuel ratio variations on petrol engine emission rates [2.10].

It becomes apparent, that the setting of the  $\lambda$  operation range always represents a compromise of optimizing different exhaust gas components. However, in terms of  $\lambda$ -controlled petrol engines equipped with manifold intake injection and 3-way catalyst,  $\lambda$ -values of approximately  $\lambda = 1$  are chosen as the best operating range with regard to the most relevant emission rates; a 3-way catalyst has the best conversion efficiency for CO, HC and  $\text{NO}_x$  close to  $\lambda=1$ .

### 2.1.2. Exhaust Gas Emission Components

A brief classification of the environmental impacts and the human health risk potential of different exhaust gas components is indicated below. The focus here is on those components, which are examined in the further course of this work within the emission measurement program (chapter 5) and the PHEM simulations (chapter 6). A distinction is made between climate-relevant components

and air pollutants. The emission components presented below are partly subject to legislative limitations, see chapter 3.

### Carbon dioxide (CO<sub>2</sub>)

Carbon dioxide is a colourless, non-combustible gas, which is formed in the reaction process of carbonaceous fuels in conjunction with oxygen. The concentrations of carbon dioxide in the ambient air (up to 0,038 Vol. %) or at workplaces (up to 0,5 Vol. %) are considered to be harmless for the human organism. With increasing concentrations (from approx. 1 - 3 Vol. %), initial health impairments occur as the gas exchange in the lungs is reduced. Concentrations above 10 % by volume represent an acute danger to human organism even in the case of short-term exposure [2.11].

Carbon dioxide is a greenhouse gas in the Earth's atmosphere that absorbs fractions of the heat radiated by the earth surface. The International Government Panel on Climate Change (IPCC) assigns CO<sub>2</sub> the Global Warming Potential (GWP) of 1, which is a measure used to assess the climate impact of gases [2.12]. All other substances are related to CO<sub>2</sub> with regard to their Global Warming Potential. Relevant CO<sub>2</sub> emission sources are the energy sector, private households and not least the transport sector. The amount of CO<sub>2</sub> emissions is approximately proportional to the fuel consumption rate of a conventional driven vehicle. There are no restrictions on the CO<sub>2</sub> emission rates in the field of powered two-wheelers so far.

### Methane (CH<sub>4</sub>)

Methane belongs to the group of alkanes with the chemical formula CH<sub>4</sub>. It is a colourless and odourless gas that is highly flammable in conjunction with oxygen. Methane itself is not harmful to human health, however, high concentrations lead to the replacement of oxygen in the lung cells. The climate impact of methane is 21 (GWP = 21) times higher than that of carbon dioxide as indicated by the IPCC and it is considered to play a significant role in climate change processes [2.13]. Methane is found in large quantities in the crust of the earth (oil deposits, coal deposits) and it is primarily formed when organic material decays anaerobically. Major natural emitters are wetlands (moors), oceans, and forest fires. Anthropogenic methane sources can be found in the agriculture sector, especially in mass factory farming, in the oil- and gas production, as well as in waste disposal sites. Low methane quantities are attributable to the transport sector and sewage sludge plants.

### Carbon monoxide (CO)

Carbon monoxide is a colourless, odourless, tasteless gas. It is a chemical compound consisting of a carbon and oxygen atom. Carbon monoxide is flammable and oxidizes in conjunction with oxygen to carbon dioxide. Carbon monoxide is a dangerous respiratory poison as it blocks the oxygen transport in the blood even at low ambient concentrations. In consequence, CO can lead to severe poisoning or even death. Even exposure to 70 to 100 ppm in the ambient air over a few hours leads to disease-like symptoms such as headache, sore eyes and shortness of breath. Exposures above 400 ppm are considered as life-threatening [2.14].

---

CO is formed in technical combustion processes when carbonaceous fuel is not completely oxidized [2.15]. It is produced in internal combustion engines when the flame extinguishes on cold combustion chamber components inside the engine, in particular, during the warm-up phase of the vehicle. In addition, when the catalytic converter has not yet reached its optimal operating temperature, CO is not further oxidized. Besides the traffic sector, relevant sources include, among others, industrial plants (blast furnaces), forest fires, private fireplaces and heating systems.

### Nitrogen oxides (NO<sub>x</sub>)

Nitrogen oxides are part of a group of nitrogenous substances in which nitrogen forms chemical components in conjunction with oxygen. The most relevant emission components in petrol engines are nitrogen monoxide (NO) and nitrogen dioxide (NO<sub>2</sub>), which are summarized as NO<sub>x</sub> emissions in the road traffic sector. Both components are considered to be harmful to health and irritating to the respiratory tract. The majority of traffic-related NO<sub>x</sub> emissions are emitted as NO, however, some shares of the NO emissions in the atmosphere continue to react to NO<sub>2</sub> [2.16]. In engine combustion processes, nitrogen and oxygen comes from the ambient air. Due to high temperatures within the flame front a reaction to NO<sub>x</sub> fractions occurs. Three-way catalysts convert NO under ideal conditions (among others, correctly adjusted  $\lambda$ -value and operating temperatures) back to non-toxic atmospheric nitrogen. Relevant sources are the transport sector, power- and combustion plants, as well as the agriculture sector.

### Volatile Organic Compounds (VOCs)

Volatile organic compounds belong to a group of organic substances in the exhaust gas resulting from the incomplete combustion of hydrocarbon-containing fuels. Usually, these substances are declared as volatile organic compounds (VOC) and a distinction is made between non-methane hydrocarbons (NMHC) and the greenhouse gas methane (CH<sub>4</sub>). NMHC emissions refer to a wide spectrum of components, including, among others, alkanes, ethane (C<sub>2</sub>H<sub>6</sub>), propane (C<sub>3</sub>H<sub>8</sub>) etc.), aldehydes (formaldehyde (HCHO)) and aromatics (Benzenes (C<sub>6</sub>H<sub>6</sub>), Toluene and Xylene). In total, hundreds of different VOCs are explored which have, among others, their origin in the combustion of fossil fuels, in the solvent industry and in biological processes. It is assumed that the worldwide share of biogenic VOCs exceed the share of anthropogenic VOCs by large amounts, however, in residential areas anthropogenic VOCs represent a significant proportion [2.16]. VOC emissions are considered as precursors to the formation of ground-level ozone. Some of the VOC components have direct harmful effects on human health. Substances such as benzene or formaldehyde are classified for humans as carcinogenic, mutagenic and show reproductive toxic effects [2.17].

Modern petrol vehicles equipped with three-way catalytic converters and  $\lambda$ -controls reduce hydrocarbon emissions and VOCs from the exhaust gas almost completely. In the cold-start phase, however, when the operation temperature of the catalyst converter has not yet reached its light-off threshold, VOC emissions are partly not oxidized. During the cold-start phase, the highest shares of HC emission fractions are emitted. Additionally, VOC emissions are increasingly released into the environment when the engine is operated under full load conditions using a rich fuel-/air mixture.

---

### Particle emissions

Particle emissions are primarily formed due to incomplete combustion in the case of a local lack of oxygen in the combustion chamber and due to the combustion of lube-oil fractions. Particle emissions consist of a large number of different substances of different shapes and sizes. They consist of organic and non-organic substances in solid and liquid phase [2.18]. Particle emissions are further differentiated according to the particle density, the soot volume fraction and the mean particle diameter. Legislation distinguishes in the traffic sector between the number and the mass of particles in the exhaust gas as defined as PN (Particulate Number) and PM (Particulate Matter) – particulate matter, in turn, is subdivided into PM 2.5 and PM 10 according to their particle diameter distribution. Although particulate emissions are predominantly an issue in diesel engines (diffusion flame without premixing of diesel fuel with oxygen), petrol engines equipped with direct fuel injection systems are an increasing source of PM emissions – particularly PM 2.5 emissions that are classified as highly respirable [2.19]. The risk of particle emissions on human health is on the one hand due to the inhalation into the respiratory track and thus into the lung air cells; on the other hand, partially toxic substances adhere to the particles, which thus also enter the human organism via the lung system and finally the blood circulation [2.20]. Although it is deemed that the greatest share of total particulate emissions are of natural origin (dust, sea salt spray), it is assumed that anthropogenic particulate emissions in residential areas can have a relevant share. From 2016 onwards, motorcycles have to comply for the first time with a particulate matter emission limit, see Chapter 3.

## **2.2 Evaporative Emissions**

Evaporative emissions are characterized as volatile organic compounds (VOC) that escape from the vehicle into the environment and that are not attributable to the combustion process itself. The formation of those emission fractions depends crucially on fuel properties, the constructive design of the vehicle - particularly the fuel-carrying components - and the application of evaporative emission reduction devices- and strategies. Not least, factors like engine temperature before stopping the vehicle and ambient climate conditions affect the amount of evaporative fumes [2.21]. Common assemblies and components that are relevant sources for the escape of hydrocarbon vapors are hoses, seals, connecting points, closures (e. g. oil-dipstick, fuel cap) and the storage tank as such. In particular, vehicle types equipped with carburetors contribute to a high extent to the outlet of hydrocarbon vapors. In terms of powered two-wheelers, older vehicle concepts and those with 2-stroke engines are primarily affected [2.22].

It is assumed that powered two-wheelers as a source of evaporative emissions in Germany are widely underestimated and that the share to the total HC-emissions in this vehicle category is deemed to be disproportionately high [1.2]. According to TREMOD the share of evaporative emissions in the total HC-emissions in this vehicle category in Germany will increase to approx. 16 % by 2030, as shown in figure 2.3.

---

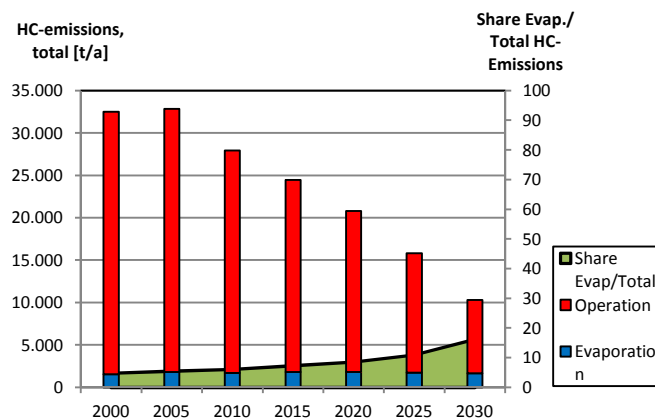


**Figure 2.3:** Powered two-wheelers hydrocarbon emissions in Germany differentiated according to operational- vs. evaporative emissions; evaporative emission share [1.2].

Evaporative emissions relate predominantly to vehicle concepts powered by short chained petrol-based fuels, since the volatility of these fuels is higher compared to those of diesel-fuel (distillation range of petrol-fuel: approx. 30°C – 200°C; distillation range of Diesel-fuel: approx. 160°C – 380°C) [2.23]. Thus, there is almost no relevant formation of gaseous phases in diesel-fuel systems and therefore diesel vehicles are largely not relevant when considering evaporative emissions in the road transport sector. A relevant factor in this context is the vapor pressure, which characterizes the evaporation properties of liquids and thus affects the formation of fuel vapors decisively. Widely used units for the measurement that describe the volatility of liquid fuels are the Dry Vapor Pressure Equivalent (DVPE) as defined in DIN EN 13016-1 and applied in EU-Legislation respectively the Reid Vapor Pressure (RVP) as determined in test method ASTM-D-323, commonly used in the U. S. [2.24][2.25].

The fuel composition affects the DVPE of liquid fuels, as for example, admixtures of ethanol in petrol fuel increases the vapor pressure and finally the volatility of the mix, resulting in possibly higher evaporative emissions. This increase is non-linear and occurs already at low mixing ratios between 0 – 5 % ethanol. In order not to oppose EU-targets to promote low-carbon- and renewable fuels in the transport sector - by implementing quotas for bio-ethanol as fixed in Directive 2003/30/EC - the limits of vapor pressure of petrol/ethanol blends were revised in Annex III of the fuel quality Directive 2009/30/EC [2.26] [2.27].

Evaporative HC emissions lead to almost the same effects as tailpipe HC-emissions, as they consist primarily of VOC's, which affect directly human health, particularly the respiratory tract and act as precursors for the formation of ground-level ozone. The greatest share of powered two-wheelers evaporative emissions are generated in urban areas according to TREMOD, as vehicles are parked commonly at the place of residence or at work, see figure 2.4. Here, the distribution of evaporative emissions from powered two-wheelers, differentiated according to motorcycles and mopeds and local area is shown.

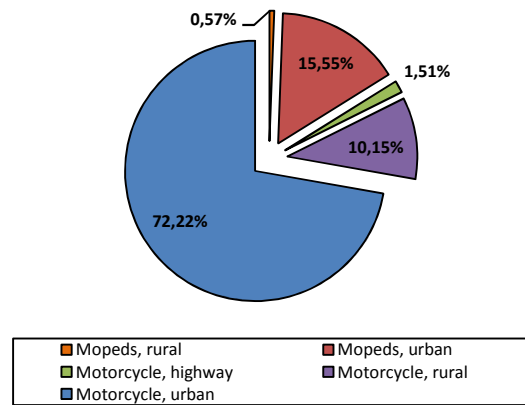


**Figure 2.4:** Powered two-wheelers evaporative emissions differentiated according local area – motorcycles and mopeds [1.2].

Figure 2.4 indicates, that approximately 87 % of powered two-wheelers evaporative emissions – both, from motorcycles and mopeds – are generated in urban districts and thus contribute to the deterioration of an already strained air-quality situation there. In order to limit the quantity of evaporative fuel fractions, modern vehicles are equipped with charcoal absorbers that store hydrocarbon vapors in the fuel storage system and prevent them to escape into the atmosphere. The inside of the charcoal canister consists of a sponge-like structure with a large charcoal surface for maximum adsorbing capacity. When the vehicle is operated the stored fuel vapors are released via a mechanical or solenoid purge valve into the air intake for combustion in the engine. The size and the loading of the charcoal canister depend on the expected vapor quantity for the individual vehicle type and are adapted to fulfill the evaporation limit values tested in the type IV test of the type approval, see chapter 3.3. Additional measures to mitigate evaporative emissions are the equipment of fuel tanks and tubing systems with low permeation materials or layers. Evaporative emissions can be assigned to five classes, as discussed below.

### 2.2.1 Diurnal / Breathing Losses

The fluctuation of the ambient temperature between day and night as well as the exposure of vehicles to hot sources (e. g. sunlight, hot asphalt) leads to a temperature and pressure variation inside the fuel system. This causes expansion- and contraction processes of fuel vapors that partly escape from the fuel storage vent system. Due to decreasing temperatures at night ambient air is pulled inside the tank system and the formation of gasoline vapors starts again. These fuel fumes are indicated as diurnal losses, since it is a process recurring every day [2.28] [2.29].

### 2.2.2 Hot Soak Emissions

Once a vehicle is switched off after use the temperature of the engine compartment continues to rise due to the missing airflow around it, which also leads to increasing fuel temperatures in the fuel- and tubing system. The evaporation into the atmosphere occurs through the ventilation systems and leaks. The quantity of the hot soak emissions depends on the temperature of the engine compartment, which is a function of e. g. the travelled distance, driving behavior, ambient

temperatures and not least fuel specifications as vapor pressure. In addition, the shutdown period has an effect on the amount of evaporative emissions. As indicated in [2.30], the highest quantity of hot soak emission occurs within 2 – 3 hours after the engine has stopped. In [2.22] an additional distinction is made between soak emissions according to the distance travelled before the engine is switched off, namely hot soak (travelled distance > 4 km before engine stop) and warm soak (travelled distance < 4 km before engine stop).

### **2.2.3 Permeation**

The transport of substances through solid materials at molecular level is defined as permeation. This process occurs as a consequence of concentration or pressure gradients between polymer layers and appears in the field of motor vehicles as the passing of hydrocarbons through plastic and rubber components in the fuel system like seals, hoses or the tank system itself. Vehicles equipped with metallic tank systems are less affected by permeation losses than those fitted with plastic tanks.

### **2.2.4 Running Losses**

Fuel fractions that evaporate from the engine and the fuel system due to the heating of the fuel from the engine, fuel pump, road, and exhaust gas system while the vehicle is operating are classified as running losses. Besides the engine heat, hot ambient temperatures reinforce the effect of fuel heating resulting in an increasing formation of vapors in the fuel system. The release mechanisms are the same as those from breathing losses and hot soak evaporation. Vehicles that are equipped with fuel return lines - primarily older vehicle concepts - have higher evaporative emissions, since the fuel flowing back from the engine into the tank is warmed up by the engine heat.

### **2.2.5 Refuelling Losses**

A distinction is made between HC emissions that occur as fuel is filled into the tank and displacing the existing fuel vapors, and those fuel fractions that are released into the environment due to spillage [2.31]. In order to absorb the escaping vapors and to allow pressure compensation in the vehicle tank system, fuel vapors are conducted through the activated carbon trap via a valve. Modern service stations are equipped with Stage II petrol vapor recovery systems according to Directive 2009/126/EC that store fuel fumes during the refilling process [2.32].

## **2.3 Non-exhaust Emissions**

Besides tailpipe- and evaporative emissions motor vehicles contribute to emission fractions that are not related to the combustion process inside the engine or to evaporative effects of the fuel carrying system. These non-exhaust emissions are attributed to particulate emissions that are formed by various processes on the vehicle side or due to interactions between the vehicle and the road surface. Here, a brief overview of relevant formation processes is given in order to include all relevant types of emissions in the powered two-wheeler segment. However, non-exhaust emissions

---

are no further issue in the later course of this work. In-depth information on this topic can be found in the corresponding literature sources.

Relevant non-exhaust emission shares occur due to the abrasion of mechanically stressed vehicle components – e. g. tires, brakes and clutches – and due to corrosion processes of certain vehicle components [2.3]. The road surface is subject to wear processes as well, so that particulate emissions also occur here. Additionally, the re-suspension of already existing particles on the road surface is considered to be a relevant source of non-exhaust particle emissions.

Since the formation of non-exhaust particle emissions underlies varying formation mechanism depending on different vehicle components, the chemical composition of generated particle emissions is diverse and partly harmful to humans and the environment. Brake wear is characterized by numerous materials from the brake pads and brake discs such as metals, binders and carbons [2.33]. The emission rate depends on a variety of factors such as, among others, the braking power, the composition of brake components (pads and discs) and, in particular, the heat generation in the braking system. Emissions from tires consist of a complex mixture of different substances, namely different types of rubber fractions, organic and inorganic compounds and metals from the inner tire structure. The majority of these components are released during the braking process, as the highest forces between road surface and tires occur. The road pavement is subject to mechanical stress due to the interaction between vehicles and the road resulting in particle emissions from the road surface. These include abrasive components like, among others, Cobalt, Molybdenum, Zinc, Tin and Nickel.

The share of non-exhaust particle emissions from the road transport sector is considered to be considerably high, particularly in residential areas [2.34]. So far, however, there are no legislative restrictions for non-exhaust emission components, but possibilities for capturing and measuring such components are currently discussed. Reference is made to the work of the PMP (Particulate Measurement Program) working Group on UN-level [2.35].

---

### **3. Emission Legislation of Powered Two-wheelers – Vehicle Classification and Test Procedures**

The emission legislation in the motor vehicle sector prescribes, among other things, the requirements for environment-related technical systems, emission limit values and the underlying test procedures, as well as durability requirements of emission control systems. This procedure is intended to minimize the impacts of road traffic pollution and to create uniform standards for legislators and manufacturers in this field. Standardized measurement procedures are necessary to obtain comparable and reproducible statements and to provide a basis for ongoing legislative actions. Within the European Union environment-related issues are regulated within the framework of EU Regulations in the motor vehicle sector and, in addition, partly also on a national level. The technical requirements are elaborated in technical working groups usually under the guidance of the European Commission. However, some test procedures and specifications are partly adopted from UN-ECE regulations and adapted to the special requirements in the EU. Each new vehicle type is tested for compliance with such requirements as a part of the European standardized vehicle type approval procedure – exceptions are made, among other things, for small-series manufacturers. In addition to the mandatory European legislation, each Member State has the possibility to impose measures to improve air quality objectives at national level. This includes, among other things, the introduction of traffic bans, environmental zones or exhaust gas retrofit solutions.

In the following chapter, certain aspects of the emissions legislation in the powered two-wheeler segment that are relevant to this work are selected and presented in detail. First, the classification of powered two-wheelers according to EU-legislation is presented in chapter 3.1. Subsequently, relevant emission test procedures and the underlying tailpipe emission limit values are introduced. In the context of this work, the legislative test procedure for determining tailpipe emissions is particularly important; relevant information is summarized in chapter 3.2. Besides to tailpipe emission, the evaporative emissions in this vehicle category are of increasing importance, as already indicated in chapter 2.2. Legislative actions for the determination of evaporative emission shares are described in chapter 3.3. There are further legally required environmental issues that apply to powered two-wheelers in the European Union. These include, among other things, test procedures for the durability of emission control devices and on-board diagnostic functionality that are prescribed in Regulation (EU) No 168/2013 [3.1]. Since these aspects are not relevant in the further course of this work, they will not be elaborated further at this point.

#### **3.1 Classification of Powered Two-wheelers according to EU-Legislation**

Powered two-wheelers are classified in accordance with Regulation (EU) No 168/2013 Article 4. Herein, motorized bicycles, two- and three-wheeled mopeds, two- and three-wheeled motorcycles, motorcycles with side cars, light and heavy on-road quads and light- and heavy quadricycles are categorized as L-category (light vehicle category) vehicles. Each of these vehicle concepts is listed in separate categories (L1e – L7e) within the L-category scheme that is determined by basic vehicle characteristics. These include, in particular, criteria such as vehicle mass and dimensions, maximum

---

vehicle speed and maximum net power of the propulsion unit. In addition, the abovementioned categories within L-category are further divided into sub-categories, which are in turn differentiated by means of supplemental sub-classification criteria such as, among others, the power-to-weight ratio of the vehicle. A further differentiation criterion within the L-category classification is the type of propulsion. Here, a distinction is made between combustion engines – these are further subdivided into positive ignition (PI) and compressed ignition (CI) engines, rotary piston engines, turbines, electric engines and hybrid propulsion solutions. The high degree of differentiation in the classification scheme of powered two-wheelers is necessary to define the requirements for the type approval test procedure for each vehicle type. Table 3.1 presents the vehicle classification scheme within the L-category. Since only motorcycles (category L3e, two-wheeled motorcycles) are covered in the later course of this work, only this vehicle category is shown here in a differentiated way. The information in table 3.1 is taken from ANNEX I of Regulation (EU) No 168/2013 [3.1].

**Table 3.1:** Vehicle classification criteria according to Regulation (EU) No 168/2013. Common classification criteria and supplemented sub-classification criteria. Top: all L-category vehicles (L1e – L7e); bottom: two-wheeled motorcycles (L3e) [3.1].

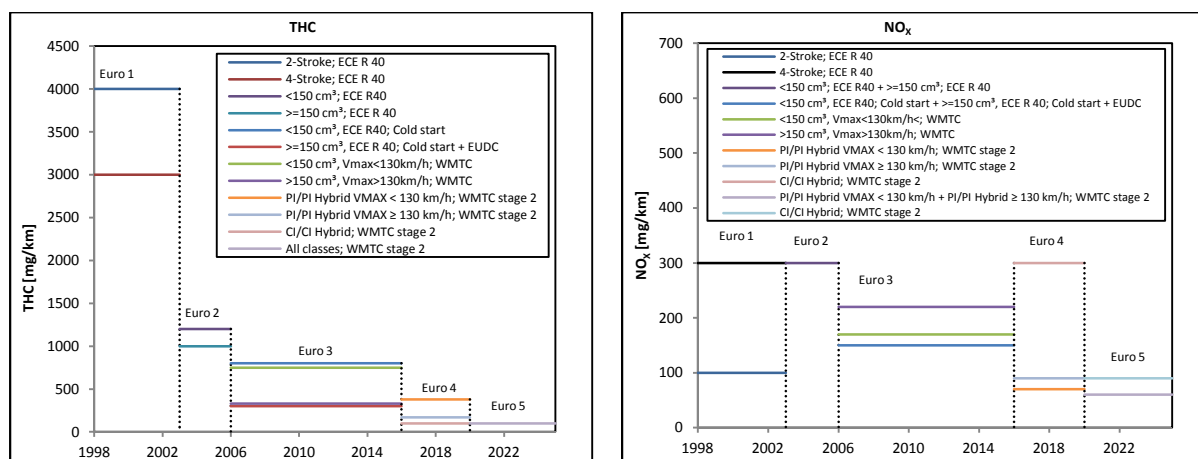
Category	Category name	Common classification criteria
L1e – L7e	All L-category vehicles	(1) length $\leq$ 4 000 mm or $\leq$ 3 000 mm for a L6e-B vehicle or $\leq$ 3 700 mm for a L7e-C vehicle, and (2) width $\leq$ 2 000 mm, or $\leq$ 1 000 mm for a L1e vehicle, or $\leq$ 1 500 mm for a L6e-B or a L7e-C vehicle and (3) height $\leq$ 2 500 mm.
Category	Category name	Common classification criteria
L3e	Two-wheel motorcycle	(4) Two-wheels and powered by propulsion as listed under Article 4(3) of regulation EG 168/2013 and (5) maximum mass = technically permissible mass declared by the manufacturer and (6) two-wheel vehicle that cannot be classified as category L1e.
Sub-categories	Sub-category name	Supplemental sub-classification criteria
L3e-A1	Low-performance motorcycle	(7) engine capacity $\leq$ 125 cm <sup>3</sup> and (8) maximum continuous rated or net power (1) $\leq$ 11 kW and (9) power/weight ratio $\leq$ 0,1 kW/kg.
L3e-A2	Medium-performance motorcycle	(7) maximum continuous rated or net power (1) $\leq$ 35 kW and (8) power/weight ratio 0,2 kW/kg and (9) not derived from a vehicle equipped with an engine of more than double its power and (10) L3e vehicle that cannot be classified under supplemental sub-classification criteria (7), (8) and (9) of a L3e-A1 vehicle.
L3e-A3	High-performance motorcycle	(7) any other L3e vehicle that cannot be classified according to the classification criteria of a L3e-A1 or L3e-A2 vehicle.

### 3.2 Hot Emission Test Procedure and Tailpipe Emission Limits

The adoption of Directive 97/24/EC on 17 June 1997 set mandatory emission standards for tailpipe emissions of powered two- and three-wheelers and defined standardized test procedures in the European type approval process [3.2]. Thenceforth, new motorcycle- and moped types had to comply with Euro 1 emission standard that includes emission limits for the exhaust gas components CO, HC and NO<sub>x</sub> as laid down in Directive 97/24/EC, chapter 5, Annexes I – III. In June 2002, the second exhaust gas limit stage (Euro 2) for mopeds came into force according to the same directive.

Up to and including the emission standard Euro 2, emission values for HC and NO<sub>x</sub> for mopeds are indicated as sum limit values whereas they are specified as individual values for motorcycles already from Euro 1 stage onwards. A distinction of exhaust gas limit values for Euro 1 motorcycles by engine type was made according to two-stroke (2S) and four-stroke (4S) models, however, that separation was abandoned in favor of a differentiation by displacement classes (< 150 cm<sup>3</sup>, ≥ 150 cm<sup>3</sup>) within the framework of the introduction of Euro 2. Motorcycles emission stages Euro 2 and Euro 3 are fixed in Directive 2002/51/EC which applied from April 2003 (Euro 2) and January 2006 (Euro 3) onwards and led to a significant reduction of exhaust gas pollutant limits in this vehicle category [3.3]. The vehicles are tested within the type I test according to the type approval driving cycles laid down in UN-ECE Reg. R47 (mopeds Euro 1 and Euro 2) and UN-ECE Reg. 40 (motorcycles Euro 1 and Euro 2) that do only reflect emission shares when the engine has already warmed up [3.4][ 3.5]. Within the scope of Euro 3, emission standard the motorcycle emission test procedure was adjusted in a way that emissions during the warm-up phase of the engine are measured additionally for all displacement classes. The test cycle laid down in UN-ECE Reg. 40 is extended to an extra urban driving cycle (EUDC) phase for vehicles ≥ 150 cm<sup>3</sup>, which corresponds to the extra-urban phase of the new European driving cycle (NEDC) applied for passenger cars. Alternatively, manufacturers can certify Euro 3 motorcycles according to Directive 2006/72/EC by applying the worldwide harmonized motorcycle test cycle (WMTC, fixed in UN-ECE GTR. No. 2), taking into account different pollutant limits contrasted to limit values in the aforementioned procedure [3.6] [3.7].

From 2016 onwards, Regulation (EU) No 168/2013, issued in January 2013, was applicable to the light vehicle category [3.1]. The regulation provides the introduction of emission standards Euro 4 and Euro 5. These new emission steps are designed to tighten already existing emission levels for HC, CO and NO<sub>x</sub> emissions within test type I within the vehicle type approval procedure, as well as to fix new exhaust gas emission values for particulate matter (Euro 4) and non-methane hydrocarbons NMHC (Euro 5) for the first time. This Regulation represents a tightened measure to mitigate ozone precursor substances and dust pollution and the resulting formation of smog - particularly in urban areas, in which a large proportion of moped- and motorcycle traffic is performed [1.2]. The underlying test cycle for Euro 4 and Euro 5 motorcycles is the WMTC stage 2 according to Annex VI, table (A1) to Regulation (EU) No 168/2013. Figure 3.1 shows the successive reduction of pollutant emissions limits of motorcycles (L3e). The emission limits of the Euro 5 emission standard for motorcycles are identical to those for passenger cars with gasoline engines and emission standard Euro 6.



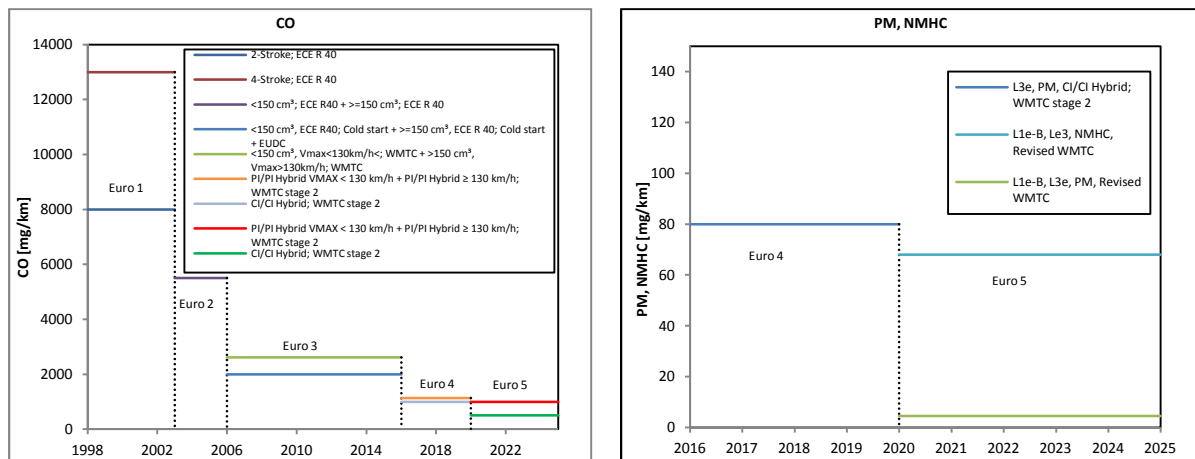


**Figure 3.1:** Motorcycle tailpipe emission limits according to emission standard Euro 1-5, vehicle specifications and underlying test procedures.

### 3.3 Evaporative Emission Test Procedure

Besides the implementation of new tailpipe emission standards, there is a restriction for evaporative emissions for Euro 4 and Euro 5 L-category vehicles for the first time. The test procedure for the determination of evaporative emissions as applied in type approval test type IV is laid down in Annex V to Regulation (EU) No 134/2014 [3.8]. In a first step from 2016 onwards newly introduced motorcycle types have to fulfill Euro 4 evaporative emission limits corresponding to Annex VI Part (C1) to Regulation (EU) No 168/2013. Therefore, vehicles are examined in gas-tight air chambers (SHED - sealed housing for evaporative emission determination) with regard to the outlet of hydrocarbon vapors as a consequence of diurnal temperature- and pressure variations inside the fuel system (tank breathing, diurnal losses) and due to hot-soak after vehicle operation. Within the introduction of Euro 5 emission standard in 2020 all L-category vehicles and subclasses including small motorcycles (L1e) have to fulfill evaporative emission limits as fixed in Annex VI Part (C2) to Regulation (EU) No 168/2013. Besides the SHED procedure, Euro 5 vehicles equipped with a non-metallic fuel storage system are analyzed according to permeation of fuel fractions through the fuel storage- and delivery system. The test procedures for the determination of tank breathing (diurnal losses), hot-soak emissions and permeation are briefly summarized as follows

#### 3.3.1 Diurnal Losses and Hot-soak Emission Test Procedure

The test procedure consists of two measuring phases in which emerging hydrocarbon fuel vapors in the form of diurnal losses and hot-soak emissions are investigated. The procedure contains a preconditioning phase, wherein the test vehicle undergoes test cycles corresponding to Part A of Annex VI to Regulation (EU) No 168/2013 on a chassis dynamometer first. Afterwards, the test vehicle is switched off for a defined soak period (between 12 and 36 hours in the case of motorcycles with a capacity > 280 cm<sup>3</sup>) before then being placed inside the SHED-chamber. Before the test begins, the test chamber is purged and the HC-analyzers are calibrated. Over a defined period, the fuel system is heated according to defined heating functions and the final hydrocarbon concentration

is recorded with a flame ionization detector (FID) inside the SHED-chamber. This procedure is followed by a further conditioning phase in which vehicles are driven again through the vehicle class-specific driving cycle, before the hot soak evaporative emission test starts. The test vehicle is moved with the engine switched off into the SHED-chamber immediately (within 7 minutes after finishing the driving cycle) and the hydrocarbon fuel vapors are measured over  $60 \pm 0,5$  minutes after the chamber is sealed. Finally the overall evaporative hydrocarbon mass emission is formed by summing up the test results from the diurnal- and the hot soak test indicated in grams / test. The limit values of 2.000 mg / test (Euro 4) respectively 1.500 mg / test (Euro 5) corresponding to Annex VI Part (C2) to Regulation (EU) No 168/2013 have to be fulfilled within the type approval tests. Figure 3.2 demonstrates the schematic sequence of the evaporative emission test procedure.

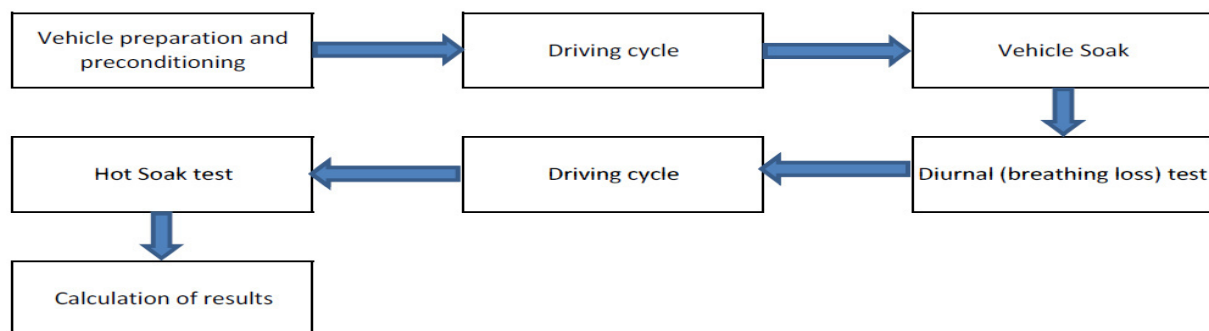


**Figure 3.2:** Sequence of evaporative test procedure according to Regulation (EU) No 134/2014 [3.8].

### 3.3.2 Permeation Test Procedure

The determination of evaporative fuel fractions due to permeation from the fuel storage- and delivery system applies for new L-category vehicle types from 2020 onwards. The test procedure is laid down in Appendix 2 of Annex V to Regulation (EU) No 134/2014. It is based on measuring the weight loss of a fuel tank over a defined test period. For this purpose, a disassembled tank system is filled with fuel, correspondingly sealed with clamps or fittings and stored under defined ambient temperature conditions ( $28 \pm 5$  °C) in a temperature-controlled chamber. The weight difference between the starting point and the end of the test has to be divided by the inner surface of the fuel tank and by the number of testing days to achieve the specific permeation rate indicated in  $\text{mg} / \text{m}^2 \cdot \text{day}$ . According to the current state of legislation all L-category vehicles and subcategories have to fulfill permeation limits of 1.500  $\text{mg} / \text{m}^2 \cdot \text{day}$  (fuel tank) and 15.000  $\text{mg} / \text{m}^2 \cdot \text{day}$  (fuel tubing) within Euro 5 emission standard.

## **4. Emission Calculation and Simulation in the European Union – Background and Models**

Within the framework of this study, emission data for a representative motorcycle are obtained based on real-world- and chassis dynamometer emission measurements. The data sets are implemented in the German emission inventory model TREMOD and the calculation of future emission trend scenarios in this vehicle category is carried out. However, the usability of such emission data gained from emission measurements requires processing steps to transform the datasets into the format of inventory models like TREMOD or COPERT. The underlying micro-, macro- and database emission models applied in this work as well as the purpose of the emission calculation- and simulation in the European Union in general are part of this chapter. The functionality and structure of the most relevant models are presented and the correlation with the key activities in this work is established.

### **4.1 Background**

The quantity of pollutant- and greenhouse gas emissions in the traffic sector in the European Union is restricted by means of regulations and measures on a national and international level. The resolution of such agreements requires a detailed understanding of the processes, which lead to problematic emission levels, air quality problems and negative environmental developments. In this context, reliable information on traffic emission sources in a high differentiation are the basis for the operation with such environment-related issues and the enforcement of legislative acts. For this purpose, appropriate emission calculation models have been developed over the last decades in the European member states that allow dealing with emission-related topics in the transport and particularly in the road traffic sector. These models have been adapted to the situation in the respective member states and they show partly variations in function and structure. The task spectrum of emission calculation and simulation models is diverse and it ranges from energy and emission assessments for individual vehicles, the calculation of road traffic emissions on single roads and local areas up to the collection of total national emission data, taking into account all kinds of road users and underlying traffic data in the state concerned.

Relevant legislative actions comprise the reporting obligations of anthropogenic pollutant and greenhouse gas emissions within the framework of the European Union, the United Nations and partly on a national level. These include, in particular, emission inventory reporting obligations within the EU-wide regulated NEC-Directive 2001/81/EC (new emission ceilings), which stipulates sector-specific quantitative limitations for several pollutant components (among others, sulfur dioxide (SO<sub>2</sub>), nitrogen oxides (NO<sub>x</sub>), volatile organic compounds (VOC) and ammonia (NH<sub>3</sub>)) for each EU member state and within the framework of the Kyoto Protocol on the reduction of national greenhouse gas emissions, adopted under the United Nations Framework Convention on Climate Change (UNFCCC) [4.1] [4.2]. Further relevant applications include the calculation of future emission trend scenarios for the estimation of the ongoing developments of air pollutants and greenhouse gases in order to

---

initiate legislative activities at an early stage. Additionally, political or technical measures that are already implemented can be assessed and analyzed with regard to their effectiveness.

In the following chapters the fundamentals of road traffic emission calculation- and simulation processes used for different applications in the road traffic sector are characterized and an overview of the most relevant models in the European Union is given. The successive levels from the micro-scale simulation of individual vehicles up to the macro-scale simulation of entire vehicle fleets are illustrated. The focus is on calculation models that apply in the further course of this work. The situation in Germany with regard to the current input parameters and calculation routines for the national accepted emission inventorying tool TREMOD is analyzed by taking into account the motorcycle input parameters in detail.

## **4.2. Emission Calculation Models**

Several emission calculation and simulation models have been developed in the European Union over the last decades in the road traffic sector, which differ with regard to design, function and their underlying input data-bases [4.3]. The activities and priorities in the field of the development of such models are primarily based on the needs and requirements of the legislative actors, the funding institutions and the individual users. However, there is a European network of national research institutes, governmental institutions and scientific experts (ERMES Group – European Research on mobile Emission Sources) under the direction of the European Commission (DG JRC – Joint Research Centre), which promotes and coordinates emissions modeling and emission measurement programs in the EU and helps to identify research demand in this working area. Experiences and knowledge concerning emission calculation issues are shared regularly within this group. The emission calculation models can be schematically divided into three main groups, namely micro-scale-, macro-scale- and database emission models that are described subsequently.

Micro-scale based emission models simulate the emission behavior of individual vehicle / engine units. A distinction is made between such models, which are suitable only for the simulation of single engines and those that are used to simulate the entire vehicle including its exhaust gas after-treatment systems. At this point, reference is made to the PHEM model (Passenger Car and Heavy Duty Emission Model) developed by the Institute of Internal Combustion engines and Thermodynamics of Graz University of Technology, which calculates the energy consumption- and specific emission rates for almost any type of vehicle and engine for almost all operating conditions. [4.4]. The PHEM model provides the basis for the calculation of emission input parameters of database- and macro-scale emission models in Europe and it is used in the further course of this work for the simulation of emission factors in the motorcycle segment. In chapter 4.2.1 the functionality and structure of the PHEM model is emphasized in detail.

The emission data sets generated in micro-scale emission models like PHEM are stored in database models such as, among others, the Handbook Emission Factors for Road Transport (HBEFA), which is the European-wide accepted basis for road transport emission data, see chapter 4.2.2 [4.5]. HBEFA includes emissions factors for almost all on-road vehicles for different driving conditions on almost all road types and local areas and it forms, among others, the emission data base for national inventory

---

models like TREMOD or COPERT, see chapters 4.2.3 and 4.2.4 [4.6] [4.7]. Besides this, emission factors generated with PHEM can also be used directly for emission calculation purposes e. g. in local applications.

Within national inventories, the specific emission factors from HBEFA are linked with national driving performance- and vehicle fleet data. These data are usually implemented in high-resolution in different manners depending on the respective situation in the focused area concerned. The linking of these three input data sets makes it possible to calculate the entire country-specific road traffic emissions in the required differentiation, e. g. according to vehicle categories, local areas, road types and emission components. The German transport emission inventorying model is explicated in detail in chapter 4.2.3 as motorcycle emission trend scenarios are calculated with TREMOD in the further course of this work (chapter 7). Particularly, the currently existing traffic- and vehicle fleet data sets for motorcycles in Germany are emphasized as they have substantial meaning for the emission calculation processes. Figure 4.1 shows the distribution of emission calculation models for national emissions reporting obligations in Europe.

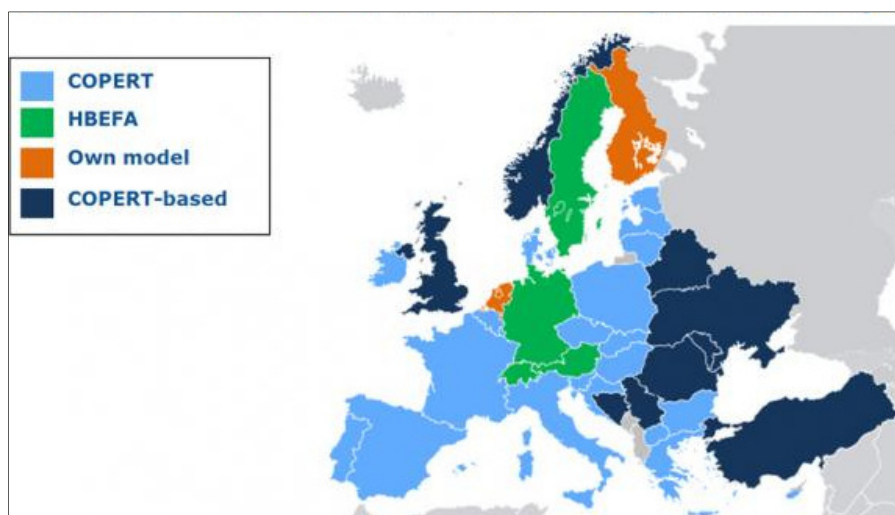


**Figure 4.1:** Distribution of road traffic emission calculation models for the national emission reporting obligations of greenhouse gases and air pollutants in Europe [4.8].

Chapter 4.2.4 gives a brief overview of the COPERT emission calculation model. COPERT is the most widely used emission calculation model within the EU and it provides also emission data on evaporative emissions in the motorcycle segment, which in turn are implemented in HBEFA and TREMOD. In essence, almost all other emission models within the EU are based on data sets from HBEFA and COPERT. These include, among others, the HBEFA Expert Version - applied in Sweden and Switzerland - and NEMO (Austria). Beyond that, some European countries developed individual emission calculations tools adapted to the prevailing situation in the country concerned e. g. Netherlands (Versit +) and Finland (LIPASTO) [4.9] [4.10].

#### 4.2.1. PHEM (Passenger Car and Heavy Duty Emission Model)

The PHEM model calculates the second-by-second power demand that is necessary to overcome the driving resistance forces acting on a vehicle during operation. On the basis of the second-by-second power data, PHEM calculates the specific exhaust gas emission and the fuel and energy consumption rates second-by-secondly based on specific emission maps, which represent the relation between engine power, engine speed and emissions, respective fuel or energy consumption rate. In turn, the emission maps are created based on real-world emissions measurements performed either on chassis dynamometers or by means of on-board emission measurements devices on the road. This makes it possible to simulate the emission behavior of an individual vehicle for almost all driving conditions, driving cycles, varying payloads or different road gradients that may occur. In addition, PHEM allows the simulation of entire vehicle segments by generating aggregated emission maps for vehicle types of similar design and technology characteristics. The last mentioned application is important particularly in the field of the emission factor calculation in the structure of national inventory models. PHEM also includes additional technical features such as, among others, a thermal behavior simulation tool for the catalyst converter or a hybrid vehicle tool, which are, however, not relevant for the applications within the motorcycle segment in this work. The last mentioned features are commonly used in the passenger car and commercial vehicle sector. In general, PHEM has been used for simulation applications in the passenger car and light and heavy-duty vehicle sector so far. A first feasibility study that investigates PHEM simulation routines in the field of powered two-wheelers has been completed in 2017 [4.11]. Figure 4.2 shows the schematic structure of the PHEM model including the relevant functions related to this work.

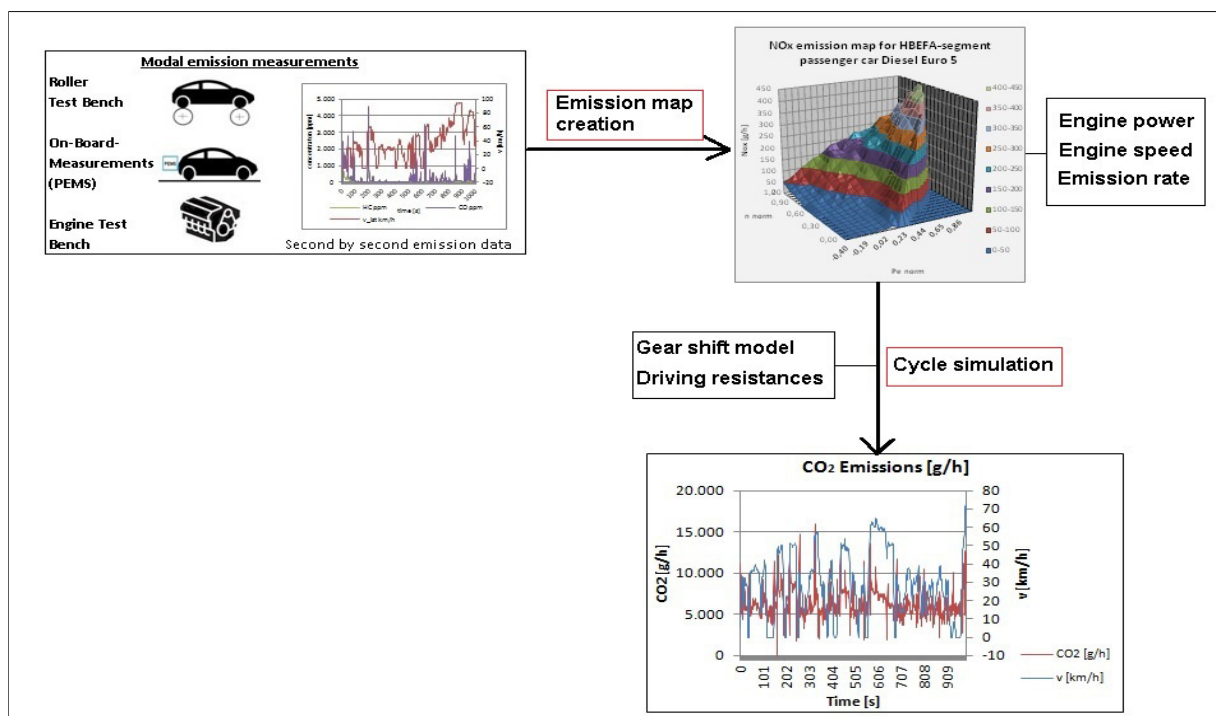


**Figure 4.2:** Schematic structure of the PHEM model.

The following chapters indicate the main features of PHEM related to this study. These include the process of the emission map generation based on exhaust gas measurement data – both, on-board-

and chassis dynamometer measurement data - and the emission simulation using driving resistance data and the PHEM gear shift model.

#### 4.2.1.1 Emission Map Creation

The basis for the creation of emission maps in PHEM are modal exhaust gas measurement data, engine power- and engine speed data, which are collected as part of chassis dynamometer or on-board emission measurements. The instantaneous measurement data have to be prepared in a way that a correct assignment of the engine load to the emission rate and the engine speed signal is ensured – engine load peaks correspond usually with emission peaks. If necessary, the exhaust gas measurement records need to be adjusted accordingly. In order to achieve the largest possible engine map coverage, it is necessary to drive through almost all relevant operating points (e. g. speed- and acceleration ranges) of the engine map in the measurement program. In particular, real-world driving cycles or driving on public roads with appropriate shares of urban, rural and motorway traffic in different driving styles (moderate to sporty) are suitable for this purpose. PHEM interconnects the second-by-second emission measurement data together with the engine power and the engine speed data into a three-dimensional emission map. This process takes place for each measured exhaust gas component and results in an individual, characteristic emission map. In the case of engine load ranges, in which no emission information from the measurement are available, PHEM interpolates or extrapolates emission values from adjacent engine map points. This method establishes a clear relationship between the parameters engine power, engine speed and exhaust gas emission rate. The engine power and the engine speed in the emission map are usually normalized and indicated in a range from 0 – 100 % of the rated engine power and the rated engine speed. Hereby, a comparability of different vehicle emission maps is made regardless of engine-specific parameters such as, among others, displacement and the number of cylinders. Although PHEM includes a cold-start model for mapping the cold-start surcharges (not yet used in the motorcycle sector), only hot emission maps are generated in this study, which map the emission behavior in the warm operating state. The following illustrations 4.3 show an example of a fuel consumption and NO<sub>x</sub> emission map of a Euro 5 diesel car.

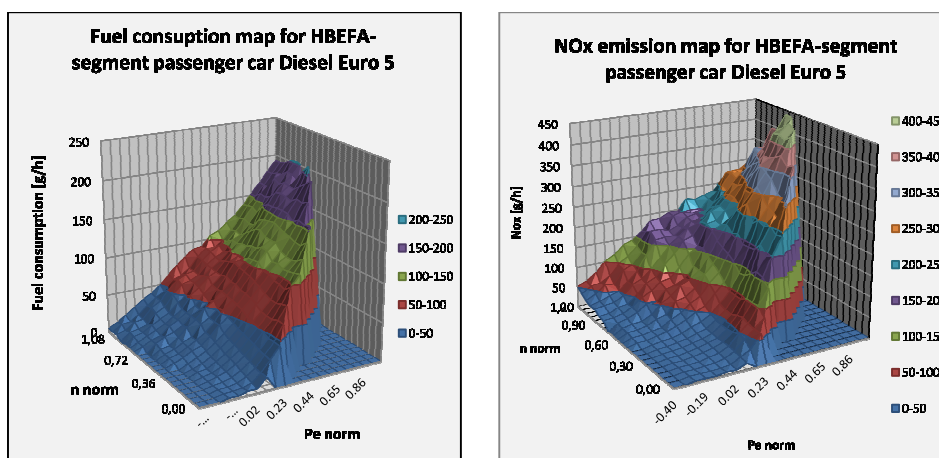


**Figure 4.3:** Fuel consumption map (left) and NO<sub>x</sub> emission map (right) for diesel passenger cars (Euro 5) generated with PHEM.

The emission concentrations in the exhaust gas are recorded via analyzers on the chassis dynamometer test bench or with mobile measurement devices. Commonly, the exhaust gas mass flow and the exhaust gas emission concentrations are measured independently and the kilometer-related emission value is determined then. The required engine speed signal and, associated therewith, the gear can be read out either directly via the OBD-CANbus interface or it can be calculated via the vehicle speed, the tire diameter and the transmission ratios. The second-by-second wheel power is measured on the chassis dynamometer test bench by measuring the braking power of the dynamometer roll. In conjunction with generic loss maps for the transmission- and auxiliary power demand the engine power can be calculated from the measured wheel power. On-board measurements, however, make it difficult to measure the engine power output directly – generally, it cannot be recorded by a PEMS system. Although it is possible to use wheel torque sensors to measure the torque on the wheel and ultimately also the engine power, this procedure is partly complex and these sensors are developed primarily for special applications [4.12]. Subsequently, a method is described in which the second-by-second engine power signal within on-board measurement programs in the motorcycle segment can be determined based on generic CO<sub>2</sub> emission maps. This method is already applied in the passenger car sector in PHEM and provides satisfactory results, in particular for the emission factor simulation for HBEFA [4.13]. In Chapter 6.1, this methodology is applied in the context of the emission map generation based on the test vehicles on-board and dynamometer emission measurements carried out in this study.

#### Emission Map Creation based on CO<sub>2</sub> Approach

Since the second-by-second CO<sub>2</sub> emission and engine speed signal of a vehicle is available, the engine load condition can be determined. This relationship is depicted in generic CO<sub>2</sub> maps. The generic CO<sub>2</sub> emission maps represent the correlation between the CO<sub>2</sub> emission rate over the normalized engine speed and power for engine types with similar technology, e. g. fuel type, combustion process (SI, CI), fuel mixture formation (carburetor or fuel injection), air supply (turbo charger or naturally aspirated engine). Regardless of manufacturer and / or vehicle models, the CO<sub>2</sub> emission behavior of similar engine technologies hardly differs in terms of efficiency and consequently CO<sub>2</sub> emissions. Variations of less than 5% for CO<sub>2</sub> emissions and fuel consumption of different engines with similar technology are reported [4.11]. Accordingly, the error in power interpolation based on generic CO<sub>2</sub> emission maps varies in this range. The generic CO<sub>2</sub> emission maps are obtained by means of emission measurements on engine test benches. Opposed to transient vehicle emission measurements, in steady-state engine measurements on engine test benches the variable time shift between engine power- and emission signal is not disturbing the time alignment of the signals, resulting in a high accuracy of engine power, speed and emission assignment in the generic emission maps. So, if one of those three parameters is not available - here, the engine power signal during the on-board measurements -, it can be derived from the generic CO<sub>2</sub> maps by means of interpolation routines, see [4.14]. In this case, PHEM calculates the required second-by-second engine power value for each CO<sub>2</sub>- / speed value gained from the measurement. In PHEM, this methodology has been implemented since 2017 and various technology-specific generic CO<sub>2</sub> emission maps are available. Basic generic CO<sub>2</sub> emission maps were derived from CO<sub>2</sub> emission data gained in a cooperation project of IVT / TU Graz and Ricardo-AEA Ltd. accomplished for the European Commission [4.15].

---

Figure 4.4 shows an example of the schematic engine power interpolation process based on generic CO<sub>2</sub> emission maps and on-board CO<sub>2</sub> emission- and engine speed data.

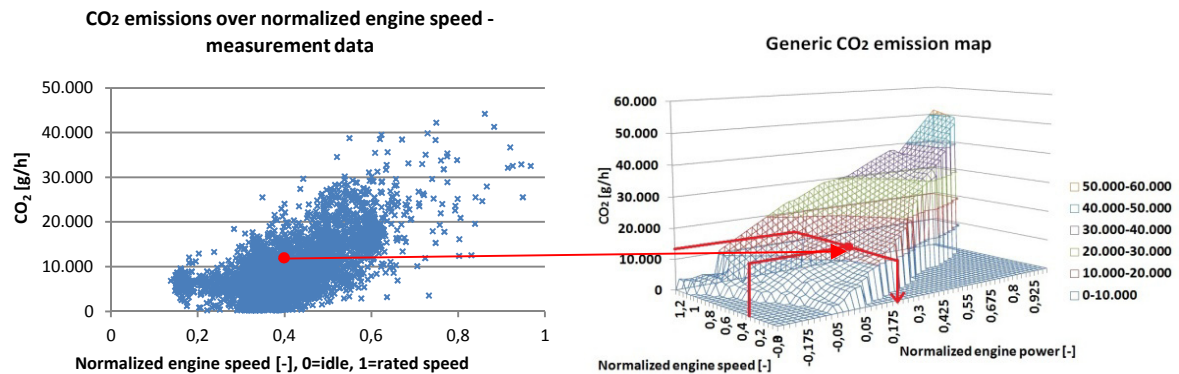


**Figure 4.4:** Second-by-second engine power calculation scheme based on generic CO<sub>2</sub> emission maps.

Based on the second-by-second engine power data, PHEM generates emission maps for exhaust gas components of any type that are measured modally. PHEM assigns emission values to normalized engine power and engine speed values. If no emission values from the measurements are available for specific points in the map grid, PHEM inter-/ extrapolates emission values for this field from adjacent fields. This methodology is applied for the emission map creation based on on-board- and dynamometer emission measurement data gained within this work, see chapter 6.1.

In the passenger car and light-duty vehicle sector, PHEM calculates the second-by-second engine power for the emission map creation by using either the generic CO<sub>2</sub> method (as far as no power signal from the measurement is available – e. g. in PEMS trips) or by calculating the total driving resistance force acting on the vehicle on the basis of vehicle specific driving resistance parameters. Hereby, it is also possible to get the required second-by-second engine power information, as the driving resistance force and the engine power demand depend on each other directly. Driving resistance parameters can be determined quite precisely for chassis dynamometer tests in the passenger car and light-duty vehicle sector, so this methodology is considered as suitable there. In the field of on-board tests, however, only approximate information on driving resistance values during an on-board trip are available. Especially for motorcycles the estimation of on-road driving resistance parameters is partly difficult; see also Chapter 6.2.4 [4.11]. The simulation of modal exhaust emissions with PHEM – and finally also kilometer-related emission values for any type of driving cycle –, however, is generally carried out by determining the second-by-second engine power demand that is necessary to overcome the driving resistance forces during the cycle / trip for each second. Then, the second-by-second emission rate is derived from the respective emission maps for each time step. This methodology is applied for the calculation of motorcycle emission factors in the later course of this study, see Chapter 6.4. The longitudinal dynamic approach for the determination of the vehicles engine power via driving resistance parameters is briefly introduced below.

Emission Map Creation via Longitudinal Vehicle Dynamics

During an on-board trip on the road, various forces act on a motorcycle. These include the air resistance, rolling resistance, road gradient and the acceleration forces supplemented by the additional power required to overcome transmission losses and the power demand required by auxiliary devices. Figure 4.5 shows schematically the relevant driving resistance forces having an effect on the required power demand of a motorcycle.

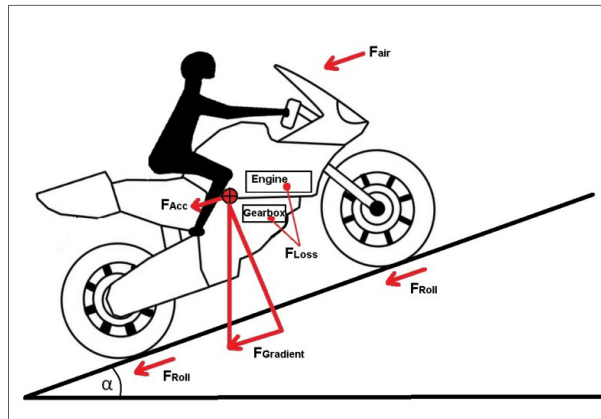


**Figure 4.5:** Resistance forces affecting a moving motorcycle.

The total driving resistance force is the sum of all individual driving resistance forces acting on the vehicle and it is calculated according to equation 4.1:

$$F_{Total} = F_{Air\ resistance} + F_{Rolling\ resistance} + F_{Acceleration} + F_{Road\ gradient} + F_{Losses,\ Powertrain} \quad (4.1)$$

Where

- $F_{Total}$  is the sum of all relevant driving resistance forces having an effect on the vehicle in [N],
- $F_{Air\ resistance}$  is the force to overcome the air resistance in [N],
- $F_{Rolling\ resistance}$  is the force to overcome rolling resistance in [N],
- $F_{Acceleration}$  is the force to overcome the acceleration resistance in [N],
- $F_{Road\ gradient}$  is the force to overcome the road gradient in [N],
- $F_{Losses,\ powertrain}$  is the force to overcome resistance in the power train, e. g. gearbox, bearings in [N].

Herein, the air resistance force is primarily determined by the design of the motorcycle and the drivers shape and it is characterized by the projected frontal area of the vehicle  $A_f$  and the aerodynamic drag coefficient  $c_d$ . The air resistance force increases with the square of the vehicle's speed  $v$  according to equation 4.2:

$$F_{Air\ resistance} = C_d \cdot A_f \cdot \frac{\rho_{Air}}{2} \cdot v^2 \quad (4.2)$$

Where

- $c_d$  is the aerodynamic drag coefficient [-],  
 $A_f$  is the projected frontal area of the vehicle and driver [m<sup>2</sup>],  
 $\rho_{Air}$  is the air density  $\left[\frac{kg}{m^3}\right]$ ,  
 $v$  is the vehicle speed  $\left[\frac{m}{s}\right]$ .

The rolling resistance force is primarily determined by constructive characteristics of the tire. These include, among others, the tire design, the rubber composition, the profile shape and particularly the tire pressure. The rolling resistance coefficient  $f_r$  comprises before-mentioned characteristics. In addition, the road surface affects the rolling resistance force - especially in unpaved terrain, the rolling resistance force can be much higher than on asphalted roads [2.2]. The vehicle mass influences the rolling resistance force approximately linearly. The rolling resistance force is calculated according to equation 4.3:

$$F_{Rolling\ resistance} = m_{total} \cdot g \cdot f_r \quad (4.3)$$

Where

- $m_{total}$  is the total vehicle mass including driver and payload [kg],  
 $g$  is the gravity constant  $\left[\frac{m}{s^2}\right]$ ,  
 $f_r$  is the rolling resistance coefficient [-].

The acceleration force is determined by the total vehicle mass  $m_{total}$ , the equivalent mass for the inertia of rotational accelerated components  $m_{rot}$  – particularly tires and gear components – and the vehicle acceleration  $a$ , see equation 4.4. The equivalent mass for the inertia of rotational parts can be calculated from the inertia and transmission ratios and has to be determined for each vehicle type in PHEM applications individually. If available, also the rotational inertia of tires, transmission and engine can be provided as input data for PHEM.

$$F_{Acceleration} = (m_{Vehicle} + m_{Rot}) \cdot a \quad (4.4)$$

Where

- $m_{rot}$  is the equivalent mass for the inertia of rotational accelerated components [kg],  
 $a$  is the vehicle acceleration  $\left[\frac{m}{s^2}\right]$ .

The resistance force to overcome the road gradient is determined by the total vehicle mass  $m_{total}$  and the sine of the road gradient  $\alpha$ . It is calculated according to equation 4.5:

$$F_{Road\ gradient} = m_{Vehicle} \cdot g \cdot \sin(\alpha) \quad (4.5)$$

Where

- $\alpha$  is the road gradient [°].

Depending on the available information on the transmission system, the losses in the powertrain can be calculated individually for each vehicle type and engine/-transmission configuration as a function of engine speed, individual gear ratios and engine power. However, one can also make an estimation based on the transmission efficiency as indicated by the manufacturer or according to generic data.

Provided that the aforementioned vehicle-specific driving resistance parameters and the speed-time course of a driving cycle or real-world trip including road gradient information are present, the longitudinal dynamic approach can be used to calculate the vehicle's second-by-second power requirement. It should already be noted at this point that some driving resistance parameters might vary during an on-board trip. In particular, the air resistance coefficient is difficult to estimate in the field of motorcycles. The air resistance parameter changes depending on the drivers position (driver sitting or lying – it has also effect on the frontal area of the vehicle), wind conditions and air density variations due to altitude differences during a trip. In addition, different road surfaces may lead to varying rolling resistance values, which also leads to differing power requirements during a trip. In particular, reliable information on the road gradient of an on-board trip are relevant for the engine power calculation. However, the road gradient is partly difficult to detect via GPS devices or topography material due to strong changes in the road gradient within short road sections (e. g. narrow road curves on mountainous roads). In Chapter 6.2.4 a parameter variation of relevant driving resistance coefficients is carried out and the influence on the simulation routine in PHEM is examined.

#### 4.2.1.2 Emission Simulation

Based on the second-by-second engine power, engine speed, gear information and specific emission maps, the second-by-second emissions for any driving cycle respectively trip can be calculated. Therefore, PHEM calculates the corresponding emission value for each time step from the characteristic emission map. In the case of engine load points, where no emission data are assigned to in the emission maps, PHEM interpolates or extrapolates the values from adjacent fields in the emission map. In combination with an implemented gear-shift model, different driving styles and gear-shift strategies can be simulated - conservative driving to sporty driving. Corresponding gear-shift points can be specified individually or the gear-shift strategy can be selected by PHEM. In the latter case, the PHEM gear-shift model selects the appropriate gear based on the power requirements within the current driving situation - e. g. in the case of accelerations or positive road gradient sections, PHEM shifts to a lower gear to provide adequate torque at the drive axle. In the case of cruising phases, a higher gear is selected to minimize the fuel consumption and the emissions. If no gear-shift information is available for the driving cycles that are to be simulated with PHEM - as for example the HBEFA / TREMOD driving cycles - the use of the PHEM gear-shift model is obligatory. The PHEM version used in the study at hand is the version 12.0.1. PHEM offers also correction functions for influences of cycle dynamics on the emission levels and a simulation tool for the exhaust gas catalyst. However, these functions have not been used in the work for motorcycles of this thesis.

---

**4.2.2. HBEFA (Handbook Emission Factors for Road Transport)**

The “Handbook Emission Factors for Road Transport” is a widely accepted emissions database in Europe that represents a basis for various environment-related applications in the road transport sector [4.16]. HBEFA allows the calculation of greenhouse gases and pollutant emissions in a high degree of differentiation. Calculations in the field of small-scale issues, e. g. in the context of air pollution control plans, up to emission inventory tasks can be carried out by using HBEFA data sets. The HBEFA was developed on behalf of national environmental authorities of Germany, Austria and Switzerland in the 1990s. Up to now, numerous other countries, among others, France, Sweden, Norway and their national authorities are involved in the continuous development and extension of HBEFA [4.17]. HBEFA provides kilometer-specific information on almost all relevant air pollutant components, climate gases, fuel and energy consumption for almost all vehicle categories in a very high degree of differentiation. The classification structure includes, among others, different vehicle categories, vehicle segments and sub-segments, different road categories, local areas and emission types (e. g. exhaust and evaporative emissions), pollutant components and a very detailed assignment of emission values to driving situations and driving conditions. Other differentiation criteria are defined, such as emission factors for different road gradient classes or also vehicle age-related correction functions for the emission factors that describe the deterioration characteristics over time.

For example, the kilometer-related CO hot emission factors for motorway operation for the motorcycle segment equipped with petrol 4-stroke (4S) combustion engines, displacement class > 750 cm<sup>3</sup> and Euro 3 emission standard can be pointed out from HBEFA. Figure 4.6 gives an overview of the most relevant differentiation criteria in HBEFA for the motorcycle segment. The HBEFA version used in the study at hand is the version HBEFA 3.2. In the course of the preparation of this study the version HBEFA 3.3 was published. This version mainly includes revised emission factors for nitrogen oxide emissions in the passenger car sector. All other emission factors of other vehicle categories were not adjusted in this update.

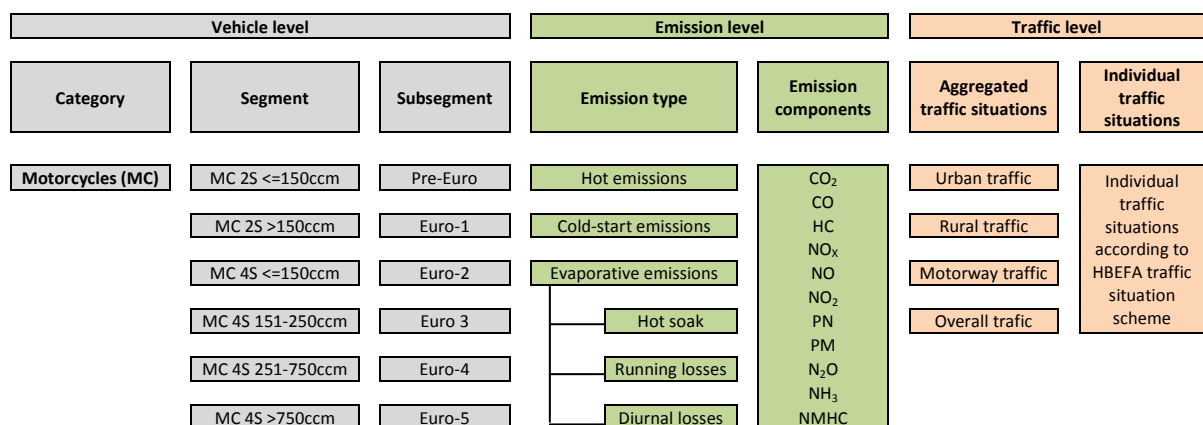


**Figure 4.6:** Differentiation criteria in the motorcycle segment in HBEFA.

In HBEFA, a system has been developed, which maps typical real-world motorcycle driving in so-called traffic situations. A traffic situation is defined as a vehicle speed profile over time. In total, there are 276 traffic situations defined in HBEFA for each vehicle category, which were derived from

extensive real-world driving investigations [4.17]. The traffic situations reflect common driving in different local areas and on different road categories taking into account varying traffic conditions (defined in HBEFA as “level of services”) and different speed limits. A total of four “levels of services” have been defined in HBEFA (version 3.2) to reflect the different traffic conditions on the road. They are classified as “stop + go”, “saturated”, “heavy” and “free flow” traffic. The exact definitions of the level of services in HBEFA are indicated in Table 4.1.

**Table 4.1:** Definition of traffic conditions in TREMOD and HBEFA – Levels of services [4.18].

Level of service	Definition
Free flow	Free flowing conditions, low and steady traffic flow. Constant and quite high speed. Indicative speeds: 90-120 km/h on motorways, 45-60 km/h on a road with speed limit of 50 km/h.
Heavy	Free flow conditions with heavy traffic, fairly constant speed, indicative speeds: 70-90 km/h on motorways, 30-45 km/h on a road with speed limit of 50 km/h.
Saturated	Unsteady flow, saturated traffic. Variable intermediate speeds, with possible stops. Indicative speeds: 30-70 km/h on motorways, 15-30 km/h on a road with speed limit of 50 km/h.
Stop + go	Stop and go. Heavily congested flow, stop and go or gridlock. Variable and low speed and stops. Indicative speeds: 5-30 km/h on motorways, 5-15 km/h on a road with speed limit of 50 km/h.

Each traffic situation has an emission factor assigned to it indicated in g / km (respectively fuel or energy consumption factor) for each exhaust gas component. Figure 4.7 shows the schematic structure of the traffic situation scheme in HBEFA.

		Speed limit [km/h]												
Area	Road type	Level of service	30	40	50	60	70	80	90	100	110	120	130	> 130
Rural	Motorway-Nat.	4												
	Semi-Motorway	4												
	Trunk Road / Primary Nat.	4												
	Distributor / Secondary	4												
	Distributor / Secondary (sinuous)	4												
	Local / Collector	4												
	Local / Collector (sinuous)	4												
	Access-residential	4												
Urban	Motorway-Nat.	4												
	Motorway-City	4												
	Trunk Road / Primary Nat.	4												
	Trunk Road / Primary-City	4												
	Distributor / Secondary	4												
	Local / Collector	4												
	Access-residential	4												
<b>Motorway</b>														
<b>Rural</b>														
<b>Urban</b>														

**Figure 4.7:** Traffic situation scheme according to HBEFA [4.18].

Due to the high degree of differentiation on the vehicle, emission and traffic level, HBEFA permits emission-related queries for almost any possible road traffic cases. Emission factors of present and older vehicle concepts are based on measurements and – in the case of passenger cars, light and heavy-duty vehicles – on PHEM emission factor simulations. However, HBEFA also contains emission data sets on future emission standards (in the field of motorcycles namely Euro 4 and Euro 5 concepts) based on assumptions derived from emission factor developments in previous emission standards. Current motorcycle emission factors that are implemented in HBEFA version 3.2 are, among others, derived from a study carried out by RWTÜV Fahrzeug GmbH in the framework of a project of the German Environmental Agency in 2003 [4.19].

Subsequently, exemplary CO emission factors for the motorcycle vehicle segment that is relevant in the further course of this study (motorcycle, 4-Stroke, Euro 3, > 750 cm<sup>3</sup>) are contrasted with previous- (Euro 1, Euro 2) and future (Euro 4, Euro 5) emission standards, see Figure 4.8. The presentation contains the specific CO emission values for each traffic situation linked with the average cycle speed of the underlying traffic situations.

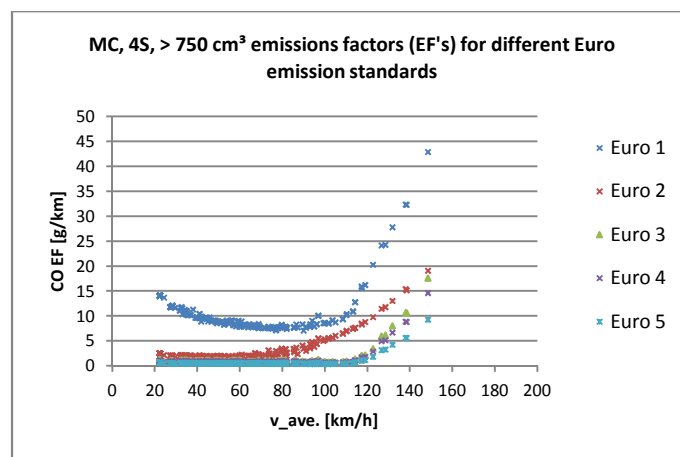


**Figure 4.8:** Motorcycle CO emission factors for different emission standards according to HBEFA 3.2.

Figure 4.8 indicates that the general CO emission factors decrease with advancing emission levels. Technical effort is necessary, in order to fulfill the legislative prescribed emission limit values (e. g. due to catalyst systems, engine management). Moreover, figure 4.8 shows that the individual CO emission factors increase towards higher average speeds for all emission standards. This correlation can be explained by the quadratically increasing engine power demand at higher vehicle speeds resulting in proportionately increasing fuel injection rates and CO emissions – e. g. due to rich fuel / air mixtures in high engine load ranges as commonly applied in the motorcycle segment, see chapter 2.1.1.

#### 4.2.3 TREMOD (Transport Emission Model)

TREMOD is a macroscopic emission calculation model that is used to calculate vehicle fleet emissions in a high degree of differentiation in Germany. It reflects all modes of transport, namely, road, air, rail and inland waterway transport. Retrospective emission and energy calculations are possible back

to the year 1960 - future trend scenarios are implemented up to the year 2030 in the TREMOD version applied in this study (version 5.63). TREMOD is used, among others, by German Federal Ministries, authorities, the German car manufacturer association (VDA) and the Deutsche Bahn AG in the field of environment-related issues with regard to emissions and energy consumption in Germany [4.20]. The development of TREMOD was initiated in the 1990's on behalf of the German Federal Environmental Agency (UBA). The model is continuously adjusted and extended to new vehicle concepts, traffic developments and emission data sets. The road traffic sector is covered in great detail in TREMOD due to the importance of this sector contrasted with total transport emissions in Germany [4.21].

The TREMOD road traffic module contains highly differentiated information on annual traffic, emissions, fuel and energy consumption and the vehicle fleet composition of almost all relevant road traffic participants in Germany. The differentiation structure of the vehicle categories, local areas, road types and traffic situations is similar to the HBEFA classification; however, it is not identical. The TREMOD road traffic module consists basically of three sub-modules that link relevant parameters for the hot emission calculation together, namely annual traffic data, vehicle fleet composition and development and hot emission factors. In the chapters 4.2.3.1 and 4.2.3.2 the vehicle fleet sub-module and the traffic data sub-module in TREMOD are described in detail. Herein, the underlying data sources are emphasized and the status of the motorcycle input database is indicated. The emission sub-module consists essentially of the emission factors of HBEFA, which are adopted either directly or weighted by traffic in TREMOD. Since only the road traffic module is applied within the framework of this study at hand, all further remarks to TREMOD in this study refer to the road traffic module. Figure 4.9 shows the schematic structure of the road traffic module in TREMOD.

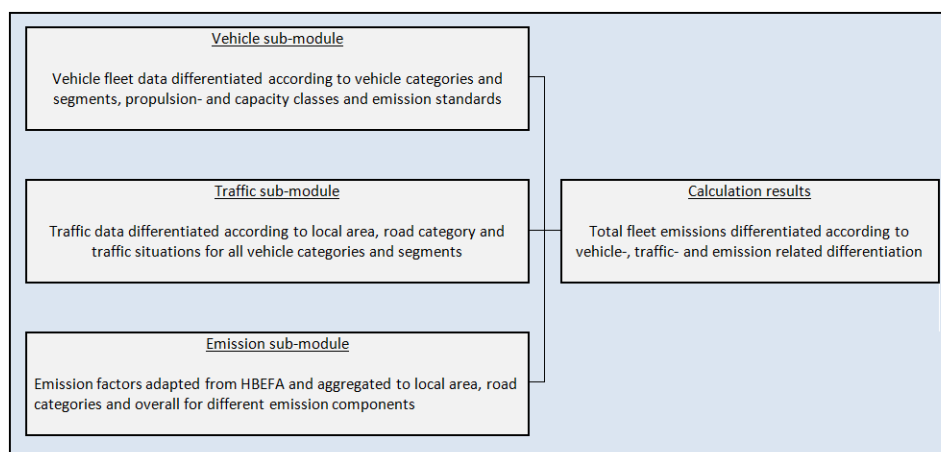


**Figure 4.9:** Schematic structure and function of TREMOD for the road traffic sector [4.22] [4.23].

#### 4.2.3.1 Vehicle Fleet Data

Information on vehicle fleet data and new vehicle registrations are taken from statistics of the German Federal Motor Transport Authority (KBA) and these data are implemented in TREMOD annually. The prediction of the prospective vehicle fleet development is based on assumptions on new registrations for new vehicle types and, in addition, based on survival curves for vehicle types that are currently on the market. Survival curves describe the vehicle age dependent percentage

decrease of individual vehicle types within the vehicle fleet over a defined period. Based on such survival curves, the proportion of those vehicles that are eliminated from the market due to age can be determined. Weighting functions are applied in TREMOD, which consider the fact that vehicles of different types, displacement classes and age have different annual driving performances, both, in total and differentiated according to local areas and road categories. Annual vehicle statistics, as well as adjustments in the vehicle stock structure are adapted in TREMOD continuously by the IFEU Institute (Institute for Energy and Environmental Research, Heidelberg GmbH) [4.24].

#### 4.2.3.2 Traffic Data

Predictions on road traffic-related emissions require robust information on the mileage performed by all road users in a specified time period in a high degree of differentiation. In TREMOD annual traffic data are differentiated according to local area – this includes urban, rural and motorway areas. Rural traffic is further differentiated according to road types, namely trunk roads, distributor roads, local roads, residential roads and motorways. Motorways are subdivided according to the number of lanes - “<= 5 lanes”- and “>= 6 lanes” motorway classes are defined in TREMOD. Urban traffic is considered in total, no further differentiation with regard to road types is carried out here. TREMOD assigns traffic data to every vehicle segment (e. g “motorcycle, 4S, Euro 3, >750 cm<sup>3</sup>) and, additionally, to every road category and aggregated local area [4.22].

Finally, traffic shares are assigned to traffic situations that are adopted from HBEFA. However, it should be noted that not all 276 traffic situations are adopted in the motorcycle segment in TREMOD. In total 28 traffic situations are implemented in TREMOD that reflect motorcycle driving in Germany. These 28 traffic situations are correlated with traffic shares. Figure 4.10 shows the structure of the traffic differentiation scheme as applied for motorcycles in TREMOD.

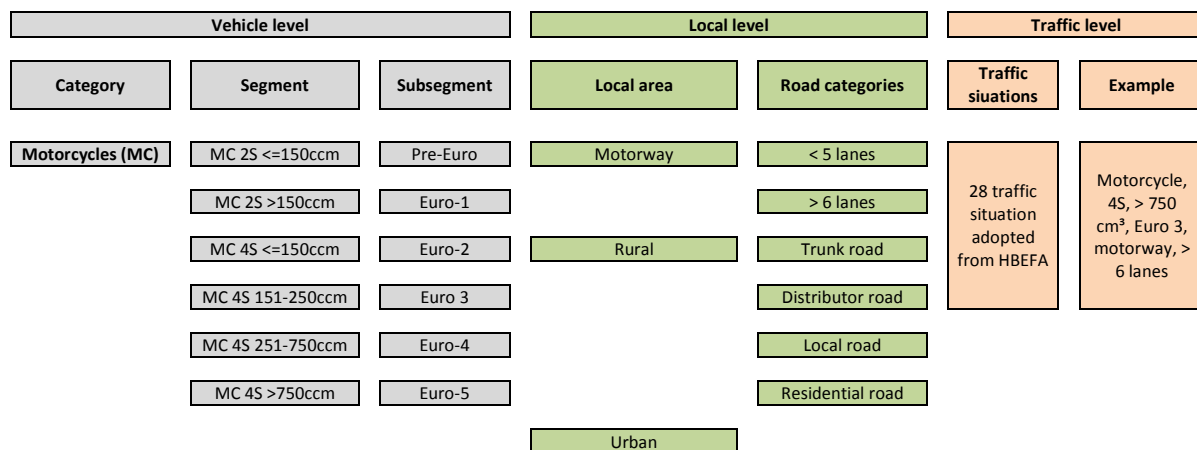


**Figure 4.10:** Traffic differentiation scheme for motorcycles in TREMOD.

Data on driving performance are generated within the framework of research projects or are calculated on the basis of statistical approaches. Relevant data sources in this context are, among others, fixed traffic counting stations that provide traffic data continuously. The Federal Highway

Research Institute (BAST) operates traffic counting stations on motorways and trunk roads on behalf of the Federal Ministry of Transport and analyzes and publishes recorded data annually [4.25]. Herein, a distinction is made between heavy and light-duty traffic - powered two-wheelers traffic is recorded as a whole. The counting system currently consists of 1744 counting stations of which 929 are installed on motorways and 815 on trunk roads in Germany. Additionally, extended traffic countings take place about every five years in Germany, in which traffic data are collected manually by qualified staff at motorways and trunk roads. Six vehicle categories, including powered two-wheelers, are recorded [4.26]. The results are collected and analyzed by the Federal Highway Research Institute, where the results are structured and published for each section of the German highway grid. The survey is carried out periodically in order to assess the traffic development over time. The overall driving performance is concluded by means of calculation and extrapolation procedures. However, above-mentioned methods cover just certain aggregated vehicle categories and road types and are based to a large extent on statistical procedures. For this reason, extensive driving performance surveys are initiated about every 10 years in Germany, in which traffic data for all relevant vehicle categories are collected in a high degree of differentiation. The concept consists of two distinct methodologies. On the one hand, vehicle owners are noticed to be part of a survey and are requested to record and communicate tachometer data at specific intervals. The second part consists of mobile camera-based road traffic counting on nearly all road types on different weekdays that are statistically determined. The overall results are obtained by combining the results from the owner surveys and counting stations by appropriate statistical methods onto the total road grid and the entire vehicle fleet [4.27]. The last extensive driving performance surveys were performed in 2002 and 2014. The combination of above-mentioned methodologies provide differentiated driving performance data for the description of the traffic structure in Germany that is used – besides emission-related issues - in the field of road and traffic planning and road safety analyzes. Complementary studies such as market analyses from the German Institute of Economic Research (DIW) and market monitoring performed by the Federal Office for Freight Transport (BAG) are taken into account for traffic data validations and adjustments in TREMOD [4.28] [4.29]. The assignment of driving performance data to traffic situations and longitudinal road gradients in TREMOD is based on driving performance investigations by Heusch-Boesefeldt from 1993 [4.30]. These results are still used to link annual traffic shares with the HBEFA / TREMOD traffic situation scheme and additionally with road sections with longitudinal road gradients.

#### **4.2.4 COPERT**

COPERT is an emission calculation model in the road transport sector that is widely used within the European Union but also in several non-European countries [4.7]. It is used for national emission reporting obligations (e. g. in the framework of the UNFCCC, the UN-ECE LRTAP Convention and to the European Union) and for answering emission-specific issues at national, regional and local level. The development has been carried out by the Laboratory of Applied Thermodynamics (LAT) of the Aristotle University of Thessaloniki and by EMISIA S. A., a spin-off company of LAT. The development has been initiated by the European Environment Agency (EEA) in the framework of the European Topic Center on Air Pollution and Climate Change Mitigation (ETC / ACM) [4.31]. Additionally, the European Commission's Joint Research Center (JRC) is involved in the scientific development process

---

of the model. COPERT is freely accessible and used by a large number of research institutions and scientists worldwide, see figure 4.11

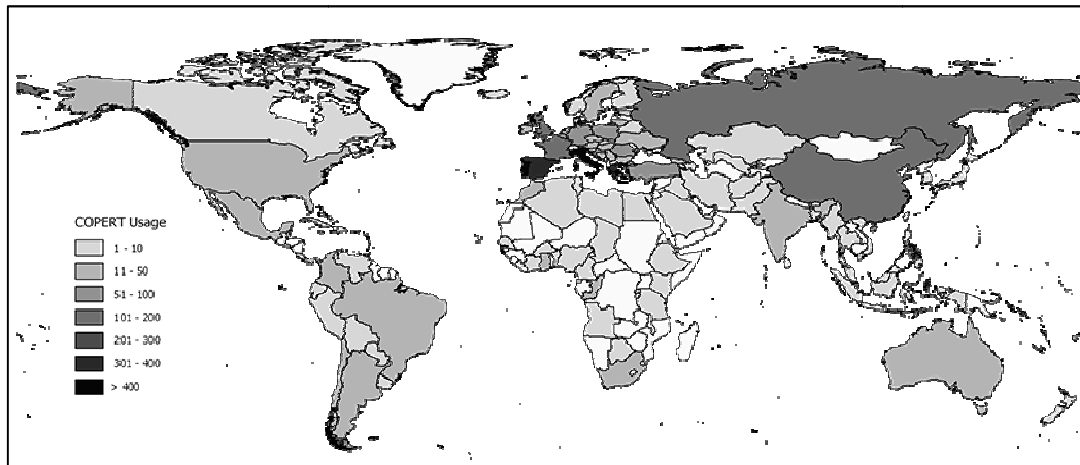


**Figure 4.11:** Worldwide distribution of the COPERT model and number of users by country [4.32].

The development of the first program versions goes back to the 1990's - meanwhile the version 5.2.2 (February 2019) is available. COPERT is programmed for windows applications, which makes it available to a wide circle of users [4.33]. The calculation of future trend scenarios is carried out with the vehicle fleet projection and scenario evaluation software Sibyl.

COPERT maps the road traffic situation in the respective countries in a high degree of differentiation. This includes, on the one hand, a classification of road users according to, among others, vehicle categories (e. g. passenger cars, light and heavy-duty vehicles, two-wheelers etc.), emission standards and propulsion types. On the other hand a distinction of emission types (e. g. hot-emissions, cold-start emissions, evaporative emissions and emissions resulting from tire and brake wear) and different emission components (e. g. hydrocarbons, carbon dioxide etc.) is made. The country-specific emissions are calculated by linking the relevant input parameters, namely emission factors, vehicle-specific traffic activity data and vehicle stock information together. The emission factors in COPERT are partly adopted from HBEFA or are derived from specific research projects; traffic activity data are available for each EU country and can be accessed via the EMISIA website. Traffic activity data have been derived from EU-wide driving performance projects. COPERT contains information on the amount of evaporative emissions in the field of powered two-wheelers differentiated according to diurnal losses, running losses and hot soak emissions. These data sets are implemented in HBEFA and are adopted for the emission trend scenario calculations in the later course of this work (Chapter 7.4).

## 5. Emission Measurement Program – Approach

Within the framework of this study a conventional motorcycle (according to EC vehicle category L3e-A3) of the TREMOD vehicle segment “motorcycle, 4S (four stroke principle), > 750 cm<sup>3</sup>, Euro 3, first registration year 2015” was subject to an intensive exhaust gas emission measurement campaign. The measurements were carried out by TU Graz, IVT, on behalf of the German Federal Highway Research Institute (BASt) as part of a joint research project in the years 2016 - 2017. In the context of this joint research project, several powered two-wheelers were measured and evaluated regarding their emission behavior and test procedures in this vehicle category for future measurement campaigns were derived. The project was completed in 2017 and all relevant findings were published in a research report [4.11]. As part of my work at BASt, I was widely involved in elaborating the measurement program, the selection of the test vehicles and the interpretation of the results. All investigations and further emission simulations within this doctoral thesis at hand are based on the measurement data gained from the TU Graz – BASt research project. Relevant information regarding the measurement program (e. g. test vehicle specifications, test routes and emission results) that contribute to the objective of this thesis, are presented below. The data sets obtained within the TU Graz – BASt research project have also been used as a basis in other scientific publications, among others in [5.1]. However, other work priorities have been set and were examined therein compared to this doctoral thesis at hand.

A total of three measurement programs were carried out, which formed the data basis for subsequent evaluations and simulations in this study (chapter 6 and chapter 7). Emission measurements using a portable emission measurement system (PEMS) were performed on public roads in order to gain information on the real world emission behavior in this vehicle category and to assess the driving dynamics by application of mobile emission measurement technology in comparison to the TREMOD motorcycle traffic situations (TS) and the legislative type approval testing cycle WMTC, see chapter 5.1. This procedure was intended to evaluate to what extent on-board measurement trips are suitable for future emission measurement campaigns in the field of motorcycles for the collection of emissions data. On-board emission measurements take into account vehicle operation points that partly cannot be reflected on roller test benches due to measurement restrictions – e. g. slippage between the vehicle tires and the test bench in strong acceleration phases - but represent partly typical driving situations in this vehicle category. The regulated emission components CO and NO<sub>x</sub>, as well as the climate gas CO<sub>2</sub> and the nitrogen compounds NO and NO<sub>2</sub> were measured within this program. Furthermore, emission measurements were carried out on an exhaust gas test bench in several driving cycles – the type approval cycle (WMTC) as well as cycles that were particularly designed for real-world emission data generation in the passenger car sector (ERMES, CADC - Common Artemis Driving Cycle) and real-world motorcycle driving cycles (RDC1, RDC2). Besides the emission components CO, CO<sub>2</sub> and NO<sub>x</sub>, HC emissions were also recorded in this measurement program (chapter 5.2). In-depth investigations of non-regulated pollutant components in the exhaust gas of motorcycles were carried out by using a FTIR-analyzer within the stationary measurement program, see chapter 5.3. Initial information on the relevance of these substances in the exhaust gas of motorcycles were collected. The emission measurement data gained in this program were intended to be used as input data sets for the creation of emission maps by using the PHEM model of TU Graz, see chapter 6.

## 5.1 On-board Emission Measurement Program

Within the scope of the measurement program, motorcycle exhaust gas measurements were carried out by means of a mobile exhaust gas measurement device. Here, a PEMS system that is also applied in type approval certification purposes of passenger cars and light-duty vehicles within the framework of Real-Driving Emission legislation (RDE) was installed on a sports tourer motorcycle and the exhaust gas emissions were measured on different test routes in Graz City and surroundings [5.2] [4.11]. Since motorcycles are not subject to legislative actions by means of on-board emission measurements, the installation of a PEMS-system on a conventional motorcycle represents partly a novel scientific approach - not least due to constructional- and traffic safety aspects that had to be taken into account. The test vehicle and the measurement setup is presented in chapters 5.1.1 and 5.1.2; the route profiles with regard to topographic properties are indicated in chapter 5.1.3. The on-board emission measurement trips were evaluated with regard to relevant driving dynamic parameters in order to obtain a comparison to the TREMOD motorcycle traffic situations, see chapter 5.1.4. The driving dynamic investigations are predominately based on prescriptions of the current RDE evaluation routines. Finally, the on-board emission measurement results are presented in chapter 5.1.5.

### 5.1.1. Test Vehicle

A high-performance motorcycle with approx. 800 cm<sup>3</sup> displacement and 66 kW rated engine power was chosen as a test vehicle and acquired for the measurement program in this study. The choice was based on the representativeness within the approval statistics in the German motorcycle fleet in order to reflect a market-relevant vehicle and against the background of a high possible payload – only high-capacity and powerful machines were taken into considerations that are approved to carry extra weights like the PEMS system. At the beginning of the test program, the test vehicle had an odometer mileage of approx. 5000 km – so, possible starting effects as they appear in new vehicles as a consequence of tight fittings and bearings resulting in partly increased fuel consumption- and emission rates could be excluded. Table 5.1 lists the relevant technical specifications that are attributed to the test vehicle.

**Table 5.1:** Technical specifications of the test vehicle

<b>Specification</b>	
Date of first registration	2015
Mileage (Beginning of test program)	Approx. 5000 km
Engine design	Water-cooled two-cylinder four-stroke in-line engine, four valves per cylinder, two overhead camshafts
Displacement	798 cm <sup>3</sup>
Rated Engine Power	66 kW at 8000 rpm
Emission standard	Euro 3
Exhaust gas after treatment system	Three-way catalytic converter with lambda control

### 5.1.2. On-board Emission Measurement Equipment - Specifications

The test vehicle was equipped with an “AVL M.O.V.E. Gas PEMS iS” device for the on-board emission measurements [5.3]. The measuring instrument meets the requirements to determine the emissions of light duty-vehicles – EC vehicle classes M1 and N1 - according to Regulation EC 646/2016 in the framework of RDE legislation. Developed for on-board emission measurement applications, the “AVL M.O.V.E. Gas PEMS iS” is able to determine concentrations of NO / NO<sub>2</sub> and CO / CO<sub>2</sub> in the exhaust gas of petrol and diesel vehicles under real driving conditions. The measuring system includes a non-dispersive ultraviolet analyzer (UV) for the simultaneous measurement of NO and NO<sub>2</sub> concentrations and cumulative NO<sub>x</sub>, as well as a non-dispersive infrared analyzer (NDIR) for the determination of the CO and CO<sub>2</sub> concentrations in the exhaust gas. The exhaust gases were sampled between the catalytic converter and the rear muffler. The device has its own power supply and an energy management via accumulators and a control unit, which offers capacity for several hours of test-driving. Carrying of calibrating gas is omitted due to very low drift values, which makes the system suitable for use even in small vehicles - detailed specifications can be found in the AVL data factsheet [5.3]. The PEMS unit was mounted using a special frame construction that was individually built for the test vehicle in the area of the pillion seat, see figure 5.1.



**Figure 5.1:** Experimental setup of the PEMS device on the test vehicle [4.11].

The conversion of exhaust gas concentrations into mass emissions requires accurate exhaust gas mass flow data. The exhaust gas mass flow was recorded modally by means of an exhaust flow meter (EFM) developed by AVL – “AVL M.O.V.E. EFM” [5.4] [4.11]. The system is based on the principle of Pitot, a differential pressure flow measurement. The continuous measurement of the exhaust gas mass flow is a decisive criterion for fulfilling the RDE regulations, which is complied with the “AVL M.O.V.E. EFM” in combination with the “AVL M.O.V.E. Gas PEMS iS” [5.5]. The EFM device consists of a tube that is connected to the tail pipe of the vehicle and which contains the pressure transducers. The signal is transmitted to a control unit with corresponding electronics via a connecting cable. The measuring principle prescribes stabilizing sections for smoothing the exhaust gas mass flow before- and behind the measuring sections, resulting in a comparatively high overall length of the EFM device (approx. 1,4 m). So, a transverse installation of the EFM behind the motorcycle above the number plate was carried out in order to meet measuring requirements while not impairing traffic safety aspects at the same time. The control unit was mounted inside the left luggage box of the motorcycle [4.11].

Additional measuring devices were installed in the test vehicle, which are briefly described as follows. The determination of the fuel consumption during the test drives was carried out with an “AVL PLU116H flow meter” [4.11]. There was an additional lambda meter for the determination of remaining oxygen in the exhaust gas installed collectively with the power supply unit inside the luggage boxes. A GPS-module was mounted at the rear of the vehicle that records the vehicle speed along with the geographical position in 1-Hz steps. Additionally, ambient air temperature and humidity was recorded. All measurement data were collected by means of an “AVL M.O.V.E. System Control Unit” which stored the recorded input data and performed the necessary data post processing [5.6] [4.11].

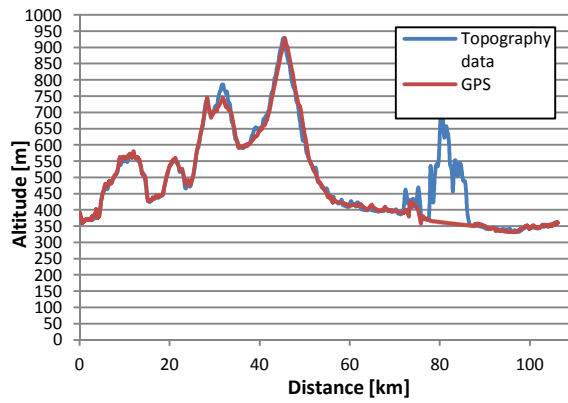
The total measurement setup weighs about 80 kg, which corresponds approx. to the weight of a pillion and/or additional luggage. Due to the transverse installation of the EFM and the side luggage boxes, the measurement equipment was rather protruding on both sides. However, the measurement configuration represents driving with a pillion and luggage in an adequate manner, even this is not a typical every-day driving situation in this vehicle category. The total vehicle weight including driver and equipment is about 350 kg [4.11].

### 5.1.3. Test Routes

Three test routes in Graz city and surroundings were chosen for the on-board measurement program. The test routes were selected so as to represent preferably realistic motorcycle driving, covering appropriate shares of urban, rural and motorway sections. Here, the test track requirements from the passenger car RDE legislation represent an approximate criterion. In addition, a curvy mountain road segment was selected to take into account ambitious motorcycle driving on rural roads. A total of three route profiles were chosen, that are named hereinafter according to geographical attributes of the routes, namely “Arzberg”, “Ries and “Gaberl”. Here, “Arzberg” and “Ries” demonstrate RDE-compliant test routes according to Regulation EU 427/2016 [5.7]. “Gaberl” reflects an ambitious test track for sporty driving on curvy extra-urban roads including a mountain pass and does not fulfill RDE track requirements, not least due to exceeding altitude requirements [4.11].

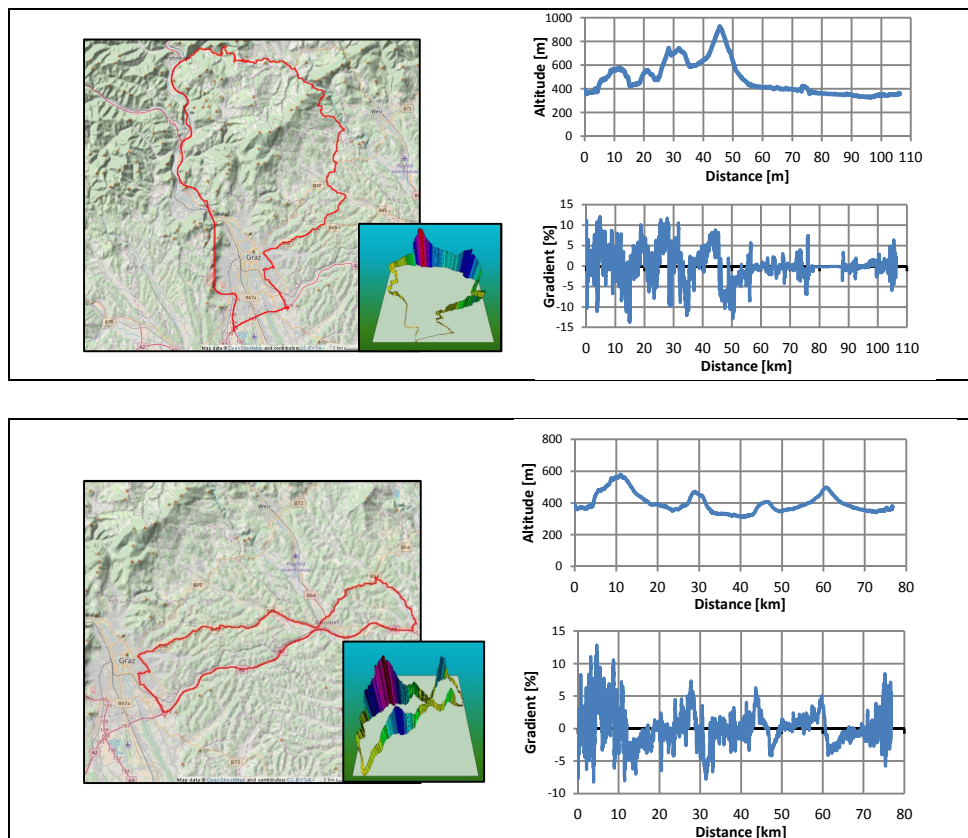
The route profiles and the vehicle speed were recorded via a GPS sensor mounted on the test vehicle. The altitude and the vehicle speed measurement data were checked regarding potential discrepancies – possible data gaps and relevant inconsistencies were corrected by interpolation routines. The obtained GPS-data were compared to topography data material in order to assess the reliability of the on-board GPS measurement setup. The GPS data sets formed the basis for the calculation of the road gradient of the test routes. Overall, there is a good correlation of the measured altitude GPS data and topographical data sets as demonstrated in the following figure 5.2 using the “Arzberg” route as an example. The topographical- and GPS data sources diverge at tunnel crossings, indicated here between km 75 and km 85 (“Plabutsch”-tunnel, west of Graz-city). Here, the topographical map material shows the elevation profile above the tunnel, whereas the GPS signal interrupts in consequence of no signal. In this segment, the missing data material was interpolated.

---



**Figure 5.2:** Comparison of measured GPS-altitude data and topography data for the “Arzberg”-Route.

The following illustrations demonstrate the route and altitude profiles of above-mentioned test tracks recorded by the GPS system installed on the test vehicle, see figures 5.3. Here, the road gradients of the test routes as well as a 3d-model of the total route profiles are pictured. The transformation of GPS data into route maps was carried out with the freely accessible online tool "GPX-viewer", which is based on map-material of “© OpenStreetMap contributors”, see Open Data Commons Open Database License (ODbL) [5.8] [5.9] [5.10]. The cartography in map tiles and documentation are licensed under the Creative Commons Attribution-ShareAlike 2.0 license (CC BY-SA) [5.11]. The 3d track presentation was carried out with the freely accessible online tool “GPX 3d viewer”, which generates a 3d route profile on the basis of altitude, latitude and longitude data [5.12].



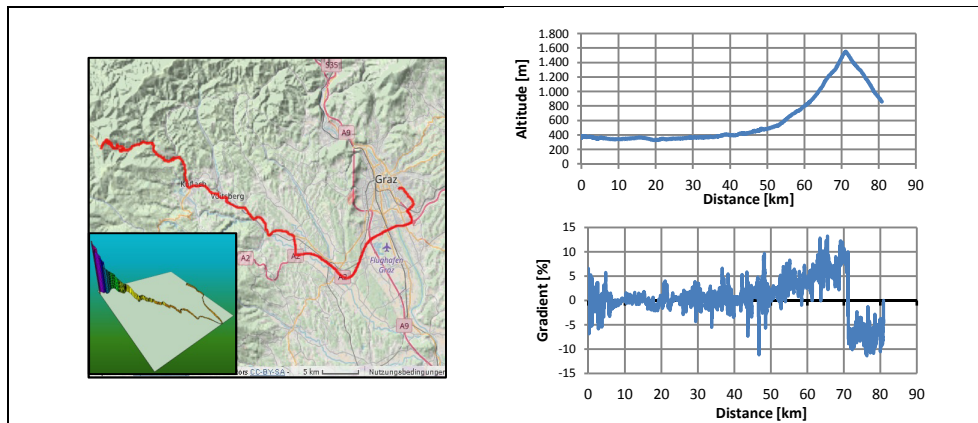


**Figure 5.3:** Route profiles “Arzberg” (top), “Ries” (middle) and „Gaberl” (bottom): maps including 3d-model, altitude profiles and road gradient characteristics.

“Arzberg” and “Ries” are both round courses that end at the start of the track (TU Graz), whereas “Gaberl” is a mountain pass track leading back to the start on the same roads – so, the route and road gradient profile of the return drive is the same. However, the mountain section of the “Gaberl” track was driven several times for emission data recording. Table 5.2 summarizes relevant track parameters of “Arzberg”, “Ries” and “Gaberl” routes.

**Table 5.2:** Relevant test route parameters

Track	“Arzberg”	“Ries”	“Gaberl”
Track length [km]	106,1	76,7	80,8
Max. height difference [m]	616	268	1218
Highest point [m a. s. l.]	929	578	1546
Lowest point [m a. s. l.]	313	310	328

#### 5.1.4 On-board Trip Dynamic Evaluation

The following investigations are intended to classify the driving dynamics of the on-board measurement trips carried out in this study compared to the TREMOD motorcycle traffic situations and the motorcycle type approval cycle WMTC. In this way, possible uncertainties and weaknesses in on-board emission recording with regard to common driving conditions in the motorcycle segment in future measurement programs should be revealed. It should be noted that the TREMOD traffic situations here are the 28 traffic situations as described in Chapter 4 that are considered as a reference for characterizing motorcycle traffic in Germany. The WMTC here was investigated for comparison purposes only in order to gain insight into the driving dynamics in the motorcycle type approval procedure and because this cycle was also used for emission measurements in the further course of this work. The influence of the measurement setup on the driving dynamics was investigated in detail. First, relevant dynamic parameters for the assessment of driving dynamics that also apply in the RDE type approval procedure are briefly introduced in chapter 5.1.4.1. In chapter 5.1.4.2 and 5.1.4.3 the results of the driving dynamic evaluations are presented in detail.

#### 5.1.4.1 Relevant Dynamic Parameters

The second-by-second vehicle speed signal (sampling rate of 1 Hz) represents the basis for the driving dynamic investigations. The speed signal was checked for incorrect values and implausibilities (e. g. tunnel crossings, see chapter 5.1.3.) and was, if necessary, corrected e. g. by interpolation methods. If no plausible correction routines were possible, these data sets were excluded from further considerations. Subsequently, relevant cycle parameters were calculated as follows [5.2].

The total trip distance was calculated according to equation 5.1.

$$d_i = \sum_{i=1}^{N_t} \frac{v_i}{3,6}, \quad i = 1 \text{ to } N_t \quad (5.1)$$

Where

- $d_i$  is the distance covered in time step  $i$  [ $m$ ],
- $v_i$  is the actual vehicle speed in time step  $i$  [ $\frac{km}{h}$ ],
- $N_t$  is the total number of samples.

The second-by-second vehicle acceleration was calculated as follows:

$$a_i = \frac{(v_{i+1} - v_{i-1})}{(2 \cdot 3,6)}, \quad i = 1 \text{ to } N_t \quad (5.2)$$

Where

- $a_i$  is the acceleration in time step  $i$  [ $\frac{m}{s^2}$ ], for  $i = 1: v_{i-1} = 0$ , for  $i = N_t: v_{i+1} = 0$ .

Only those second-by-second speed changes are defined as accelerations that show values of  $a_i \geq 0,1 \frac{m}{s^2}$ .

The average cycle speed is defined as the quotient of the total covered distance by the total cycle driving time. Here, one has to distinguish between the average cycle speed including stop shares and without considering stop phases, see equations 5.3 and 5.4 [5.2].

Average cycle speed including stops phases:

$$v_{i,ave.} = \frac{d_i}{T_i}, \quad i = 1 \text{ to } N_t \quad (5.3)$$

Where

- $v_{i,ave.}$  is the average cycle speed including stop phases,
- $T_i$  is the total cycle time up to time step  $i$  [ $s$ ].

Average cycle speed without stops phases:

$$v_{i,ave.,without\ stops} = \frac{d_i}{(T_i - T_{Stop})}, \quad i = 1 \text{ to } N_t \quad (5.4)$$

Where

$v_{i,ave.,without\ stops}$  is the average cycle speed without stop phases,

$T_{Stop}$  is the total standing time within the trip with  $v_i = 0\ km/h$  [s].

According to Regulation (EU) No 2016/646 the measured speed signals were assigned to three speed classes, namely urban driving ( $v_i \leq 60\ \frac{km}{h}$ ), rural driving ( $60\ \frac{km}{h} < v_i \leq 90\ \frac{km}{h}$ ) and driving on motorways ( $v_i > 90\ \frac{km}{h}$ ) [5.2]. A relevant parameter that characterizes the dynamic of a trip is the relative positive acceleration (RPA). It describes the acceleration work over the driven distance and is calculated as follows, see equation 5.5.

$$RPA_i = \frac{1}{d_i} \sum_{i=1}^{N_i} \frac{a_i \cdot v_i}{3,6}, \quad \left( a_i > 0,1\ \frac{m}{s^2} \right), \quad i = 1\ to\ N_t \quad (5.5)$$

Where

$RPA_i$  is the relative positive acceleration for urban, rural and motorway shares [m/s<sup>2</sup> or kW/(kg·km)],

$N_i$  is the number of samples up to time step i.

Within RDE legislation RPA is used as a boundary limit to ensure that measurement trips fulfill upper and lower dynamic limits, see Regulation (EU) No 2016/646, Annex 7a [5.2]. The evaluation method within RDE Regulation (EU) No 646/2016 was developed for the passenger car and light commercial vehicle sector and it therefore provides only an approach for evaluating the driving dynamics of motorcycles - not least because of significantly higher power / mass ratios and higher dynamic ranges in this vehicle category. However, it provides a robust comparability of driving cycles and real-world measurements on the road in terms of dynamic characteristics and it was therefore applied in this study.

#### 5.1.4.2 Basic Trip / Cycle Parameters

The on-board measurement trips, the TREMOD traffic situations and the WMTC were investigated with regard to relevant basic cycle parameters first. These include the average vehicle speeds for the RDE speed classes urban, rural and motorway and the vehicle speed frequency distribution in general (figure 5.4). Additional driving dynamics-related parameters are summarized in table 5.3. A differentiation of the on-board trips was carried out by showing the on-board trips once in total and once excluding the "Gaberl"-trip. Hereby, the influence of the "Gaberl" share on the overall on-board trip dynamics was examined, as this route represents intentionally sporty, ambitious driving, whereas "Arzberg" and "Ries" trips were carried out under RDE-legislative compliant conditions. The type approval driving cycle WMTC is displayed for comparison purposes, but it is not treated further. The WMTC shows partly significant differences in relevant cycle parameters compared to the on-board trips and the TREMOD traffic situations, which, however, have no relevance in the later course of this work.

Figure 5.4 shows the cumulative speed distribution of the WMTC, the on-board trips – with and without the “Gaberl” share - and the traffic weighted TREMOD traffic situations. The urban traffic share within the on-board trips is more pronounced than in the TREMOD traffic situations scheme – approx. 45 % (on-board trips) compared to 35 % (TREMOD traffic situations). Excluding the “Gaberl” trip, there is a further shift towards higher proportions in urban driving (49,3 %) in the on-board trips, because the “Gaberl” track consists predominately of federal rural roads with speed limits above 60 km/h. With regard to rural and motorway driving shares, the differences between the on-board trips and the TREMOD traffic situations are less pronounced, as indicated in table 5.3.

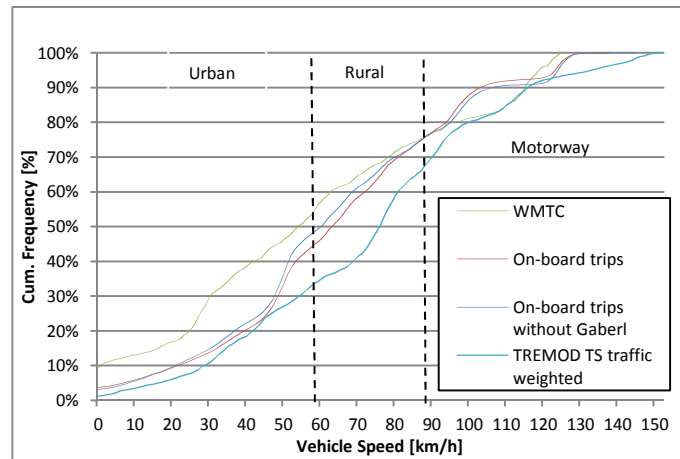


**Figure 5.4:** Cumulative speed frequency distribution of the on-board trips with- and without “Gaberl”-trip, traffic weighted TREMOD TS and WMTC – all trips / cycles including stop phases.

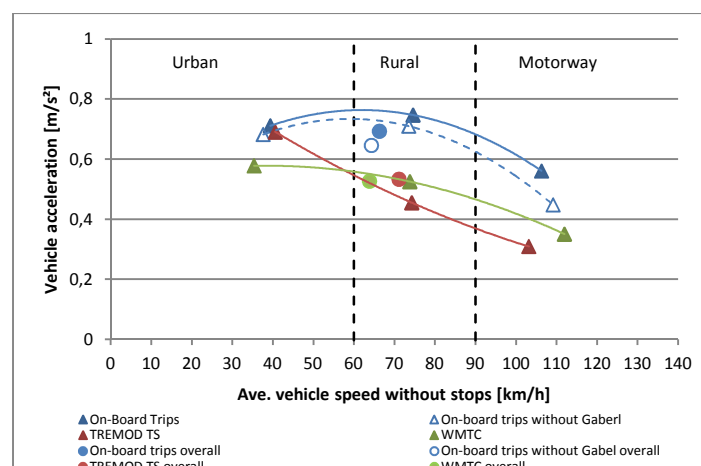
Concerning the average vehicle speed without stop phases of the on-board trips and the TREMOD traffic situations, the deviation for urban, rural, motorway and overall driving lies in a narrow margin between – 12,7 % to + 5,8 %, see table 5.3. This shows a high degree of correspondence of both data sets – the on-board trips and the TREMOD traffic situations , not least because the TREMOD traffic situations were derived and weighted based on real-world motorcycle driving data. There is also a high degree of correspondence concerning further trip parameters like acceleration and deceleration shares, stop phases and stops per km, as indicated in table 5.3. However, it should be noted, that the TREMOD traffic situations represent motorcycle driving of almost all relevant motorcycle classes in Germany – this includes different engine power- and displacement classes and various vehicle types, while the on-board trips performed in this study reflect driving with an individual vehicle. Thus, deviations between individual cycle / trip parameters are generally possible here.

**Table 5.3:** Relevant cycle- / trip parameter of onboard trips – with and without “Gaberl”-trip – traffic weighted TREMOD TS and WMTC

Cycle- / Trip parameter	On-board trips	On-board trips without Gaberl	TREMOD TS (traffic weighted)	WMTC
Total Distance [km]	525,8	362,0	21,4	28,9
Share stop duration [%]	2,9	3,1	1,4	9,5
Average speed with stops, overall [km/h]	65,1	64,2	73,1	57,8
Average speed without stops, overall [km/h]	66,3	64,3	73,7	63,9
Average speed without stops [km/h]	Urban	39,4	37,6	35,4
	Rural	74,6	73,5	74,3
	Motorway	106,3	109,2	103,2
Maximum speed [km/h] (not traffic weighted)	137,7	135,5	151,5	125,3
Share accelerations [%]	31,5	30,0	34,0	33,2
Share deceleration [%]	32,3	31,0	32,7	28,3
Accelerations per km [-]	4,3	4,3	4,6	2,3
Stops per km [-]	0,2	0,2	0,3	0,4
Average stop duration [s]	9,2	10,1	2,3	15,5
Urban share	45,0%	49,3%	35,0%	56,2%
Rural share	31,2%	26,7%	35,1%	20,3%
Motorway share	23,8%	24,0%	29,9%	23,5%

### 5.1.4.3 Driving Dynamics Results

Figure 5.5 represents the average urban, rural, motorway and overall vehicle acceleration values over the underlying aggregated, average vehicle speeds according to the RDE evaluation routines. Table 5.4 summarizes the percentage deviations of the on-board trips and the type approval cycle WMTC – overall, and differentiated according to local level – in relation to the TREMOD traffic situations. It should be noted here that TREMOD traffic situations, which contain speed shares of different RDE speed classes (e. g. the traffic situation “URB/Distr/50/Heavy” contains approx. 80 % RDE classified urban traffic and 20 % RDE classified rural traffic with a total share in the German motorcycle traffic of approx. 15,3 % according to TREMOD) were assigned to the respective aggregated RDE speed classes in figure 5.5 according to the traffic shares within this traffic situation and according to the share of this traffic situation to total motorcycle traffic. So, based on 15,3 % motorcycle traffic that this traffic situations represents in TREMOD, about 12,2 % were allocated to RDE urban- and 3,1 % were assigned to RDE rural speed class in figure 5.5.

**Figure 5.5:** Average vehicle acceleration values over average vehicle speed without stops according to urban, rural and motorway speed classes and overall – on-board trips in total and excluding the “Gaberl”-trip.

Overall, the on-board trips show approximately 30 % higher average positive acceleration values compared to the TREMOD traffic situations, see figure 5.5 and table 5.4. Within the speed ranges rural and motorway, the average positive acceleration values are with 60 %, respectively 80 % even more pronounced than the TREMOD traffic situations. However, in lower speed ranges < 60 km/h (urban), the acceleration dynamics of the on-board trips are nearly identical compared to the reference TREMOD (approx. + 3 %). Taking into account the fact that the driving dynamic increases with lower vehicle speeds this result is partly discrepant with regard to the on-board trip results. It is assumed here that the handling of the motorcycle with a PEMS-setup is more difficult compared to vehicle configurations without extra loadings, particularly during the starting phase of the vehicle. Although the additional weight (approx. 80 kg) corresponds approx. to a normal-weight pillion, the test setup had additional overhanging equipment (e. g. the EFM tube, side-boxes), which complicated slow driving and the start-up phase considerably. Not least, attention had to be paid to ensure that the safety of the driver and other road users was always maintained. At higher speed ranges, however, the test setup probably did not influence the acceleration dynamics notably, as the vehicle had more longitudinal stability and enough engine power so that the additional weight did not greatly affect the vehicle dynamic characteristics. It should be noted that additional test drives on public roads with motorcycles with and without PEMS-systems are required to describe the impact of the PEMS system on the vehicle dynamics in a more detailed way. For this purpose, different vehicle types should be driven by the same drivers on same test routes to generate comparative statements. In particular, powerful vehicle concepts are relevant for these purposes, since the influence on the driving dynamics is correspondingly lower opposed to driving with small, less powerful machines. However, such data sets were not available at the time of the evaluation of the driving dynamics in this chapter, so the results here have to be considered as an initial indication. The test vehicle used in this study probably represents a lower limit for the use of PEMS systems in the field of powered two-wheelers [4.11]. However, it can be assumed that the exhaust gas measurement technology will continue to evolve, making systems smaller and lighter and allowing them to be used on less powerful machines in future.

**Table 5.4:** Average vehicle speed without stops and aggregated positive acceleration values of the on-board trips – with and without “Gaberl” share – compared to traffic weighted TREMOD motorcycle traffic situations (TS) and WMTC; differentiated according to local level and overall; all percentage deviations are related to the TREMOD TS.

Trip / cycle	Local level	V_ave. without stops [km/h]	V_ave. deviation to TREMOD TS [%]	Mean positive acceleration [m/s <sup>2</sup> ]	Mean positive acceleration - deviation to TREMOD TS [%]
On-board trips	Urban	39,4	-3,00%	0,71	2,99%
	Rural	74,6	0,40%	0,75	64,23%
	Motorway	106,3	3,00%	0,56	81,44%
	Overall	66,3	-6,80%	0,69	29,99%
On-board trips without Gaberl	Urban	37,6	-7,30%	0,68	-1,17%
	Rural	73,5	-1,00%	0,71	56,07%
	Motorway	109,2	5,80%	0,45	44,97%
	Overall	64,3	-9,60%	0,65	21,15%
TREMOT TS	Urban	40,6		0,69	
	Rural	74,3		0,45	
	Motorway	103,2		0,31	
	Overall	71,1		0,53	

<b>WMTC</b>	Urban	35,4	-12,90%	0,58	-16,33%
	Rural	73,8	-0,60%	0,52	15,46%
	Motorway	112	8,50%	0,35	13,42%
	Overall	63,9	-10,20%	0,53	-1,21%
<b>Gaberl</b>	Urban	36,2	-10,8%	0,82	18,8%
	Rural	74,6	0,46%	0,81	79,13%
	Motorway	102,2	-0,98%	0,8	158,8%
	Overall	67,2	-5,49%	0,81	52,6%

As shown in table 5.4, within the speed ranges > 60 km/h (rural and motorway driving) the driving dynamics of the on-board trips is significantly higher in terms of average positive acceleration values compared to the TREMOD traffic situations. One can expect here that the “Gaberl” share shifts the acceleration dynamics of the overall on-board trips upwards due to the deliberately sporty driving style. However, the “Gaberl” share makes only about 31 % of the total on-board trip distance of which about half of the distance here is the trip to the mountain pass performed in normal traffic conditions. So, approx. 15 % of the total on-board trip distance represents the sporty up- and downhill driving at the mountain pass. Overall, the positive acceleration values of the on-board trips without the “Gaberl” share are approx. 8 % below the values of the total on-board trips including “Gaberl”. However, in the speed range > 90 km/h (motorway) the acceleration values of the on-board trips including “Gaberl” are about 24 % higher than the acceleration values of on-board trips without concerning the “Gaberl” share, as it was often accelerated during the mountain pass trips with maximum throttle in speed ranges also above 90 km/h. For comparison purposes the individual “Gaberl” route dynamic parameters are indicated in table 5.4 too. Here, it turns out, that the mean positive acceleration value of 0,8 m/s<sup>2</sup> for the motorway speed range is exceptionally high compared to the motorway speed range of the on-board trips (0,56 m/s<sup>2</sup> for the on-board trips including “Gaberl” and 0,45 m/s<sup>2</sup> for the motorway speed range of the on-board trips without the “Gaberl” share). The curvy mountain pass driving also increases the rural traffic share of the on-board trips from 26,7 % to 31,2 % - compared to the on-board trips without “Gaberl” - as it took place particularly in speed ranges between 50 – 100 km/h. Opposed to that, the other on-board trips (“Arzberg” and “Ries”) took place according to RDE conform conditions in normal road traffic and had to be adapted to the current traffic situations. So, high accelerations were partly not possible, not least due to safety aspects. Further considerations of the on-board trips in the simulation part of this study (chapter 6) always include the “Gaberl” share, as it is considered to be quite realistic to represent motorcycle driving for recreational purposes and it did not affect the overall on-board trip dynamic results to an unusual extent as proven above.

The TREMOD traffic situations were derived from the WMTC in-use database, which is composed of real-world driving profiles of various motorcycles of different displacement and performance classes in different countries - primarily recorded at the end of the 1990's [5.13]. Thus, the TREMOD traffic situations map the driving behavior of a vehicle fleet selected at the time of the development of the WMTC, while the on-board trips in this study represent the driving dynamics of an individual vehicle of the upper power spectrum in 2017. The question arises as to what extent the driving patterns of motorcycles applied in TREMOD and HBEFA are still representative against the background of a steadily increasing traffic density on German roads in recent years and decades [4.27]. The validation of the motorcycle driving patterns in TREMOD would require a novel real-world driving analysis, in which the speed-time profiles of a representative vehicle fleet are recorded under real driving conditions on the road. This procedure may allow verifying or discarding the existing motorcycle traffic situations in TREMOD and helps to re-assess the traffic shares to the traffic situations. In addition, in-depth investigations should be taken into consideration in which the traffic situations are

specified according to power or displacement classes in TREMOD. This might help to gain a possible higher degree of differentiation of motorcycle traffic data for simulation purposes.

In a next step, the on-board trips, the TREMOD traffic situations and the WMTC were investigated regarding to their mean relative positive acceleration values (RPA, see definitions in chapter 5.1.4.1), see figure 5.6 and table 5.5. Herein, the individual TREMOD traffic situations (figure 5.6 a) as well as the aggregated urban, rural, motorway and overall values (figure 5.6 b) are compared. The TREMOD traffic situations pictured in figure 5.6 a), which contain speed shares of different RDE speed classes, are divided according to these speed classes and displayed as separate points in the diagram. Each of these points has its own RPA value and a corresponding average cycle speed value. The driving shares of different RDE speed classes within one traffic situation-/ trip are proportionally allocated to the aggregated RDE speed classes urban-, rural- and motorway in figure 5.6 b).

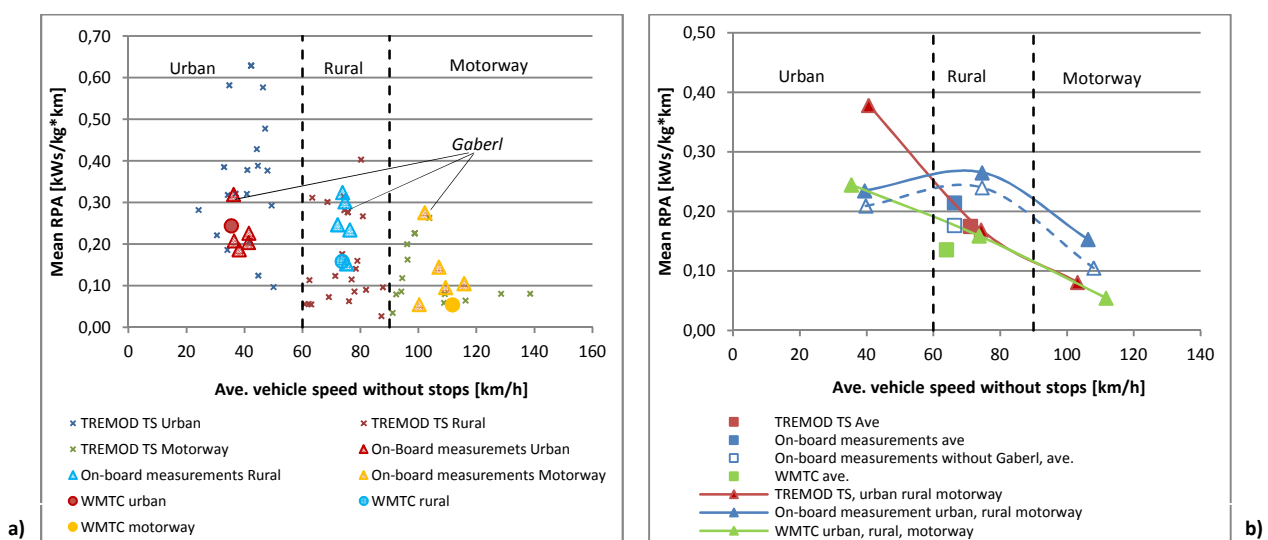


**Figure 5.6:** a) Mean RPA values of individual TREMOD motorcycle traffic situations, WMTC and on-board measurement trips over average cycle speed without stops; b) aggregated RPA values according to urban, rural, motorway and overall speed classes for TREMOD motorcycle traffic situations (traffic-weighted), WMTC and on-board measurement trips (with and without “Gaberl”-trip) over average cycle speed without stops.

A decline in the RPA values with increasing average vehicle speed becomes apparent, for both, the individual (figure 5.6 a) and the aggregated trips /cycles, figure 5.6 b). It turns out that some of the TREMOD urban traffic shares are partly significantly above the on-board urban driving shares and the WMTC with respect to RPA. It should be noted that some of these TREMOD cycles are characterized by high average cycle speeds and a high traffic saturation (heavy or saturated traffic) – e. g. the traffic situation “Rural/Motorway/120/Saturated”. However, the urban share within this traffic situation is comparatively low namely approx. 8 %. High urban RPA values in this traffic situation result from short and strong accelerations in the urban speed range, see figure 5.7. This might be explained by the driving dynamics in saturated traffic conditions on highways, in which the traffic comes almost to a standstill in short intervals followed by renewed acceleration phases.

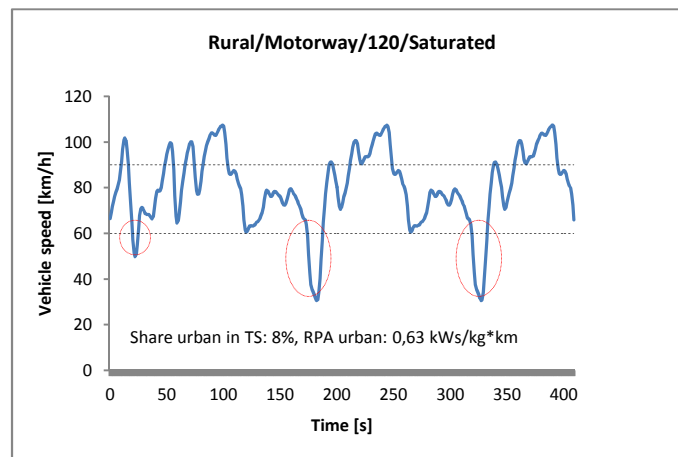


**Figure 5.7:** Example of a motorcycle traffic situation with a high urban RPA value: “Rural/Motorway/120/Saturated”.

Even the share of the urban traffic in such traffic situations is partly low, it can lead to a shift upwards of the aggregated urban RPA value for the TREMOD traffic situations, because the share in the total motorcycle traffic in TREMOD can be partly quite high. The aggregated urban RPA value of the TREMOD traffic situations is clearly above the on-board trip urban RPA value (approx. 60 % higher), see figure 5.6 b).

The on-board trips including the “Gaberl” share show higher RPA values opposed to the on-board trips without taking into account the “Gaberl” share – the deviation here ranges from + 10 % for rural traffic to + 45 % for motorway traffic. Overall, the dynamic of the on-board-trips including the “Gaberl” share concerning RPA is approx. 22 % above the TREMOD traffic situation RPA value; without consideration of the “Gaberl” share, the dynamic is almost equal to that of the TREMOD traffic situations, namely approx. + 1 %.

**Table 5.5:** Mean RPA values of the on-board trips (with and without “Gaberl” share) compared to the TREMOD motorcycle traffic situations and WMTC; differentiated according to local level and overall; all percentage deviations are related to the TREMOD traffic situations.

Trip / Cycle	Local level	Mean RPA [kW/kg*km]	Mean RPA deviation to TREMOD TS
On-board measurements	Urban	0,235	-37,91%
	Rural	0,265	56,82%
	Motorway	0,153	89,13%
	Overall	0,214	22,27%
On-board measurements without Gaberl	Urban	0,209	-44,63%
	Rural	0,24	42,01%
	Motorway	0,105	29,50%
	Overall	0,177	0,93%
TREMOD TS	Urban	0,378	
	Rural	0,169	
	Motorway	0,081	
	Overall	0,175	
WMTC	Urban	0,245	-35,31%
	Rural	0,159	-5,91%
	Motorway	0,055	-32,65%
	Overall	0,136	-22,32%

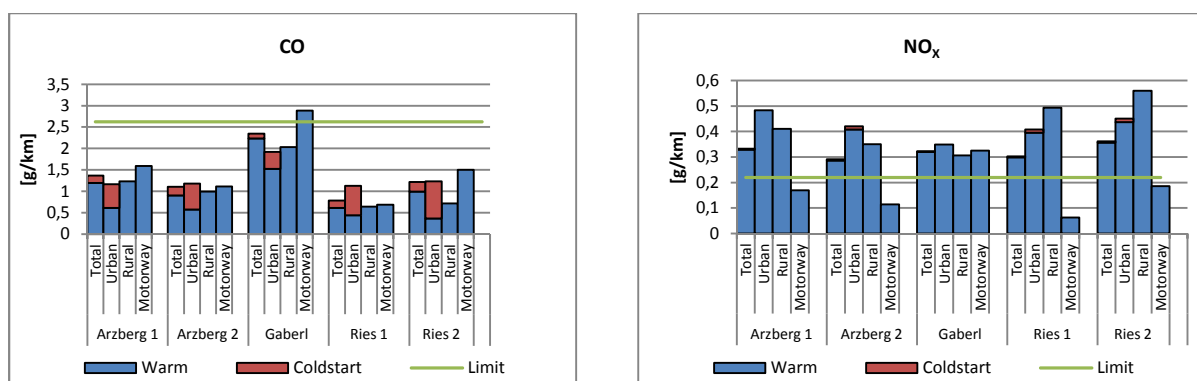
It turns out that the driving dynamics of the on-board trips performed within this project partly deviate from the existing mapping of motorcycle traffic in Germany with TREMOD. However, the

results generated here are to be considered under different aspects. In low speed ranges (0 – 60 km / h) it seems that the PEMS system influences the driving dynamics significantly, whereas it can be rather neglected at higher speeds in rural and motorway traffic. Here, the on-board trips show clearly higher dynamics compared to the TREMOD cycles. Further measurements of motorcycles with and without PEMS systems may be helpful in order to describe the influence of measuring devices like PEMS on the driving dynamics more precisely.

It should be noted that the TREMOD traffic situations map all motorcycle vehicle segments as a whole, whereas the on-board trips in this study were performed with an individual vehicle of the upper power class. It is necessary to investigate whether the TREMOD motorcycle traffic situations as such still represent the German motorcycle traffic in an acceptable way and whether the distribution of motorcycle traffic shares to the TREMOD traffic situations is still appropriate. In this context, it seems appropriate to differentiate the TREMOD traffic situations further with regard to vehicle segments and / or performance classes. For this purpose, representative on-board measurement campaigns including driving with various vehicle concepts on different road types in different geographical regions, local areas and traffic conditions may be meaningful. As a part of prospective activities in the field of motorcycle emission factor determination, uniform standards with regard to the evaluation of on-board emission measurement data and the setup of mobile emission measurement technology on motorcycles (e. g. the PEMS system, EFM tube) should be defined - possibly within the ERMES group.

## 5.2 On-board Emission Measurement Results

The kilometer-related emission results of the individual on-board trips for the emission components CO<sub>2</sub>, CO, NO<sub>x</sub>, NO, NO<sub>2</sub> are presented in figure 5.8. Here, the results are differentiated according to hot- and cold-start emissions and according to RDE speed classes urban, rural, motorway and overall. The CO emission results within the first two kilometers after engine start are used to assess cold-start surcharges. Within this trip distance, a "normal" emission level is reached. In addition, the Euro 3 tailpipe emission limit values of CO and NO<sub>x</sub> are indicated for comparison purposes, however, legislative emission values have no significance here, since the tailpipe emissions in this vehicle category are determined in WMTC on chassis dynamometers, see chapter 3. Table 5.6 summarizes the results for all aggregated measurements. All measurements in this project were carried out by using commercial fuel (E5) complying with Directive 2009/30/EC [5.14]. The test drives took place in the summer months in temperature ranges between 15 - 30 C °.



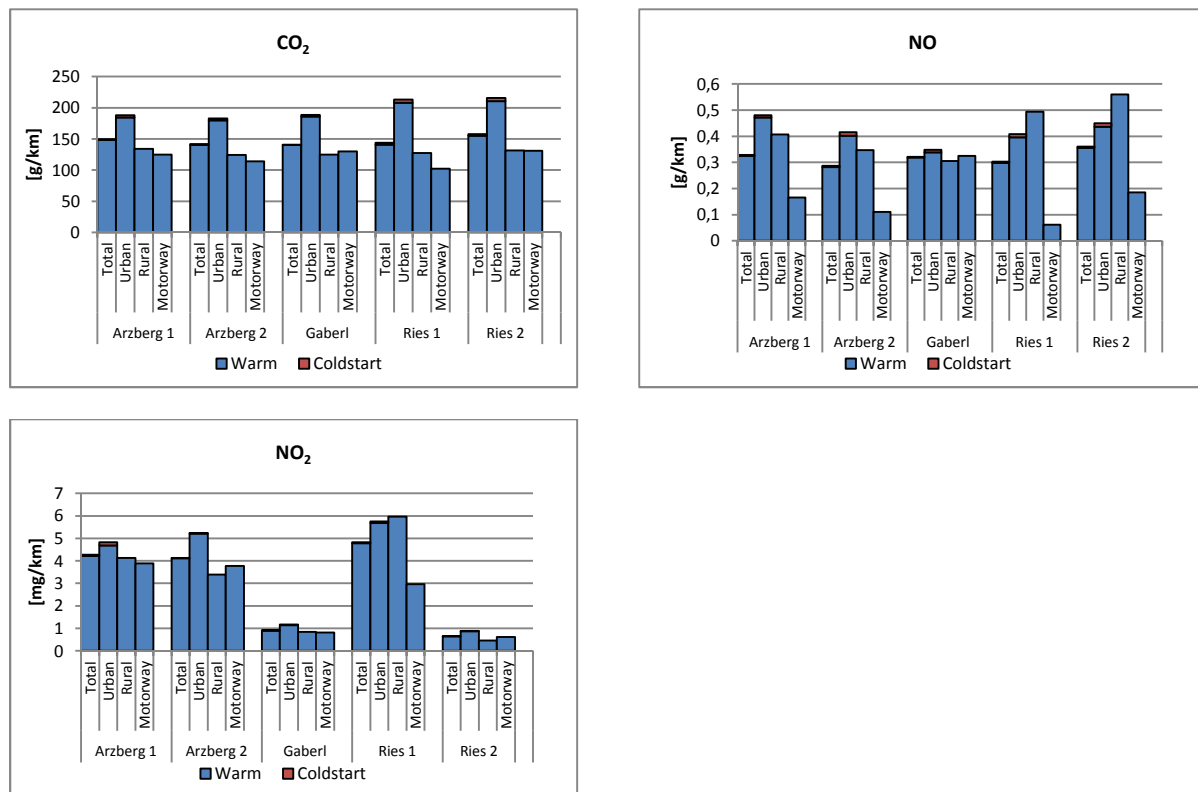


**Figure 5.8:** Kilometer-related emission results of the on-board trips for CO<sub>2</sub>, CO, NO<sub>x</sub>, NO, NO<sub>2</sub> differentiated according to RDE speed classes urban, rural, motorway and overall and differentiated according to hot- and cold-start emissions.

Basically, there is a good comparability between the emission results of the individual on-board measurement trips. Only the CO emission results of the “Gaberl” trip and the NO<sub>2</sub> emissions recorded during “Gaberl”- and “Ries 2” trip partly show some inconsistencies. It turns out that increased CO emissions during the “Gaberl” trip occurred due to many full-load phases during the mountain pass driving. This might also explain the correspondingly low NO<sub>2</sub> emissions values during the “Gaberl” trip. Due to the excess of CO in the exhaust gas, the NO<sub>2</sub> fractions are primarily used for the oxidation of CO and HC, since it is more reactive compared to oxygen. However, the low NO<sub>2</sub> emissions of the “Ries 2” trip cannot be directly explained by this relation. In general, one has to underline that the NO<sub>2</sub> concentrations in the exhaust gas of the test vehicle are comparatively low of just a few mg/km compared to the other measured emission components – the share of NO<sub>2</sub> to total NO<sub>x</sub> is approx. 0,3 – 1,5 %.

Cold-start emissions are relevant in the field of CO- and HC emissions (HC was only measured in the dynamometer test program), as the share in total emissions is deemed to be rather noteworthy. The duration of the cold-start phase depends on several parameters, among others, the catalyst temperature, the driving style, ambient conditions and cannot be quantified in general. However, a stable emission level was achieved within the first two kilometers after engine start in each on-board measurement trip. Table 5.6 indicates high deviations in cold-start CO emissions compared to hot CO emissions, particularly in urban traffic (0 – 60 km / h) – here, cold-start related CO emissions are approx. 80 % higher compared to hot urban CO emissions. Although the warm-up phase made up less than 5 % of the total trip time, up to 20 % of the CO emissions were emitted here, see figure 5.9. – herein, the modally and cumulative CO emissions in “Arzberg 1” trip are shown. In addition, a high

share of CO emissions occurred during strong acceleration phases - particularly on gradient road sections - that shifted the overall result upwards.

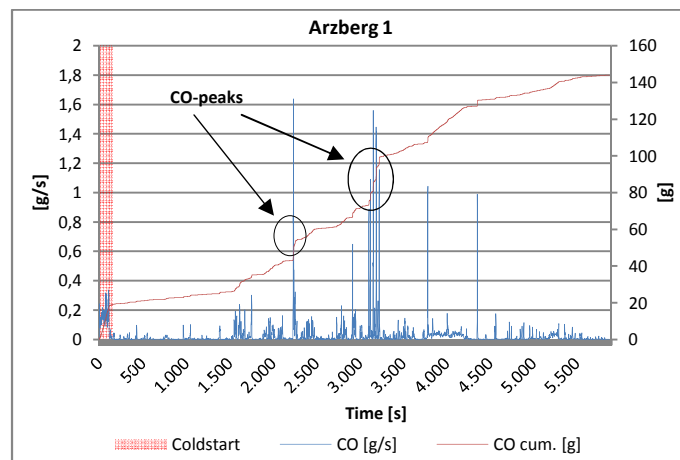


**Figure 5.9:** Second-by-second- and cumulative CO-emissions recorded for the “Arzberg 1”-trip.

Since the test routes in this study were chosen to be relatively long, the urban CO emission result shifted the overall CO emission results upwards relatively slightly – the overall CO emission results are approx. 12 % higher compared to the overall CO emission results by not including cold-start surcharges. However, TREMOD indicates an average driving distance of 14 km for motorcycles per trip resulting in more cold-start phases than pictured with the on-board trips here, which might lead to even higher overall CO emissions related to the driven distance. Against the background that motorcycles are operated to a high extent for private purposes and parked in residential areas, motorcycles may contribute disproportionately to CO emissions in urban areas during the first kilometers after start. Nonetheless, despite the high additional loading and untypical driving resistances, the legally prescribed CO emission limit was kept during all test drives. The other emission components do not show relevant cold-start surcharges (approx. + 1 – 2 % compared to the hot emission results).

**Table 5.6:** Kilometer-related emission results of the on-board trips differentiated according to RDE speed classes urban, rural, motorway and overall and differentiated to warm- and cold-start emissions.

Local area	CO <sub>2</sub>		CO		NO <sub>x</sub>		NO		NO <sub>2</sub>	
	warm [g/km]	cold-start [g/km]	warm [mg/km]	cold-start [mg/km]	warm [mg/km]	cold-start [mg/km]	warm [mg/km]	cold-start [mg/km]	warm [mg/km]	cold-start [mg/km]
∅ Urban	190,8	194,5	753,6	1.345,0	412,8	421,6	408,4	419,3	3,6	3,6
∅ Rural	127,3		1.365,2		385,7		384,1		2,5	
∅ Motorway	122,1		1.720,0		190,6		188,8		2,3	
∅ Overall	144,0	145,7	1.349,0	1.513,7	317,3	320,9	315,2	318,9	2,7	2,7

For the later trend scenarios calculations (chapter 7), the start-related cold-start surcharge is indicated here. The cold-start emissions per starting process - CO emissions within the first two kilometers from the start minus the average warm urban CO emissions – weighted over all on-board trips result in a value of approximately 16,4 g CO / start.

### 5.2.1 Uncertainties in the On-board Emission Measurement Program

The use of a passenger car PEMS system in a motorcycle application contains some uncertainty factors. In particular, the measurement of the exhaust gas mass flow via the EFM turned out to be difficult due to the requirements of the installation – e. g. a homogenization section required before the sensors. So, in order to validate the measurement accuracy of the PEMS system, reference measurements were carried out on the exhaust gas roller test bench at IVT, TU Graz [4.11]. Validation measurements were performed with the EFM installed transversely to the driving direction - in this design the device was used on the road - and alongside in vehicle direction (only applied for this validation measurement). In both cases, a good agreement of the measurement accuracy between the PEMS- and the CVS system was determined – the deviation lies in a range of < 15 %, depending on the emission components [4.11].

The additional weight of the measuring equipment combined with the significantly increased air resistance shifted the on-board emission results upwards. The total vehicle weight of approximately 350 kg - driver plus measuring equipment - represents the upper limit for this vehicle type (permissible total weight: 420 kg). Basically, such a loading is not an unusual scenario - driving with pillion and luggage - but it is also not assumed to be representative for typical motorcycle driving. It is assumed that the influence of the measurement equipment on the emissions decreases with increasing total vehicle weight and engine power. Thus, powerful, heavy motorcycles seem to be more suitable for PEMS applications compared to light machines [4.11].

The increased air resistance of the vehicle is noticeable particularly in higher speed ranges, however, it is difficult to classify the higher air resistance effects on the emission results here. Initial estimations for the air resistance parameter can be made on the basis of literature values. In addition, the driver might change his position at higher speeds to reduce the forces acting on his body – e. g. bending down on motorway segments. Although efforts were made to minimize this influence as far as possible in this study, even small changes in the driver position lead to modifications in air resistance- and frontal area values that unpredictably influence the emission results. In the further course of the work, this influence is investigated on the basis of a parameter variation with PHEM, see chapter 6.2.4.

### 5.3 Chassis Dynamometer Emission Measurement Program

Exhaust gas emission measurements were carried out on the IVT two-wheeler dynamometer test bench. Besides the emission components measured with the PEMS device on the road, additional emission components were recorded and evaluated, e. g. HC emissions. The test program included measurements in different driving cycles. In addition to the legislative type approval testing cycle WMTC, real-world cycles developed specifically for determining emission factors were applied here, see chapter 5.3.2 [4.11]. Different measurement systems (PEMS-, CVS-, FTIR device) were used at the same time to check the validity of the emission results.

---

### 5.3.1 Two-wheeler Test Bench Facilities

The dynamometer measurements were carried out on an AVL Zöllner two-wheeler dynamometer test bench [4.11]. The test bench can be operated in stationary and transient mode. The brake force control is based on the current vehicle acceleration and speed and relevant vehicle data such as the vehicle mass and driving resistance data [4.11]. Table 5.7 shows relevant technical specifications of the two-wheeler test bench applied in this study.

**Table 5.7:** Technical specifications of IVT two-wheeler test bench [4.11].

Specification	
Brake	electromechanical
Max. vehicle speed	160 km / h
Max. vehicle mass	350 kg
Roller $\varnothing$	20"
CVS flow	2, 4, or 6 m <sup>3</sup> / min
Regulated airstream cooler	+/- 10 % of vehicle speed (max. 48.000 m <sup>3</sup> / h)

The exhaust gas emissions were recorded via an open CVS device with an AVL AMA i60 analyzer [4.11]. The AVL AMA i60 combines various analyzer technologies (FID, CLD, IRD, PMD, QLC) to measure the exhaust gas components CO, CO<sub>2</sub>, NO / NO<sub>2</sub> / NO<sub>x</sub>, O<sub>2</sub> and total HC. The emission signal was recorded continuously with a resolution of 10 Hz and the total emission results of a test run (bag values) were stored as well. The position of the exhaust gas sample was fixed behind the rear muffler and the EFM device. The ambient conditions in the test chamber such as the air humidity and temperature are adjustable and these data were plotted during the measurements [4.11]. The test bench fulfills all requirements for the vehicle type approval process of powered two-wheelers. Additional information according the measurement procedure and –equipment can be found in the TU Graz - BAST report [4.11].

### FTIR Measurement System

The measurement of additional exhaust gas components was carried out with a FTIR (Fourier-transform infrared spectroscopy) measurement device from the IAG company (model: versa06) [5.15]. The FTIR device records the infrared spectrum of a gas mixture. Since each molecular structure has an individual infrared spectrum, the infrared transformation can be used to determine the concentration of each substance whose infrared spectrum is known. However, the evaluation was carried out only for relevant substances that were present in adequate concentrations in the exhaust gas (some emission components were present only in trace concentrations and they were partly below the measurement accuracy of the FTIR-device) [4.11]. The unregulated emission components evaluated in this study include CH<sub>4</sub>, C<sub>6</sub>H<sub>6</sub>, C<sub>4</sub>H<sub>6</sub>, C<sub>2</sub>H<sub>2</sub>, C<sub>2</sub>H<sub>6</sub> and HCHO. Due to the dimensions and operational requirements of an FTIR-device, no mobile FTIR's are currently available in the motorcycle vehicle sector, so the FTIR measurements are limited to stationary applications.

### 5.3.2 Test Cycles

The exhaust gas measurements were carried out in different test cycles. The type approval testing cycle WMTC, the CADC and the ERMES cycle - used to generate emission factors in the passenger car and light commercial vehicle sector – were chosen for emission testing in this project. In addition, real-world driving cycles (RDC 1 and RDC 2) developed for reflecting typical motorcycle driving were selected for the test program as well [4.11]. The latter ones include road gradient segments, which are simulated via the dynamometer brake adjustment of the test bench. The following figures 5.10 show the speed-time profiles of the dynamometer test cycles.

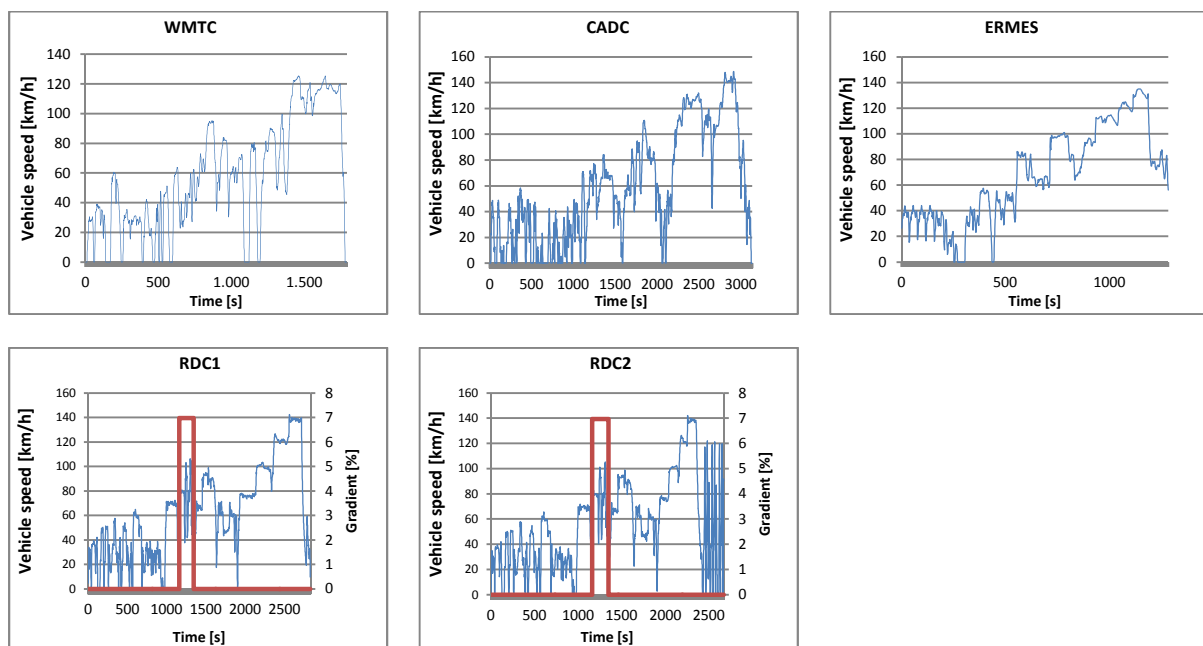


**Figure 5.10:** Test cycles applied in the dynamometer emission measurement program.

## 5.4 Dynamometer Emission Measurement Results and Evaluation

The following illustrations present the kilometer-related emission results of the regulated emission components CO, NO<sub>x</sub>, HC and, in addition, the climate gas CO<sub>2</sub> for all individual test runs including the legislative emission limit values, see figure 5.11. The results are differentiated according to hot- and cold-start emissions and according to RDE-speed classes urban, rural, motorway and overall. The overall HC- and CO emission values including cold-start shares averaged over all cycles are significantly above the results without taking into account cold-start surcharges; detailed information are indicated in table 5.8. Related to urban driving, the deviations are partly remarkable higher. Here, the urban CO emission values including cold-start surcharges are approx. 180 % higher than the results without considering cold-start effects. The urban HC emissions values are approx. 90 % higher (taking into account cold-start emissions) compared to the urban HC emission results without considering these emission shares. The cold-start emissions per starting process – again, the emissions within the first two kilometers from the start minus the average warm urban emissions – weighted over all dynamometer measurements result in a value of approximately 8,3 g CO / start

and 2,2 g HC / start. Similar to the results of the on-board measurement program the relevance of cold-start emission fractions in this vehicle category – in particular in urban driving after the engine starts – is accentuated again.

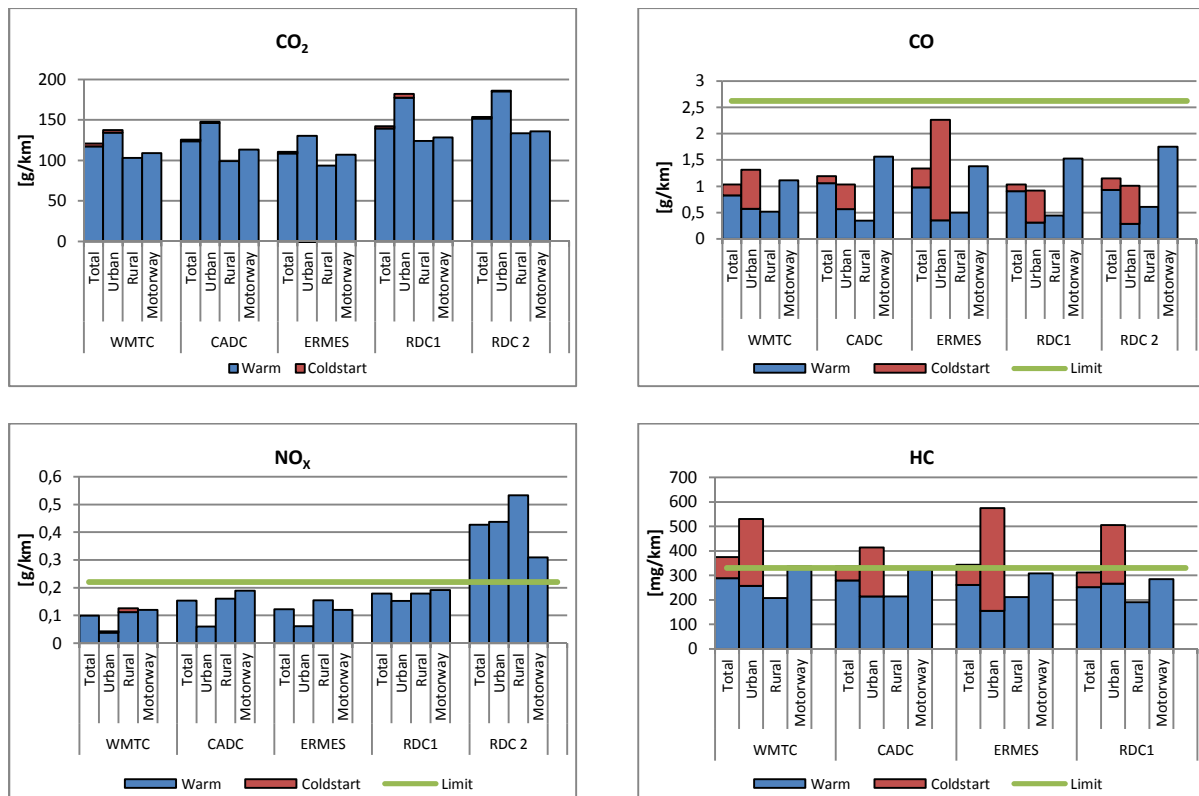


**Figure 5.11:** Kilometer-related emission results of the chassis dynamometer test program for CO<sub>2</sub>, CO, NO<sub>x</sub>, and HC according to RDE speed classes urban, rural, motorway and overall and differentiated to hot- and cold-start emissions.

The averaged CO<sub>2</sub> emissions aggregated over all test cycles are approx. 11 % below the on-board CO<sub>2</sub> emission measurement results - NO<sub>x</sub> emission results in the dynamometer program are even approx. 50 % lower compared to the on-board measurement program. Here, in particular, the lower driving resistances and vehicle mass compared to the measuring program on the road becomes noticeable. An exception is the RDC 2 cycle, which shows similar results for CO<sub>2</sub> and NO<sub>x</sub> compared to the on-board measurement program. In particular, the high dynamics at the end of the test cycle lead to a significant increase in the total CO<sub>2</sub> and NO<sub>x</sub> emission levels. There are no measurement results for HC emissions in RDC 2 available due to an error of the FID analyzer during the measurement [4.11]. Overall, all emission measurement results represent a valid data base for further simulations in PHEM in chapter 6. The averaged emission values indicated in table 5.8 were determined over all valid test runs in the driving cycles described in chapter 5.3.2. Again, the driven distance of two kilometers after engine start was defined as the distance for the determination of the cold-start surcharges.

**Table 5.8:** Kilometer-related emission results of the chassis dynamometer test program for regulated emission components and CO<sub>2</sub> differentiated to RDE speed classes urban, rural, motorway and overall and according to hot- and cold-start emissions.

	CO <sub>2</sub> warm [g/km]	CO <sub>2</sub> cold-start [g/km]	CO warm [mg/km]	CO cold-start [mg/km]	NO <sub>x</sub> warm [mg/km]	NO <sub>x</sub> cold-start [mg/km]	HC warm [mg/km]	HC cold-start [mg/km]
Ø Urban	160,35	161,54	417,06	1174,66	176,03	191,72	231,80	489,48
Ø Rural	115,18		485,19		256,44		203,34	
Ø Motorway	119,23		1496,27		190,02		311,56	
Ø Overall	130,91	133,29	949,95	1138,80	207,53	210,78	269,29	489,48

Figure 5.12 shows the results of the FTIR analyzer for the emission components CH<sub>4</sub>, C<sub>6</sub>H<sub>6</sub>, C<sub>4</sub>H<sub>6</sub>, C<sub>2</sub>H<sub>2</sub>, C<sub>2</sub>H<sub>6</sub> and HCHO for the test cycles concerned - again differentiated according to RDE speed classes urban, rural, motorway and overall and according to hot- and cold-start emissions. Relevant concentrations in the exhaust gas became apparent for methane (CH<sub>4</sub>) and benzene (C<sub>6</sub>H<sub>6</sub>) showing approx. 20 mg / km in total. Methane emissions are approx. 20 % higher when taking into account the cold-start surcharges – resulting primarily from the urban driving shares in the test cycles –, whereas benzene shows no difference between hot and cold-start emissions. All other relevant emission components show concentrations of less than 5 mg / km [4.11]. Detailed information on the emission results of the FTIR measurements are presented in table 5.9.

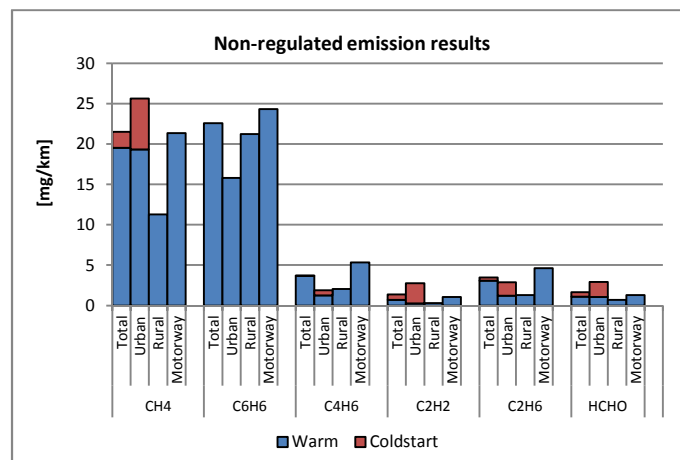


**Figure 5.12:** Kilometer-related emission results of the FTIR-measurements for CH<sub>4</sub>, C<sub>6</sub>H<sub>6</sub>, C<sub>4</sub>H<sub>6</sub>, C<sub>2</sub>H<sub>2</sub>, C<sub>2</sub>H<sub>6</sub>, HCHO averaged over all valid test runs according to RDE speed classes urban, rural, motorway and overall and differentiated to hot- and cold-start emissions.

Particularly, the emission components acetylene (C<sub>2</sub>H<sub>2</sub>), ethane (C<sub>2</sub>H<sub>6</sub>) and formaldehyde (HCHO) show high cold-start emission values compared to the emissions recorded when the engine is in warm operation mode - these values are partly ten times higher than the "hot" emission values recorded (e. g. in the case of C<sub>2</sub>H<sub>2</sub>). However, one has to consider that these emission values amount only a few milligrams C<sub>2</sub>H<sub>2</sub> per kilometer in total. The values in table 5.9 are averaged over all valid test runs in the dynamometer measurement program with the FTIR-analyzer in operation. The emissions were recorded in five driving cycles as described in chapter 5.3.2 – cold-start surcharges, again, were determined within the first two kilometers after engine start. However, since no additional calculations with regard to cold-start emissions of non-regulated emission components in

this study are carried out, starting-process related information for cold-starts in g / start for the non-regulated emission components were not calculated.

**Table 5.9:** Kilometer-related emission results of the chassis dynamometer test program for unregulated emission components differentiated to RDE speed classes urban, rural, motorway and overall and according to hot- and cold-start emissions.

	CH <sub>4</sub>		C <sub>6</sub> H <sub>6</sub>		C <sub>2</sub> H <sub>2</sub>		C <sub>4</sub> H <sub>6</sub>		C <sub>2</sub> H <sub>6</sub>		HCHO	
	warm [mg/km]	cold-start [mg/km]	warm [mg/km]	cold-start [mg/km]	warm [mg/km]	cold-start [mg/km]	warm [mg/km]	cold-start [mg/km]	warm [mg/km]	cold-start [mg/km]	warm [mg/km]	cold-start [mg/km]
Ø Urban	19,32	25,62	15,81	15,62	0,27	2,76	1,26	1,905	1,21	2,89	1,06	2,92
Ø Rural	11,27		21,23		0,29		2,06		1,28		0,68	
Ø Motorway	21,37		24,32		1,05		5,34		4,57		1,28	
Ø Overall	19,53	21,5	22,58	22,06	0,7	1,373	3,65	3,706	3,06	3,46	1,11	1,63

## 6. PHEM Simulation

The emission factor simulation for the relevant emission components CO<sub>2</sub>, CO, NO<sub>x</sub>, HC and CH<sub>4</sub> in the systematic of HBEFA and TREMOD for the test vehicle was carried out in this study with the PHEM model, version 12.0.1. The creation of the emission maps and the underlying methodology is presented in chapter 6.1. Here, a distinction is made between simulations, which were carried out on the basis of emission maps based on on-board measurements and those emission maps created on the basis of the data gained in the dynamometer measurement program. Emphasis is laid on the validation of the simulation procedure by re-simulations of the measurement trips in chapter 6.2. In this context, it is evaluated, whether the emission simulation routines in PHEM based on the generated emission maps are suitable for simulation purposes in the context of HBEFA and TREMOD. Additionally, possible weaknesses in the simulation procedure were identified and evaluated in this chapter. An approach for the simulation of TREMOD motorcycle emission factors is presented in chapter 6.3. In this chapter, the development of a real-world vehicle configuration for TREMOD applications is discussed on the basis of different test vehicle configurations – the on-board- and the dynamometer vehicle configuration. Finally, emission factors in the structure of TREMOD were simulated with PHEM for the test vehicles segment and the results were contrasted with the current emission factor database in TREMOD, see chapter 6.4.

### 6.1 Motorcycle Emission Map Creation

The compilation of emission maps with PHEM requires second-by-second engine speed, engine power and emission concentration signals. PHEM generates emission maps by assigning the instantaneously measured emission data to the underlying engine speed and power signal. The engine speed signal was recorded by means of a CAN-bus interface and the measurement of the exhaust gas concentrations was carried out with the PEMS system respectively with the CVS device and relevant analyzers of the chassis dynamometer test bench. Measurements of the engine power / or torque are technically and economically complex and are difficult to realize in the field of motorcycles under real driving conditions, see chapter 4.2.1.1 [4.12]. In addition, the calculation of the second-by-second engine power via the PHEM driving resistance approach is not sufficiently accurate for on-road measurements due to uncertainties with regard to air, rolling and road gradient resistance parameters. Thus, a direct engine power recording was not directly possible here. Opposed to the on-board measurements, the braking force of the dynamometer roll of the test bench could have been used as a signal source to calculate the vehicle wheel torque and thus, also the second-by-second engine power signal. However, it was necessary to use the same engine power calculation procedure for both emission map variants – the on-board- and the dynamometer maps - in order to obtain comparable results.

In this work, the second-by-second engine power signal required for the emission map creation was determined via an approach, which is based on second-by-second CO<sub>2</sub> and engine speed signals gained from the measurements combined with generic engine technology-specific CO<sub>2</sub> emission maps, as already described in chapter 4.2.1.1 [4.14]. This approach was developed to calculate the required second-by-second engine power for PHEM applications based on on-board emission

---

measurements with PEMS systems in the passenger car- and light commercial vehicle sector, in which usually no power signals are available. As on-board emission measurements become more and more relevant in the field of passenger cars- and light commercial vehicles - not least due to the RDE regulations -, valid engine power data can be generated for PHEM hereby. It should be noted that only hot emission data from the measurements were taken into account for the emission map creation in this study; cold-start emissions were not further considered in this context.

### 6.1.1 Emission Map Results

Figure 6.1 shows the generated emission maps based on the on-board emission measurements for the exhaust gas components CO<sub>2</sub>, CO, and NO<sub>x</sub>. The emission rates are indicated in g/h and the values are assigned to absolute engine power and speed of the test vehicle. Characteristic emission maps for the exhaust gas components NO and NO<sub>2</sub> were not created; on the one hand the share of NO to total NO<sub>x</sub> in the measurement program was > 99,5 % and possible NO emission maps would be therefore almost equal to the NO<sub>x</sub> maps. In the case of NO<sub>2</sub>, however, the concentrations recorded were negligibly low, (approx. 0,5 % to total NO<sub>x</sub>), so that no conclusive relations and gradations between the parameters engine power, speed and NO<sub>2</sub> concentration could have been compiled. All generated on-board emission maps show an adequate coverage of almost all engine load points.

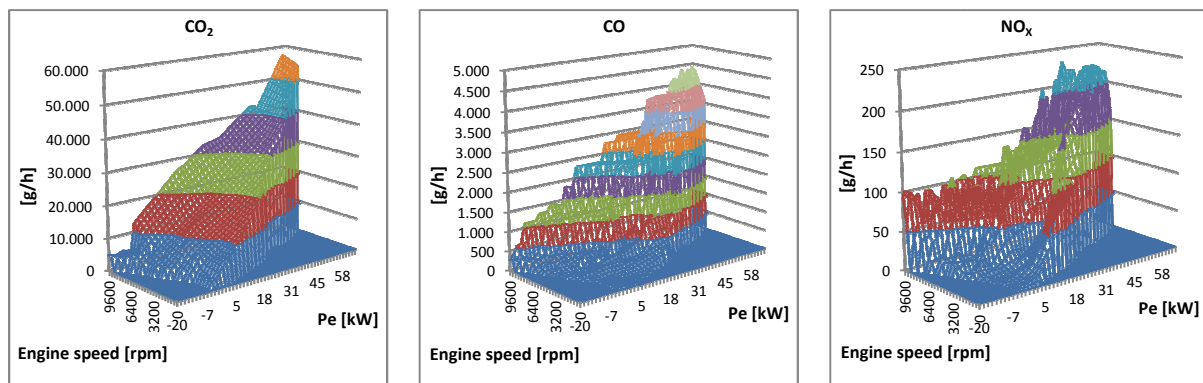


**Figure 6.1:** Emission maps generated with emission data from the on-board measurement program – CO<sub>2</sub>, CO, NO<sub>x</sub>.

In figure 6.2 the results of the emission map creation based on the dynamometer measurements are presented – the engine power calculation was based on the same generic CO<sub>2</sub> emission map approach as already applied for the on-board emission map creation. As HC and CH<sub>4</sub> emissions were also measured within the dynamometer test program these emission maps were created, too. It is noticeable that the CO<sub>2</sub> emission map generated from the dynamometer measurements is almost identical to the CO<sub>2</sub> emission map compiled with data from the on-board measurements. Although the driving resistances in the on-board tests were partly significantly higher (positive road gradients, air resistance etc.) resulting in overall higher engine power demand, the correlation between the CO<sub>2</sub> emission rate, engine power and -speed must always be the same. Since the second-by-second engine power for the on-board- and the dynamometer CO<sub>2</sub> map creation is calculated based on the same generic CO<sub>2</sub> emission map the on-board- and the dynamometer CO<sub>2</sub> emission maps are almost

identical to the generic CO<sub>2</sub> emission map. Minor deviations may occur due to the averaging process and the assignment of emission values in the engine map.

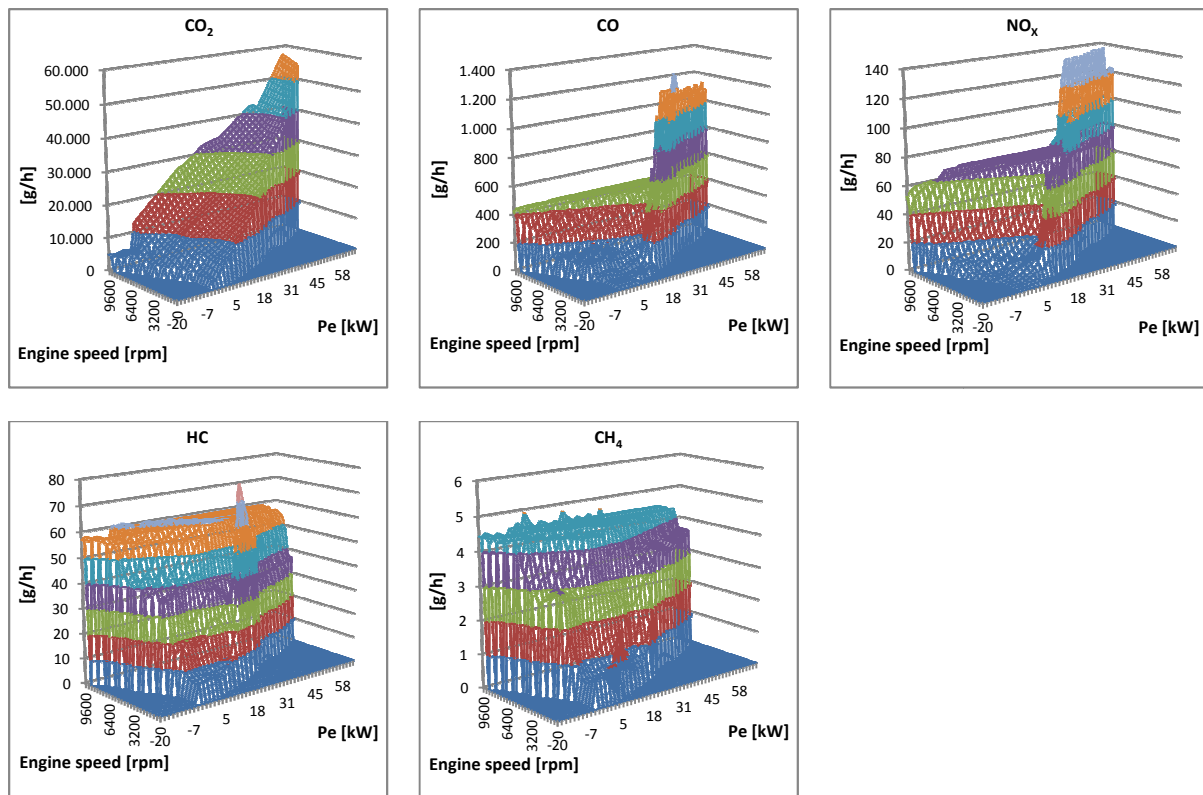


**Figure 6.2:** Emission maps generated with emission data from the dynamometer measurement program – CO<sub>2</sub>, CO, NO<sub>x</sub>, HC and CH<sub>4</sub>.

Opposed to the on-board emission maps, the pollutant emission maps generated based on the dynamometer measurements show clearly insufficient map coverage of wide areas of the engine operation range. Thus, no assignment between engine power and speed and emission rate could be generated for all engine operation points. Within the dynamometer measurement program high engine loads could partly not be driven on the dynamometer test bench due to physical restrictions – e. g. slippage between the vehicle tires and the test bench role during strong acceleration phases – resulting in a lack of emission data in high engine operation points. However, the measurements performed in the motorcycle real-driving cycles RDC 1 and RDC 2 compensated this data lack in the emission maps partially, due to road gradient sections with high engine power demand [4.11]. Figure 6.3 shows the speed-acceleration distribution of the dynamometer driving cycles contrasted with the on-board trips (including the “Gaberl”-share) and the type approval cycle WMTC – once, the second-by second acceleration values over vehicle speed a) and aggregated to acceleration classes b). It becomes apparent that the on-board trips show higher acceleration values, particularly in the speed range between 50 – 100 km / h, resulting in better emission map coverage in this operation range.

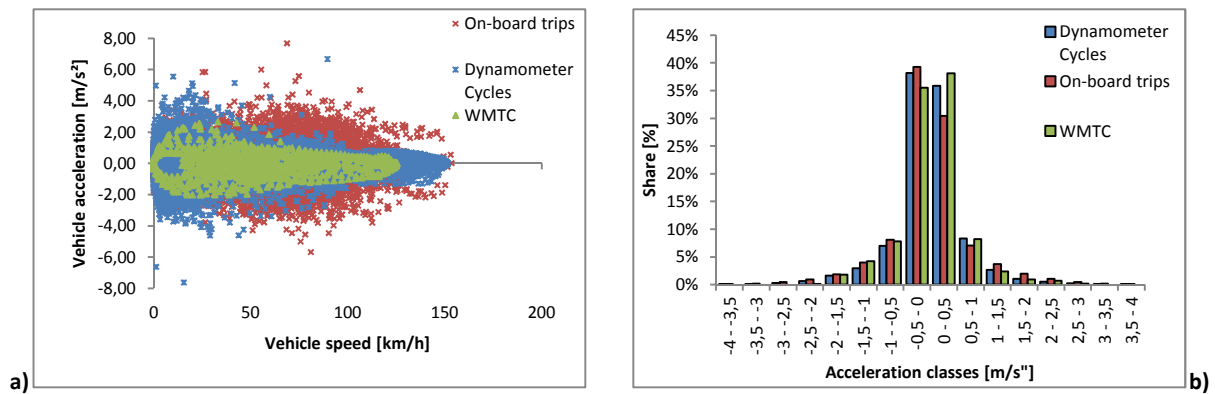


**Figure 6.3:** Speed-acceleration distribution of dynamometer driving cycles (blue) and on-board trips (red) from the test vehicle of the measurement program – WMTC (green) indicated for comparison purposes. **a)** Individual acceleration values over vehicle speed **b)** aggregated to acceleration classes.

In general, the emission levels of the dynamometer pollutant emission maps are considerably less pronounced compared to the on-board emission maps. Additionally, the total distance travelled in the dynamometer measurement program was evidently shorter – approx. 155 km compared to approx. > 500 km in the on-board measurement program - resulting in less data material for the emission map creation. Overall, it becomes obvious that the on-board emission maps reflect the emission behavior of the test vehicle comparatively better – statements regarding the robustness of the emission maps were derived from validation simulations, as applied in chapter 6.2.

## 6.2 Validation of the Emission Simulation

The assessment of the robustness of the emission simulation with PHEM was carried out by re-simulating the measurements performed in this study – the on-board- and the dynamometer measurements - based on the respective emission maps from chapter 6.1. This procedure is intended to identify deviations between the emission measurement results and the PHEM simulations and it helps to reveal potential weaknesses in the simulation routine. The engine speed during the test drives was simulated in order to assess the quality of the PHEM gear shift model for motorcycle applications, see chapter 6.2.1. The CO<sub>2</sub>- and the pollutant emissions were simulated subsequently in chapter 6.2.2 and 6.2.3. The emission measurements performed were simulated on a second-by-second basis and cumulatively, in which all individual measurement trips were composed together. In this way, the suitability of the different simulation configurations for TREMOD / HBEFA applications was evaluated. Since the emission maps do not consider cold-start surcharges, only measurement shares in which the test vehicles engine has reached the hot operation temperature were considered.

### 6.2.1 Engine Speed Simulation

As described in Chapter 4.2.1, the emission simulation of any driving cycles can be performed based on engine speed signals from the measurements - if available - or by using the PHEM-integrated gear shift model that calculates engine speeds based on predefined gear shift characteristics. However,

TREMOM motorcycle driving cycles do not include gear shift information or engine speed signals, so the PHEM gear shift model was applied for the gear shift simulation and finally the engine speed calculation here. Since it was difficult to derive up- and downshift points from the measurement data – the clutch actuation times led to high engine speed fluctuations at low vehicle speeds -, the predefined settings in PHEM were selected for the gear shift simulation provisionally. In the course of this, PHEM determines the gear shift points based on parameters such as, among others, current engine- and vehicle speed and required engine power to overcome the second-by-second driving resistance forces acting on the vehicle. First, it was investigated to what extent the basic engine speed settings in the PHEM gear shift model deliver robust results of the engine speed for a motorcycle trip simulation. Therefore, the dynamometer measurements and the on-board trips - each lined up over all measurements – were simulated with PHEM and the simulated second-by-second and the cumulative engine speed were contrasted with the engine speed data recorded in the measurements. The cumulated engine speed over a measurement trip has technically no relevance – however, it serves a comparison parameter for the assessment of the simulation here. The following figures 6.4 a) and b) show the deviations between the measured and the simulated engine speed.

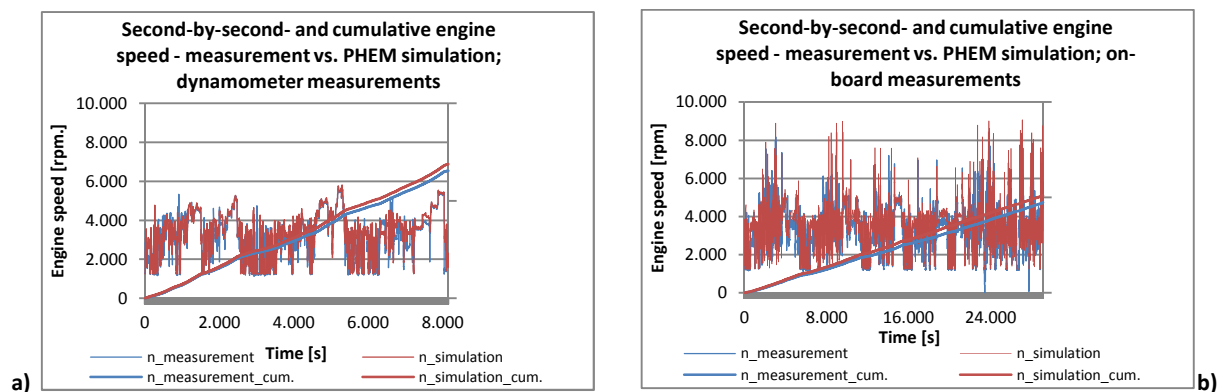


**Figure 6.4:** Second-by-second and cumulative engine speed – measurement vs. PHEM simulation; **a)** dynamometer measurements, **b)** on-board measurements.

The deviation between the measured cumulative engine speed and the PHEM simulation results are approx. 5,1 % in the case of the dynamometer engine speed simulation and approx. 7,7 % in the on-board trip engine speed simulation. It was expected that the deviation between the engine speed measurements and the simulations in the on-board trips are more pronounced compared to the dynamometer simulation results due to higher driving dynamics and stronger acceleration phases - figure 6.4 b) shows that the up-shifting points are partly significantly higher within the on-board measurement program. However, it turns out that the PHEM gear shift model already matches the engine speed in an appropriate range with the predefined settings [4.11]. In future elaborations on motorcycle simulations with PHEM, it is recommended to investigate the gear shift characteristics of real-world motorcycle driving more detailed – e. g. in the context of driving behavior analyses with more different drivers involved - in order to derive vehicle segment specific gear shift definitions. This procedure may even increase the robustness of the engine speed simulation in the motorcycle segment in PHEM. The PHEM gear shift model simulation results for the test vehicle concerned are

acceptable and the predefined settings were applied to the emission factor simulation in the further course of this work.

### 6.2.2. Re-simulation of the Dynamometer Tests

The dynamometer emission measurements were re-simulated with PHEM in order to evaluate the robustness of the PHEM simulation routines for the TREMOD emission factor simulation in the motorcycle segment. Since the driving resistance data of the test vehicle / dynamometer test bench configuration were precisely known via the roller test bench settings, a direct comparison between the emission measurement and the simulation results is feasible here. All dynamometer measurements were lined up and simulated based on the emission maps generated from the dynamometer test program. The driving resistance data for the PHEM simulation are equal to the dynamometer test bench settings taken from the UN WMTC Regulation and the resistance data were also compared to literature information [6.1] [2.2] [4.11]. Table 6.1 indicates the driving resistance data applied for the dynamometer measurement re-simulation in PHEM.

**Table 6.1:** Driving resistance data of the test vehicle for the dynamometer measurement re-simulation in PHEM.

Vehicle reference mass including driver [kg]	Vehicle loading [kg]	Air resistance coefficient $C_w$ [-]	Cross sectional area [m <sup>2</sup> ]	$C_d \times A$ [m <sup>2</sup> ]	Rolling resistance coefficient $F_{RO}$ [-]
270	0	0,45	1,15	0,52	0,0089

Figure 6.5 show the PHEM re-simulation results of the dynamometer measurements compared to the dynamometer emission measurement results itself for the emission components CO<sub>2</sub>, CO, NO<sub>x</sub>, HC and CH<sub>4</sub> – both second-by-second and cumulative. The driven distance for the methane emission recording is shorter compared to the other emissions components due to a temporary measurement error in the FTIR measurement – thus, only the valid data material from the measurement was taken for the CH<sub>4</sub> re-simulations. Overall, there is an acceptable correspondence between the emission measurements and the simulation results for all emission components concerned; maximum deviations can be found in HC- and CO emissions with approx. + 12,3 % and + 10,5 %. The deviation in the CO<sub>2</sub> emission simulation results is marginal and lies < 0,1 %. It can thus be assumed that the CO<sub>2</sub> emission maps and the underlying generic map compilation method show a high degree of robustness. Due to the drive of several rotating parts (pumps, transmission components etc.) and related inertia forces the fuel consumption and thus the CO<sub>2</sub> emissions do not reach a value of zero – neither in the measurement nor in the PHEM simulation. The cumulated, simulated NO<sub>x</sub> emissions are approx. 4,4 % above the measurement results and the CH<sub>4</sub> simulation is approx. 9,5 % above the measurement results.

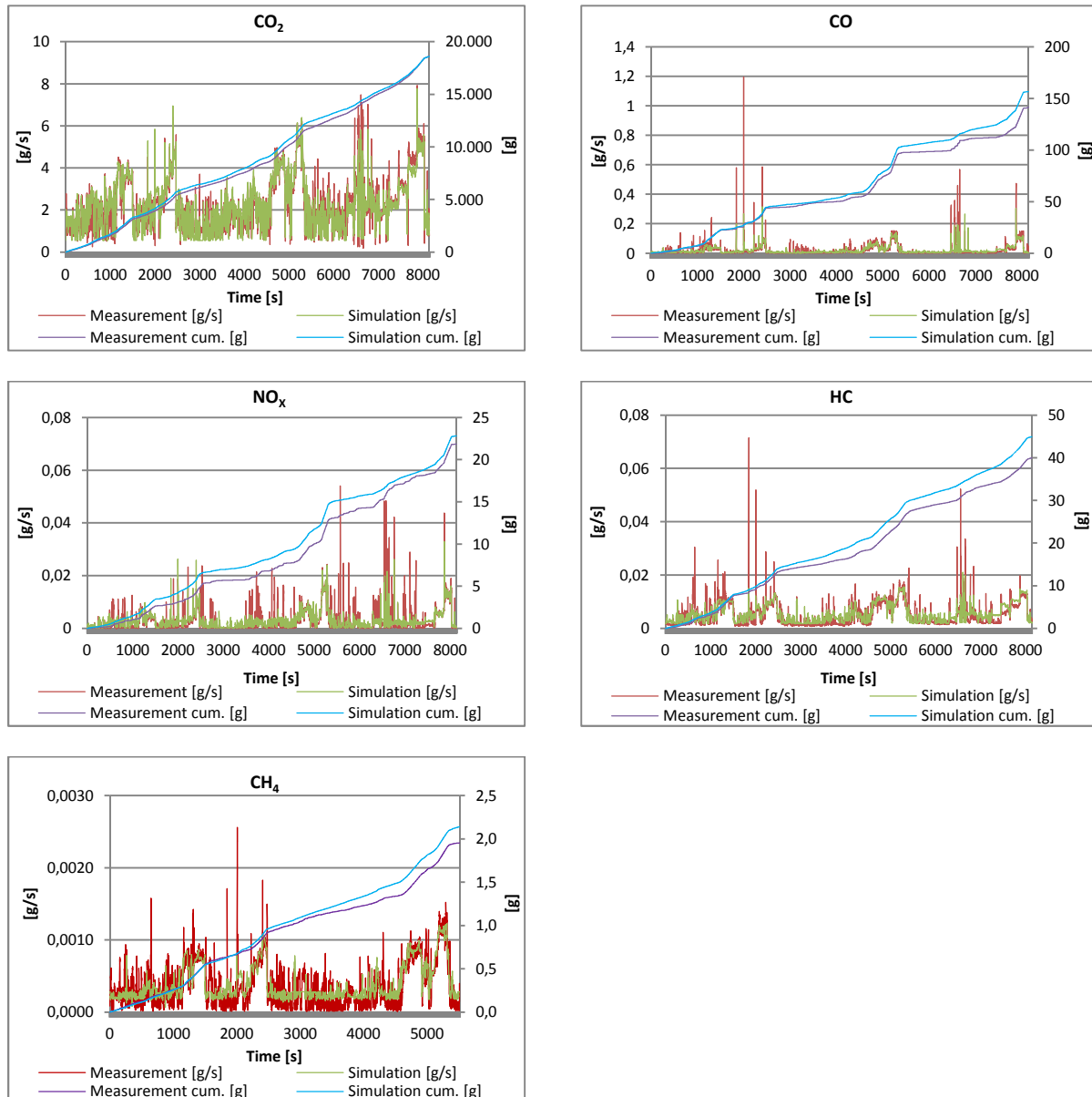


**Figure 6.5:** Second-by-second and cumulative dynamometer emission measurement- and PHEM simulation results of lined-up dynamometer tests based on emission maps generated from the dynamometer measurement program.

All emission components show an overall higher cumulative emission level in the PHEM-simulation compared to the measurement results. This might be an indicator that the pollutant emission maps are partly too high concerning the emission level. Due to emission peaks within the second-by-second emission courses the cumulative emission levels are partially up-shifted, however, this effect is more pronounced in the measurement courses. It becomes apparent that the emission peaks are partly not met by PHEM. These emission peak values are sometimes several times more pronounced compared to the average emission level of the measurements. As a result the emission peaks are too low in the simulations. However, the emission peaks in the considered dynamometer measurements are only exceptional occurrences compared to the total measurement record, which do not influence the overall result in a highly decisive manner. Table 6.2 lists the percentage deviations of the simulation results related to the measurements.

**Table 6.2:** Deviation between the cumulative dynamometer emission measurement results and the PHEM simulation results of lined-up dynamometer tests based on emission maps generated from the dynamometer measurement program.

	CO <sub>2</sub>	CO	NO <sub>x</sub>	HC	CH <sub>4</sub>
Deviation to the measurement results	<0,1%	10,5%	4,4%	12,3%	9,5%

The influence of the driving dynamics on the simulation result is briefly investigated below. As an example, the RDC 1 cycle is considered and the difference between measured- and simulated CO emissions over the cycle engine power over time is displayed, see figure 6.6.

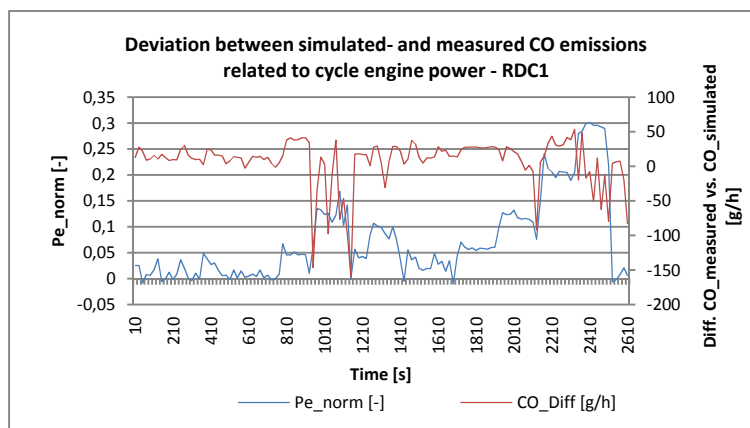


**Figure 6.6:** Deviation between simulated and measured CO emissions related to cycle engine power in RDC1 cycle.

Here, it becomes clear that deviations between the measured and simulated CO emissions occur in cycle segments in which high engine loads due to accelerations or gradient sections are necessary. For the further simulations in chapter 6.4, this means that the uncertainty of the simulation of the 28 TREMOD motorcycle traffic situations decreases with increasing cycle time and decreasing cycle dynamics: a) the longer the cycle, the less is the individual emission peak influence on the overall result b) the lower the dynamics of the driving cycle the lower is the probability of occurrences of emission peaks.

In figure 6.7, the duration and the RPA values of the 28 motorcycle traffic situations in TREMOD are presented. Most of the TREMOD traffic situations show a rather short duration of less than 10 minutes. As already investigated in chapter 5.1.4.3 the driving dynamic increases with decreasing average cycle speed as existing primarily in urban traffic situations. The TREMOD urban traffic situations are characterized mostly by short durations linked with high RPA values. Thus, one can assume that the emission simulation of these urban traffic situations is affected by greater uncertainties contrasted with the motorway- and rural traffic situations.

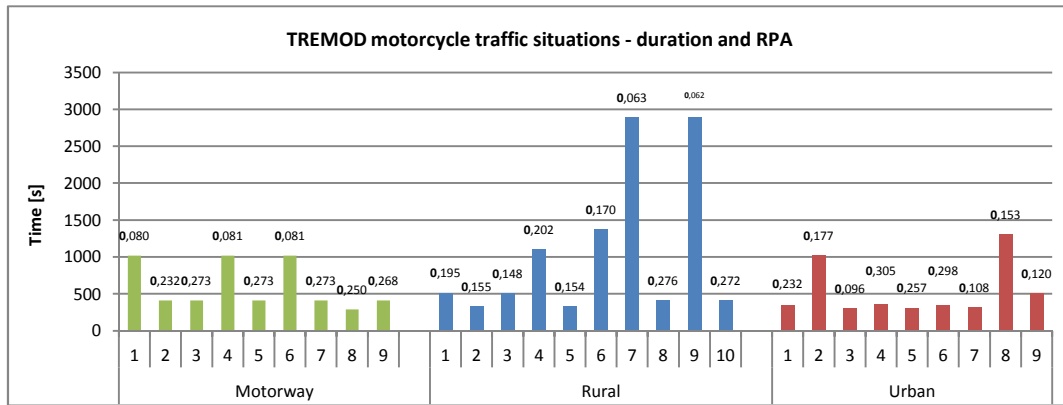


Figure 6.7: Duration and RPA values of the individual TREMOD motorcycle traffic situations.

### 6.2.3 Re-simulation of the On-board Trips

The on-board trips were re-simulated with PHEM based on the emission maps generated from the on-board measurement program, both on a cumulative and second-by-second basis. Again, all simulated test runs were composed together and only the hot emissions were concerned. The PHEM gear shift model was applied for calculating the required gear and engine speed information. The simulation results are presented in figures 6.8. Contrary to the dynamometer measurement simulations, adjustments in the application of driving resistance data in PHEM were necessary in order to capture the real-world driving conditions of the conducted test drives on the road. The air resistance coefficient  $C_w$  and the cross sectional area  $A_f$  of the test vehicle with the PEMS system were estimated based on my own assumptions and literature information [2.2].

Since the rolling resistance coefficient could not be derived directly from the measurements, it was determined via a parameter variation approach in PHEM. For this purpose, the other relevant driving resistance data  $C_w$ ,  $A_f$ , and  $C_w \times A_f$  were fixed and the rolling resistance coefficient was varied until the simulated  $CO_2$  emissions of the on-board trips corresponded to the  $CO_2$  emission results from the measurement. Thus, the simulated engine power also corresponded to the engine power demand during the trips. As a result of this approach, a rolling resistance coefficient of 0,0249 was determined. The literature indicates values of 0,015 – 0,02 for the friction pairing of motorcycle-tires and road pavements [2.2]. The relevant driving resistance data used in PHEM for the on-board trip re-simulations are listed in table 6.3. There is an additional driving resistance due to the alternator, however, compared to the above-mentioned resistance forces, the additional resistance due to the electric machine is comparably low (max. 400 W electric power) and therefore PHEM standard settings are adopted.

Table 6.3: Driving resistance data for on-board trip re-simulations in PHEM.

Vehicle reference mass including driver [kg]	Vehicle loading [kg]	Air resistance coefficient $C_w$ [-]	Cross sectional area $A$ [m <sup>2</sup> ]	$C_d \times A$ [m <sup>2</sup> ]	Rolling resistance coefficient $FRO$ [-]
270	80	0,8	1,35	1,08	0,0249

Figure 6.8 presents the PHEM re-simulation results for the on-board trips for CO<sub>2</sub>, CO and NO<sub>x</sub> emissions compared to the emission measurement results – on a second-by-second basis and cumulatively. The deviations in the PHEM on-board trip simulations are partly more pronounced in contrast with the dynamometer measurement simulations, particularly in the field of the pollutant components CO and NO<sub>x</sub> – the deviations here are approx. + 34,6 % in CO- and approx. – 12,8 % in NO<sub>x</sub> emissions. Overall, the simulated CO emission level is higher pronounced opposed to the measured CO emission level. Due to many high engine load phases during the on-board trips combined with positive road gradient sections, correspondingly more CO emission peaks occurred. However, the emission peaks are better reflected in the on-board trip simulation routine due to a significantly better coverage of the on-board CO emission map compared to the dynamometer CO emission map.

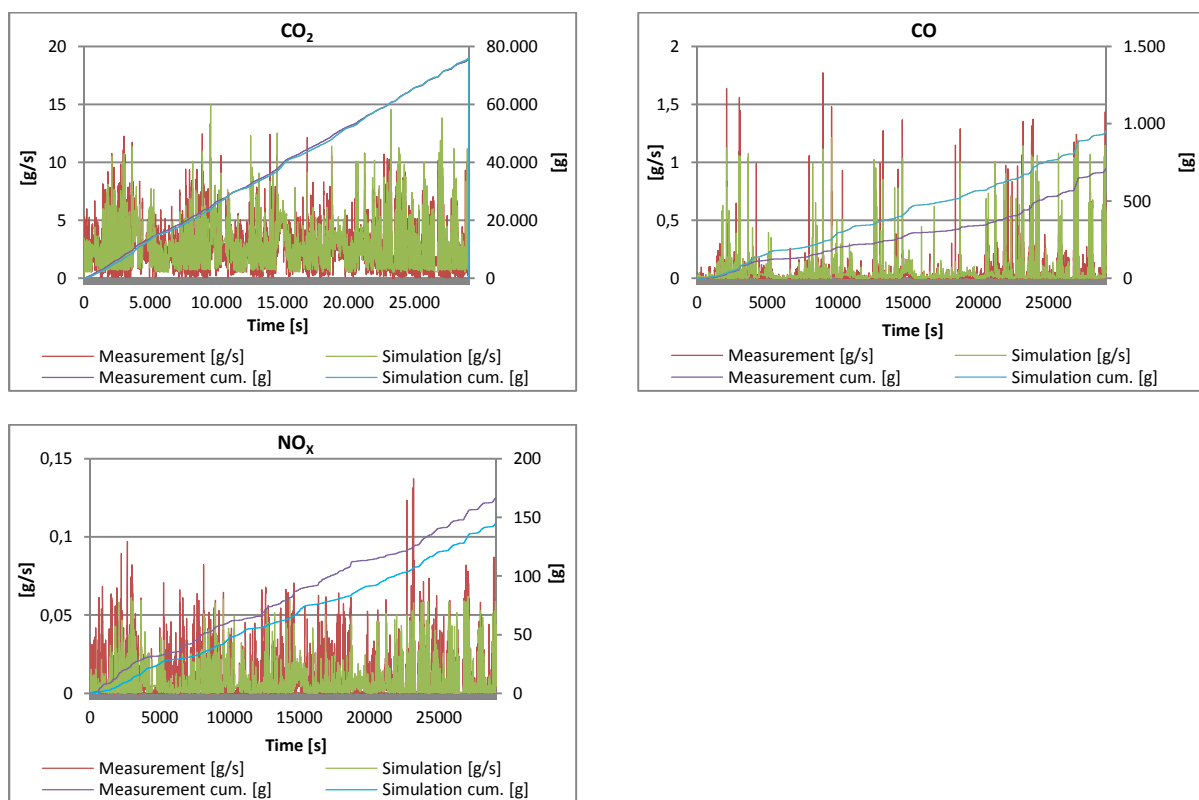


**Figure 6.8:** Second-by-second and cumulative on-board measurement results and PHEM simulation results based on emission maps generated from the on-board measurement program.

The measured CO emission peaks, however, are still more pronounced than the simulated ones. In the case of the NO<sub>x</sub> emission simulation, the cumulated simulation results are beneath the measured NO<sub>x</sub> emission level (- 12,8 %). Significantly more NO<sub>x</sub> emission peaks occur during the on-board trips opposed to the dynamometer measurements too, in which the measured NO<sub>x</sub>-peaks are also more pronounced compared to the simulated ones, which has the effect that the simulated- and measured cumulative NO<sub>x</sub> emission courses diverge increasingly over time. The CO<sub>2</sub> emission simulation led, as prescribed above, to correlating values compared to the measured CO<sub>2</sub> results (the deviation is approx. 0,5 %). Table 6.4 lists the deviations between the simulated- and measured emission results for the on-board trips.

**Table 6.4:** Deviation between the cumulative on-board emission measurement results and the PHEM simulation results of lined-up on-board trips based on emission maps generated from the on-board measurement program.

	CO <sub>2</sub>	CO	NO <sub>x</sub>
Deviation to the measurement results	0,5%	34,6%	-12,8%

The on-board trip simulation results indicate that the overall emission level of the CO emission map is partly too high pronounced, whereas it is slightly too low for the NO<sub>x</sub> emission map. In order to assess this issue more sophisticated, further on-board emission measurements are recommended with different motorcycle types and emission maps have to be generated and validated. In addition, the catalyst temperature should be taken into account then, since this parameter might change in the course of a measurement trip and affects the conversion rate of CO-, HC- and NO<sub>x</sub> emissions. As a result of this, different emission rates may occur under otherwise identical operating conditions. Besides this, some driving resistance parameters used in the simulation might be partly uncertain as they might change during a trip. Here, factors like a variable driver position or different road surface conditions have to be mentioned. Furthermore, changes in the air density due to altitude variations and ambient temperature changes within a measurement trip have an influence on the simulation results. Within the PHEM simulation settings, however, only fixed driving resistant values for parameters described above can be set for each simulation run. The influence of an inaccurate detection of the road gradient is relevant for the emission behavior as well, since the inclined road force affects the engine power demand and finally the emissions significantly. Particularly, when driving on curvy mountain roads, strong road gradient changes can be found within short distances, both over longitudinal- and also over the transverse direction of the road (curves), which makes it difficult to obtain robust road gradient signals. In chapter 6.2.4 the results of a parameter variation are presented in which the influence of different vehicle simulation parameters, e. g. vehicle loading, air resistance, rolling resistance, air density and the road gradient on CO<sub>2</sub>, CO and NO<sub>x</sub> emissions is examined.

#### 6.2.4 Driving Resistance Parameter Variation

The intention of the following driving resistance parameter variation is to evaluate the sensitivity of individual driving resistance parameters in the PHEM simulation process by modifying one driving resistance parameter in the calculation process, whereas the other calculation parameters remain the same. The simulation was carried out for different values of air density,  $C_{wx}A_f$ , vehicle loading, rolling resistance coefficient and road gradient. According to the generally valid driving resistance equation (see chapter 4.2.1.1) the driving resistance parameters have varying effects on the engine power demand resulting in a varying emission behavior of the vehicle. The driving resistance parameters were modified in 5 % steps and the variations in CO<sub>2</sub>, CO and NO<sub>x</sub> emission simulation results were recorded. The on-board trips – all trips again composed together – were simulated and compared to the baseline PHEM simulation results (reference results) described already in chapter

6.2.3. In figure 6.9 the PHEM simulation results of CO<sub>2</sub>, CO and NO<sub>x</sub> emissions for varying driving resistance data are presented.

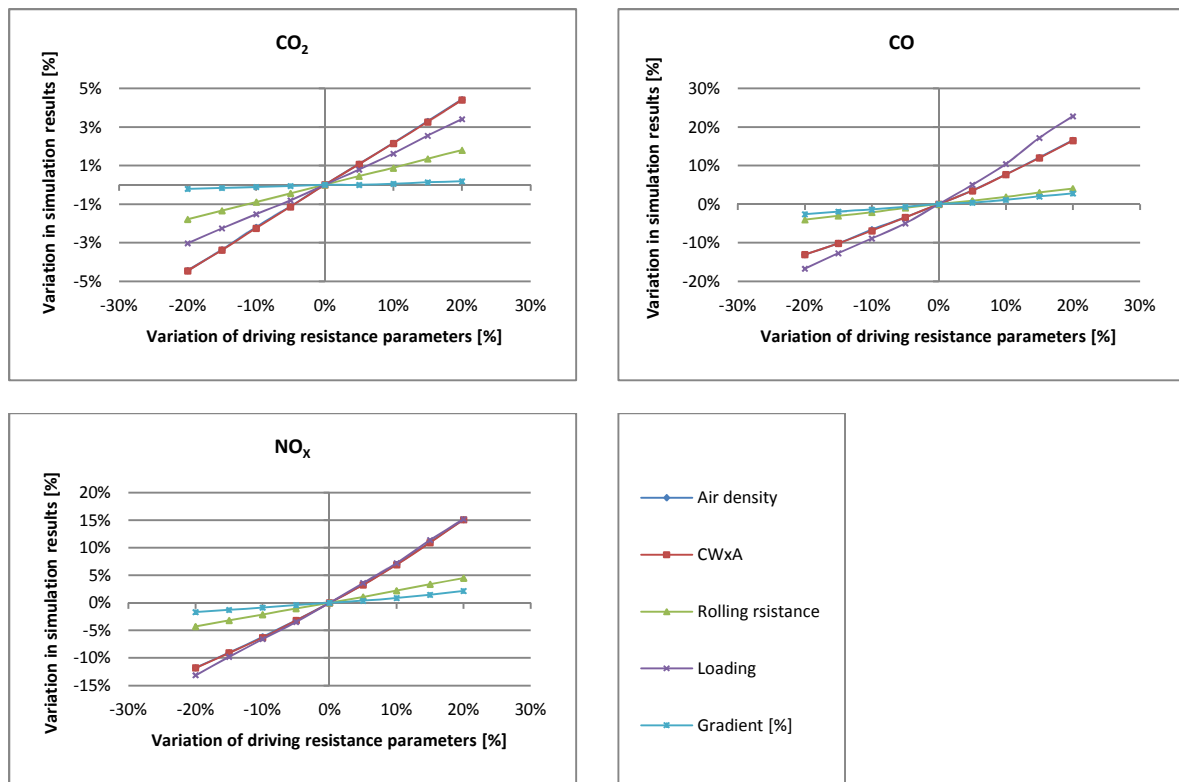


**Figure 6.9:** Deviation of the simulated, cumulated emission results (CO<sub>2</sub>, CO and NO<sub>x</sub>) of the on-board trips by variation of relevant driving resistance parameters in PHEM.

According to the driving resistance equation, a change in the air density and the  $C_{wxA_f}$  value leads to a linear change in the total driving resistance force. This effect leads almost to linear changes in the emission simulation results, see figure 6.9. Since a change in the air density value as well as in the  $C_w$  value has the same linear effect on the change in emissions, the course of the air density variation is identical to the  $C_w$  value variation course in figure 6.9. It should be noted, however, that only the effect of a varying air density value on the air resistance force can be investigated here. Varying air densities may also result in engine process-related variations (e. g. lower oxygen concentrations in the combustion process may result in decreasing engine power, provided that no altitude detection technology is installed – usually in vehicle concepts equipped with turbochargers), which may also affect the emission behavior of combustion engines. So, the air density related driving resistance force decreases with increasing altitude, but at the same time the engine power is likely to decrease as well. To what extent the second mentioned effect determines the emission behavior is not further investigated here.

The baseline PHEM re-simulation results of the on-board trips in chapter 6.2.3 were calculated based on a fixed air density value of  $\rho = 1,2 \text{ g/cm}^3$  which corresponds to an altitude above sea level of approx. 300 m (Graz city). The “Gaberl” mountain pass test drives cover altitudes up to approx. 1550 m, which corresponds to an air density decrease of approx. 11 % (corresponds to approx.  $\rho = 1,06 \text{ g/cm}^3$ ) contrasted to the baseline level (300 m). At this altitude level, the pollutant emissions CO and

$\text{NO}_x$  in the simulation decrease by about 8 % and  $\text{CO}_2$  by 2% due to decreasing air resistance forces. However, since the mountain pass route represent only a section of the on-board trip program, one can say that the effect of a varying air density during an on-board trip may have a minor relevance on the PHEM simulation results. By subdividing the mountainous road segments into sections according to different altitude levels and simulating these zones separately with adjusted air density values, the simulation results may become slightly more accurate. In the case of the TREMOD traffic situations, however, air density changes do not have to be taken into account, since they do not contain any road gradient sections in the motorcycle segment.

Overall, a high variability in the PHEM simulation results can be identified by varying the  $C_w \times A_f$  value. In the case of a 20 % up-shift of the  $C_w \times A_f$  parameter in PHEM the deviations from the basic PHEM simulation result are approx. + 4,5 % for  $\text{CO}_2$  and approx. + 16 % for the pollutant components CO and + 15 % for  $\text{NO}_x$ . Against the background that both,  $C_w$  and  $A_f$  are difficult to estimate for the on-board vehicle configuration with the PEMS-setup, a higher deviation between the simulation and the measurement results may occur. In the motorcycle segment of sport-tourer machines the literature indicates  $C_w$  values of approx. 0,4 - 0,5 (drivers position: sitting) and 0,35 - 0,45 (drivers position: lying down), which corresponds to a variability up to 20 - 30 % in the  $C_w$  value for the same vehicle configuration. Added to this, the PEMS measurement setup and the resulted modification of the vehicle's front area, additional flow resistances (EFM tube), as well as a possible changing in the drivers position during a trip lead to a high sensitivity of the  $C_w \times A_f$  value in the measurement. However, it should be noted that the air resistance force is primarily affected by the vehicle speed as it increases with the square of the vehicle speed. Thus, an increased sensitivity on the simulation results is expected particularly in higher speed ranges.

The variation of the total vehicle mass shows a major influence on the driving resistance forces and finally on the emission simulation results. Deviations from the reference simulation values of approx. + 3,5 % for  $\text{CO}_2$ , + 15 % for  $\text{NO}_x$  and up to + 23 % for CO - simulated with + 20 % extra vehicle loading occur. In the PHEM simulation routine, however, only a very small uncertainty on the simulated emission results is expected since the total vehicle mass can be determined exactly before each measurement trip. Taking into account the test vehicles fuel tank volume of 15 l, a vehicle weight variability of approx. 3 % based on 350 kg total vehicle weight may occur during a trip due to fuel consumption. As a result of this, the impact on the pollutant emissions is less than 3 % according to PHEM.

The rolling resistance coefficient and the road gradient show the slightest influence on the PHEM simulation result in this analysis. Deviations from the baseline reference are below 5 % for all emission components concerned, again calculated for a 20 % increase in the respective resistance parameters. It is expected, however, that the difference between the recorded and the actual road gradient is sometimes significantly greater, e. g. in narrow road curves on mountain roads, resulting in pollutant emission peaks. The GPS based gradient determination might reach its system limits here. Possibly, an inclinometer based approach that includes the continuous measurement of the vehicles longitudinal angle makes more sense in future research projects.

Based on the presented above driving resistance parameter variation, a high degree of sensitivity in the PHEM simulation process was identified due to difficulties in the determination of robust driving resistance parameters in the motorcycle segment - both as a result of the complex measurement setup itself and due to parameter variations during the measurement trips. Therefore,

---

comprehensive driving investigations – e. g. coast-down tests for the determination of real-world driving resistance data for different vehicle / driver configurations in the motorcycle segment are necessary in order to optimize the driving resistance settings in PHEM. Optionally, in the course of such investigations, the influence of different road pavements and surface conditions as well as cross wind effects at different wind speeds may be investigated in order to minimize uncertainties in rolling resistance coefficients in the simulation process.

### 6.3 Vehicle Configuration for the TREMOD / HBEFA Emission Factor Simulation – Approach

As already mentioned in Chapter 4, the emission inventory models like TREMOD or COPERT are intended to map the emission behavior of average vehicle types of the vehicle fleet. However, within the measurement program performed in this study two motorcycle configurations were used, which both do not reflect real-world driving. On the one hand, the on-board vehicle configuration, which is characterized by above average high payload and air resistance values, as well as the dynamometer vehicle configuration, in which the driving resistance values are clearly too low compared to driving resistance values occurring in real-world traffic. Consequently, an approach was elaborated in which a real-world vehicle configuration (Real world VEH) was defined for the simulation of the motorcycle emission factors in TREMOD. Herein, real-world driving resistance data were derived from literature information and from the test vehicle configurations from the measurement programs. Table 6.5 displays the real-world vehicle configuration (right column) as applied in the subsequent simulations compared to the on-board- (RDE VEH) and the dynamometer- (dynamometer VEH) vehicle configuration from the measurement program.

**Table 6.5:** Different test vehicle configurations in comparison; on-board, dynamometer and real-world test vehicle configuration.

	RDE VEH (on-board)	Dynamometer VEH	Real-world VEH
Vehicle mass including driver [kg]	270	270	270
Vehicle loading [kg]	80	0	0
$C_w$ value [-]	0,8	0,447	0,447
Cross sectional area $A_f$ [m <sup>2</sup> ]	1,35	1,17	1,17
$C_w \times A$	1,08	0,52	0,52
Rolling resistance coefficients $f_{RO}$	0,0249	0,0071 (WMTC Norm)	0,02 (literature)

The unladen vehicle weight plus approx. 75 kg (corresponds to a driver's normal weight) was chosen for the real-world vehicle configuration approach (approx. 270 kg). This vehicle mass corresponds to the one of the dynamometer vehicle configuration and reflects a typical motorcycling situation with regard to total vehicle mass. The air resistance coefficient  $C_w$ , the vehicle front area  $A_f$  and  $C_w \times A_f$  in the real-world vehicle configuration are adopted from the dynamometer vehicle configuration. The rolling resistance coefficient was taken from literature references and a constant value of 0,2 was applied for the real world vehicle configuration. The rolling resistance coefficient is approx. 20 % below the approximated value of the on-board vehicle configuration and approx. three times higher than the value applied in the dynamometer measurement program. Consequently, the real-world

vehicle configuration is between the on-board- and the dynamometer vehicle configuration with regard to driving resistance data. However, one driver without additional load represents the lower limit for typical driving - higher loads (two persons or extra luggage) are certainly possible in real-world driving.

In order to evaluate the PHEM simulation for different vehicle configurations, the test drives were simulated with PHEM again - an assessment for the most suitable vehicle / emission map configuration for the simulation of the TREMOD motorcycle emission factors was elaborated from this. The emission measurements performed – again, all on-board- and dynamometer measurements lined up - were simulated based on the on-board- and the dynamometer emission maps for all three vehicle configurations and for all emission components. The cumulative simulation results were contrasted with the measurement results. First, the on-board trips were re-simulated this way; the results are presented in figure 6.10. The absolute deviation between the simulation results for the real-world vehicle configuration and the measurement is indicated in table 6.6. As described in chapter 6.1.1 the CO<sub>2</sub> emission maps generated from the on-board- and the dynamometer measurements are almost identical; therefore, only the simulation results calculated based on the CO<sub>2</sub> dynamometer emission map are shown in figure 6.10.

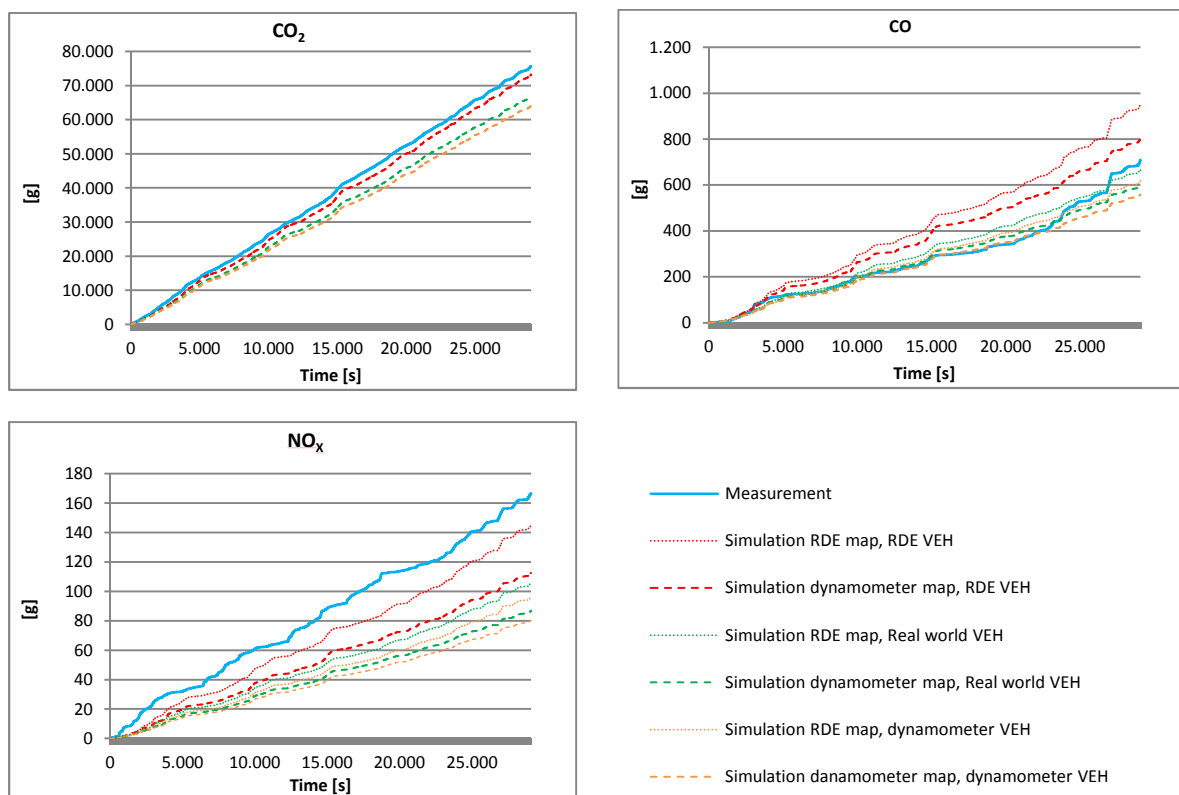


**Figure 6.10:** Cumulative PHEM simulation results for the on-board measurement trips based on on-board- and dynamometer emission maps for different vehicle configurations; comparison of measurement results.

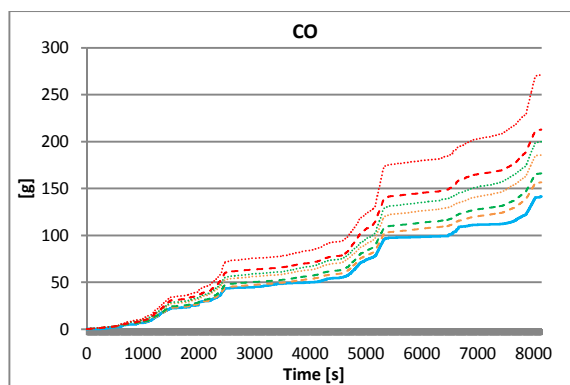
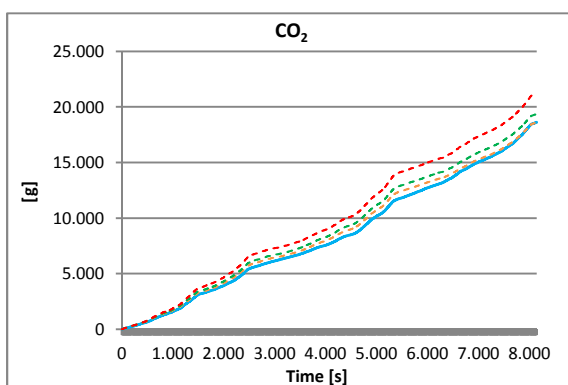
The course of the cumulative emissions for the real-world vehicle configuration (real-world VEH) lies between the simulation results of the on-board- (RDE VEH) and dynamometer vehicle (dynamometer VEH) configuration, both for the simulation with on-board- and dynamometer emission maps. The

simulation results based on the on-board emission maps are closer to the measurement for all emission components, as the level of the on-board emission maps is generally higher in contrast to the dynamometer emission maps. It should be noted at this point that the deviation in the results of the real-world vehicle simulation compared to the measurement results has no relevance for assessing the simulation quality with PHEM as such; only simulations with the same vehicle configuration as applied in the measurement are suitable therefore – e. g. on-board trip measurement results compared to simulation results with the on-board vehicle configuration (RDE VEH) and on-board emission maps; respectively dynamometer measurement results compared to simulation results with dynamometer emission maps and the dynamometer VEH configuration. This assessment was already performed in chapters 6.2.2 and 6.2.3 and yielded acceptable simulation results. In the case of an ideal PHEM simulation (elimination of all possible uncertainties in the simulation process and ideal emission measurement data) the simulation results with on-board- and dynamometer emission maps would be almost identical.

**Table 6.6:** Deviations between the on-board trip re-simulation results and the emission measurement results for the “real-world vehicle configuration”; simulation based on on-board and dynamometer emission maps.

	CO <sub>2</sub>	CO	NO <sub>x</sub>
Deviation between real-world VEH. simulation (dynamometer map) and measurement	-8%	-15,7%	-47,8%
Deviation between real-world VEH simulation (RDE map) vs. measurement	-8%	-6,1%	-36,4%

The figures 6.11 show the re-simulations results of the dynamometer measurements for different vehicle / emission map configurations. HC- and CH<sub>4</sub> emissions were simulated additionally, since these measurement data were only available from the dynamometer measurement program – accordingly, the HC- and CH<sub>4</sub> simulations were carried out only with dynamometer emission maps.



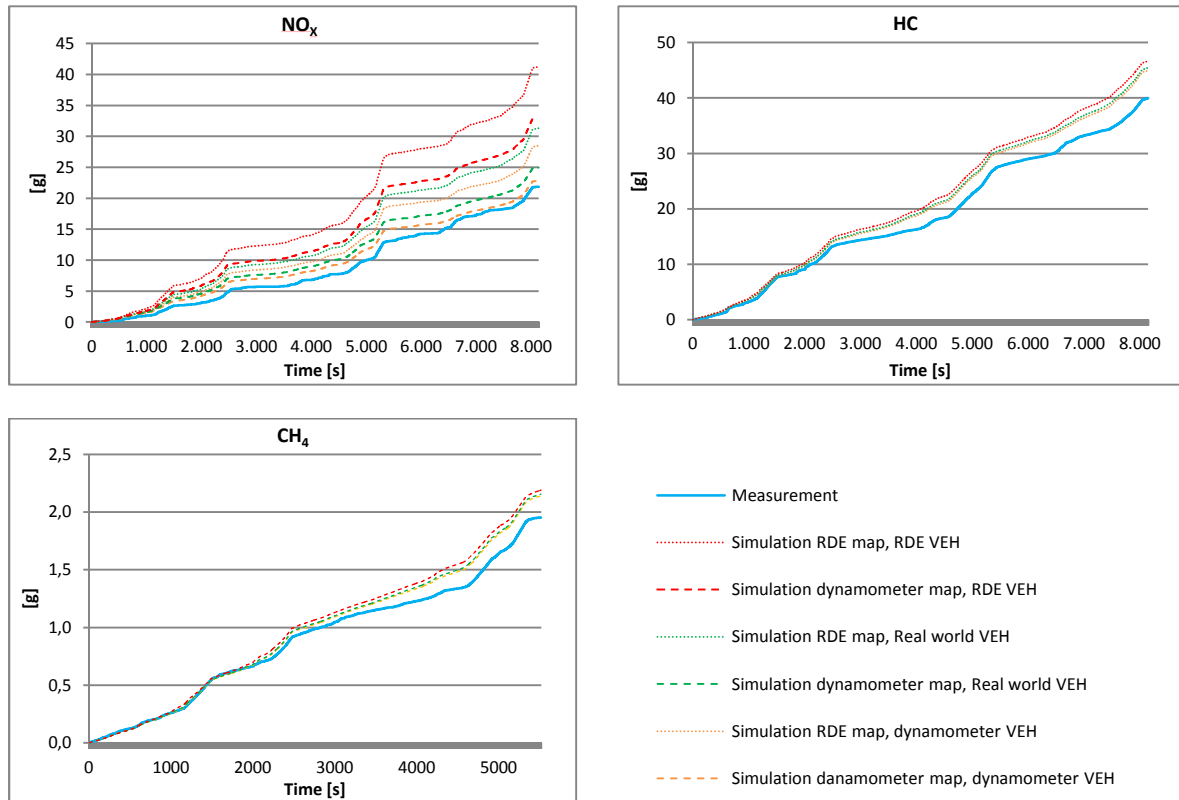


**Figure 6.11:** Cumulative simulation results for dynamometer measurements based on on-board- and dynamometer emission maps for different vehicle configurations; comparison of measurement results.

Again, the simulation results of the real-world vehicle configuration lie between the simulation results of the RDE VEH- and the dynamometer VEH configuration. Contrary to the on-board trip simulations, all cumulative simulation results here are above the measurement results, since the driving resistance data of the real-world vehicle configuration are higher than the values applied in the dynamometer measurement program, see table 6.7.

**Table 6.7:** Deviation between the dynamometer measurement re-simulation results and the emission measurement results for the “real-world vehicle configuration”; simulation based on on-board and dynamometer emission maps.

	CO <sub>2</sub>	CO	NO <sub>x</sub>	HC	CH <sub>4</sub>
Deviation between real-world VEH. simulation (dynamometer map) vs. measurement	8,1%	17,2%	14,1%	13,5%	10,3%
Deviation between real-world VEH. simulation (RDE-map) vs. measurement	8,1%	41,1%	43,1%	-	-

Deviations in CO and NO<sub>x</sub> simulation results may be assigned to various uncertainties in the simulation and measurement routine. Relevant driving resistance parameters were investigated extensively in chapter 6.2.4. Uncertainties in the on-board measurement equipment (e. g. the PEMS system, EFM tube etc.) cannot be further investigated here. However, the stationary emissions measurements on the chassis dynamometer using the PEMS system at the same time revealed that certain deviations between both measuring systems are not avoidable. Not least, in the field of the

RDE legislation development emission limit values are adapted to the accuracy and robustness of the on-board measurement devices.

Additional emission measurements as well as further developments in PHEM, e. g. exhaust gas after-treatment simulation tools, as already implemented in the passenger car and heavy-duty vehicle sector may help to improve the accuracy of the simulation. These uncertainties are not a motorcycle-specific problem, but occur in other vehicle categories as well, however, the development in PHEM is already more sophisticated and significantly more experience and measurement data are available (see publications on the ERMES website). It is assumed that the major part of the deviations between measurement and simulation is attributable to inadequate emission map coverage in high engine load areas and a lack of mapping of emission peaks, particularly for the pollutant components CO and NO<sub>x</sub>. By contrast, the CO<sub>2</sub> and thus the engine power simulation showed adequate results, which confirm that the engine power simulation in the motorcycle segment works already efficiently.

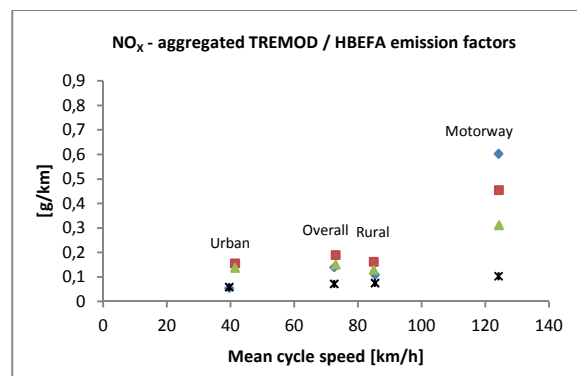
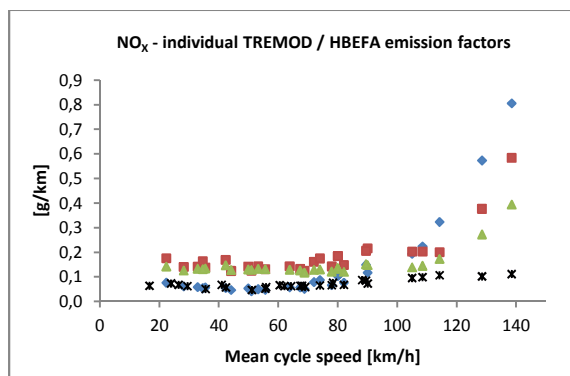
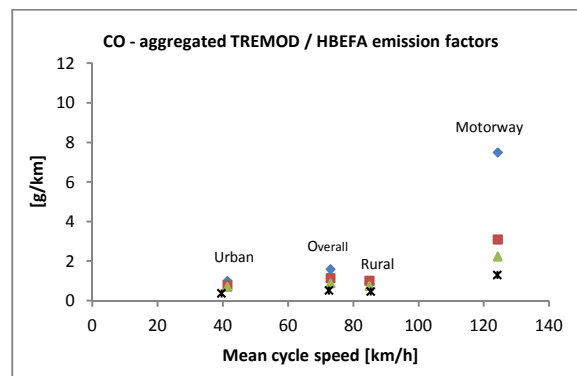
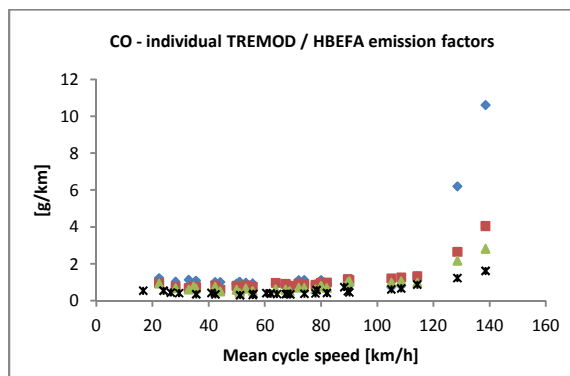
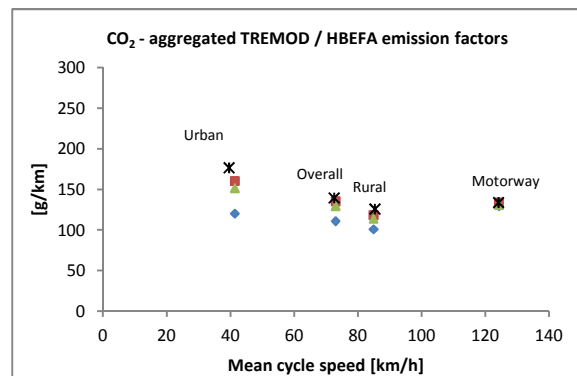
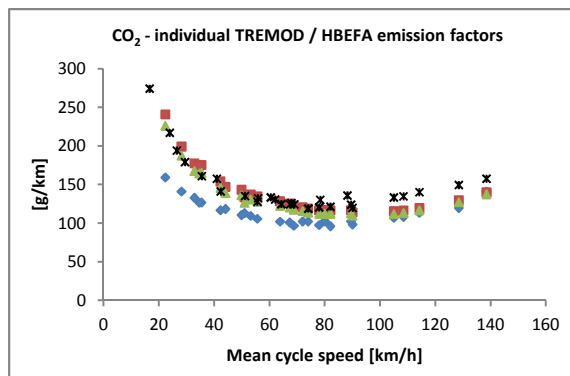
Not least due to a better coverage of the on-board emission maps, the simulation of the TREMOD motorcycle emission factors was carried out for the real-world vehicle configuration using the on-board emission maps, see chapter 6.4. The TREMOD motorcycle traffic situations show partly high driving dynamics, particularly in lower speed ranges, which would not be sufficiently represented by simulations based on the dynamometer emission maps. However, for comparison purposes, both simulation variants with the on-board- and the dynamometer emission maps were carried out.

#### **6.4 TREMOD Motorcycle Emission Factor Simulation**

The PHEM simulation results for the 28 TREMOD motorcycle emission factors for the vehicle segment “motorcycles, 4S, Euro 3, > 750 cm<sup>3</sup>, first registration year 2015” are presented below - the individual emission factor results and, additionally, the traffic-weighted emission factors aggregated according to local level, namely urban, rural, motorway and overall. The aggregated emission factors are traffic-weighted according to their traffic shares in the German motorcycle fleet according to TREMOD. As already mentioned in chapter 6.3, the PHEM simulations for the emission components CO<sub>2</sub>, CO and NO<sub>x</sub> are based on on-board- and dynamometer emission maps, whereas the HC- and CH<sub>4</sub> emission factor simulation is based only on emission maps generated from the dynamometer test program. The simulations were carried out with the PHEM batch mode, which allows simulating any number of driving cycles within one process step. It simplifies the simulation process particularly for HBEFA / TREMOD applications due to the high number of driving cycles implemented there. The following figures 6.12 show the simulation results of the 28 TREMOD motorcycle traffic situations compared to the existing emission factor database in TREMOD version 5.63 respectively HBEFA version 3.2 and HBEFA version 4.1. However, a direct comparison of the emission factors simulated in this project with those of the HBEFA 4.1 version is partly difficult, because the vehicle layer assignment in HBEFA 4.1 in the motorcycle segment has changed. Instead of the vehicle layer > 750 cm<sup>3</sup> (as applied in HBEFA v. 3.2), there will be only the vehicle layers > 250 cm<sup>3</sup> and < 250 cm<sup>3</sup> in the motorcycle segment future. As a result, the emission factors of the vehicle layer to which the test vehicle from this project belongs to are certainly lower in HBEFA 4.1, since vehicles of lower power- and displacement classes were used for the emission factor generation of this new created vehicle layer. For this reason, the comparison with HBEFA 4.1 emission factors is more a comparative purpose - since this study here includes partially work for the development of the HBEFA 4.1 version (among

---

others, the application of PHEM in the motorcycle segment). So, the HBEFA 4.1 values contrasted with the simulation results are indicated in figure 6.12 and table 6.8 only for comparison purposes. A further interpretation of the HBEFA 4.1 values is not included in the following paragraphs. Table 6.8 indicates the absolute emission values for the simulated, aggregated emission factors as well as the percentage deviation contrasted with the TREMOD / HBEFA 3.2 and 4.1 reference databases. It should be pointed out that the TREMOD / HBEFA motorcycle emission factors here reflect a fleet mix of the vehicle segment “motorcycles, 4S, Euro 3, > 750 cm<sup>3</sup>” between 2006 and 2016, while the simulation results represent one individual vehicle of this vehicle segment with the first registration year 2015.



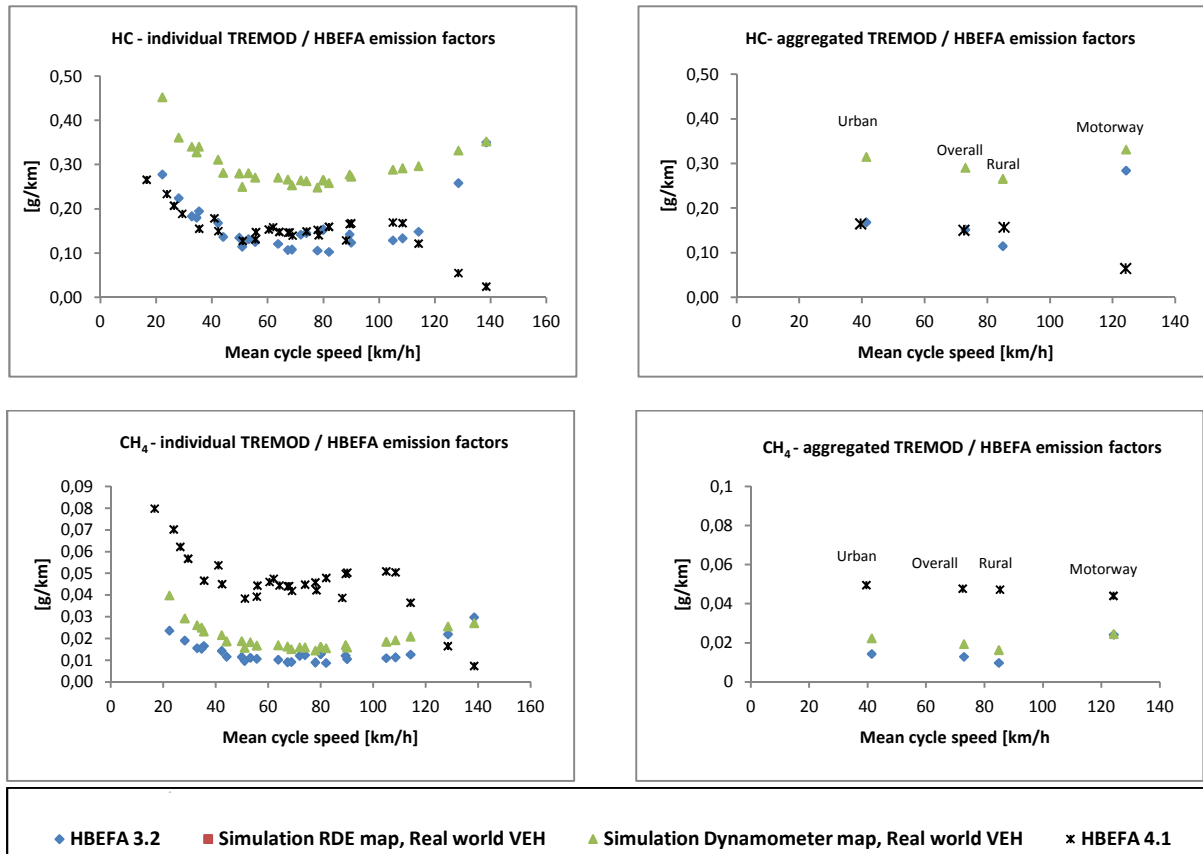


**Figure 6.12:** Comparison between the individual TREMOD 5.53 / HBEFA 3.2 and HBEFA 4.1 motorcycle emission factors for the vehicle segment “motorcycles, 4S, Euro 3, > 750 cm<sup>3</sup>” and the PHEM simulation results for the emission components CO<sub>2</sub>, CO, NO<sub>x</sub>, HC and CH<sub>4</sub> – simulation results with RDE (on-board) emission maps and dynamometer emission maps. Left column: individual emissions factors; right column: aggregated emission factors according to urban, rural, and motorway speed classes and overall.

The CO<sub>2</sub> emission factor simulation with PHEM resulted in overall higher emission values for all 28 TREMOD motorcycle emission factors compared to the TREMOD reference database, both for the individual- and aggregated emission factors simulated with both emission map variants. Due to the higher emission level of the on-board emission maps the simulation results based on these maps are higher compared to the emission factors simulated with the dynamometer emission maps. It is noticeable that the deviations to the TREMOD reference values decrease with increasing average cycle speeds. The deviation of the aggregated urban CO<sub>2</sub> emission factor simulated on the basis of the on-board CO<sub>2</sub> emission map contrasted with the TREMOD reference value is + 33,5 % (+ 26,1 % for the dynamometer CO<sub>2</sub> map simulation). Concerning the aggregated motorway driving cycles the deviation to the TREMOD reference is only + 3,5 % (on-board CO<sub>2</sub> map simulation) respectively + 1,2 % (dynamometer CO<sub>2</sub> map simulation). Typically, the individual CO<sub>2</sub> emission factors show a minimum in the speed range between approx. 70-90 km / h, because the engine power demand is minimal here. In lower speed ranges, however, frequent accelerations lead to increased CO<sub>2</sub> emissions, whereas at higher speeds (approx. > 90 km / h) the driving resistances increase significantly, resulting in increased fuel consumption and finally CO<sub>2</sub> emissions. It can be assumed that the test vehicle depicts a rather powerful / above-average vehicle of the TREMOD motorcycle segment “motorcycles, 4S, Euro 3, > 750 cm<sup>3</sup>” as both simulation variants (on-board- and dynamometer CO<sub>2</sub> map simulation) show generally higher CO<sub>2</sub> emission factors compared to the

TREMODO reference data. Overall, the deviation of the aggregated CO<sub>2</sub> emission factor lies in an acceptable range with approx. + 22,1 % (on-board CO<sub>2</sub> map simulation) and + 16,7 % for CO<sub>2</sub> for the dynamometer CO<sub>2</sub> map simulation.

The TREMOD CO emission factors show a strong increase towards higher average cycle speeds of the individual traffic situations compared to the PHEM simulation results. During high engine load phases motorcycle engines often operate with rich fuel / air mixtures and the fuel is not converted completely, resulting in an increase in CO- and HC emissions, see chapter 2.1.1. The deviation of the overall on-board CO map simulation results to the TREMOD reference is approx. – 28,4 %; the deviation of the overall dynamometer CO map simulation results to the TREMOD reference is even higher, namely approx. – 44,3 %. The TREMOD vehicle segment “motorcycles, 4S, Euro 3, > 750 cm<sup>3</sup>” represents engine technologies from 2006 to 2016 (time span in which Euro 3 was in force) so the CO emission level of vehicles manufactured at the lower end of this time span may be partly significantly higher compared to newly registered vehicles in this segment. It is assumed that these older vehicles shift the TREMOD CO emission factors upwards. However, there were no indications found within the measurement programs in this study showing average motorway CO emissions up to 7,5 g / km (aggregated motorway CO emission factor) as TREMOD / HBEFA indicates, which was finally also not reflected in the PHEM simulation results. In combination of a high weighting of individual motorway emission factors in TREMOD (e. g. the emission factor “Rural / motorway / 130 / freeflow” represents approx. 62 % of total motorway traffic in Germany with a CO emission factor of approx. 10,6 g / km according to TREMOD) the overall motorway CO emission factor is shifted upwards and finally also the overall CO emission factor increases. This once again shows the decisive influence of a robust traffic data allocation to the individual TREMOD traffic situation as it affects the emission calculation results of inventory models significantly. With regard to urban CO emissions, the on-board- and the dynamometer CO map simulation results are below the TREMOD reference (- 22,1 % within the on-board CO map simulation, respectively – 29,7 % within the dynamometer CO map simulation). The on-board CO map simulation results of the aggregated rural CO emission factor is slightly above the TREMOD reference (+ 16,4 %) – the dynamometer CO map simulation compared to the existing reference is slightly below, namely – 13,4 %.

Overall, the NO<sub>x</sub> emission factor simulation results lie above the TREMOD reference, namely approx. + 35,8 % within the on-board NO<sub>x</sub> map simulation respective + 8,2 % within the dynamometer NO<sub>x</sub> map simulation. The NO<sub>x</sub> emission factors slightly increase at lower speeds (urban traffic) and at higher speeds (motorway traffic). The latter case is due to the disproportionately high driving resistances, whereas in low speed ranges an increasing driving dynamic leads to an increase in accelerations and finally in NO<sub>x</sub> emissions. In the speed range of approx. 60 - 80 km / h, a minimum in NO<sub>x</sub> emissions is noticeable. In addition to engine power requirements, the level of NO<sub>x</sub> emissions is also affected by the temperature- and the general condition of the exhaust gas after-treatment system. Different driving styles lead to varying catalyst temperatures resulting in different NO<sub>x</sub> emission conversion rates during a measurement trip. The simulated, aggregated NO<sub>x</sub> emission factors for urban- and rural traffic are partly clearly above the TREMOD reference values: urban: + 185,7 % (on-board NO<sub>x</sub> map simulation), respective + 153,1 % (dynamometer NO<sub>x</sub> map simulation); rural: + 48,8 % and + 18,5 % simulated with on-board- and dynamometer NO<sub>x</sub> emission maps. The motorway NO<sub>x</sub> emission factors of the simulation are below the TREMOD reference, namely - 24,6 % (on-board NO<sub>x</sub> map simulation) and - 48,3 % (dynamometer NO<sub>x</sub> map simulation).

---

As already mentioned, HC and CH<sub>4</sub> emission factor simulation results are available only based on the dynamometer emission maps. The simulation results are partly disproportionately above the TREMOD emission factors - in total + 91,2 % (HC), in which the largest deviation can be determined for rural HC emission factors namely + 131,1 % and the lowest for motorway driving, namely + 16,6 %. HC emission factors also show a characteristic emission minimum in the speed range of 60-80 km / h due to before-mentioned physical effects. The simulated overall CH<sub>4</sub> emission factor lies approx. 50 % above the TREMOD / HBEFA 3.2 database. Largest deviations between the simulation results and TREMOD can be found in rural driving, namely + 67 %. However, with regard to the aggregated motorway CH<sub>4</sub> emission factor, the simulation results and the TREMOD datasets are almost identical (deviation approx. + 1,5 %).

**Table 6.8:** Deviation between the individual- and aggregated TREMOD / HBEFA motorcycle emission factors for the vehicle layer concerned “motorcycles, 4S, Euro 3, > 750 cm<sup>3</sup>” and the PHEM simulation results for emission components CO<sub>2</sub>, CO, NO<sub>x</sub>, HC and CH<sub>4</sub> – simulation with on-board- and dynamometer emission maps.

CO <sub>2</sub>	HBEFA 3.2 / TREMOD v. 5.53 [g/km]	HBEFA 4.1 [g/km]	Simulation results RDE map, Real world VEH [g/km]	Deviation from HBEFA 3.2 / TREMOD v. 5.53	Deviation from HBEFA 4.1	Simulation results dynamometer map, Real world VEH [g/km]	Deviation from HBEFA 3.2 / TREMOD v. 5.53	Deviation from HBEFA 4.1
∅ Urban	120,24	176,74	160,54	+33,5%	-9,2%	151,65	+26,1%	-14,2%
∅ Rural	100,96	125,92	118,46	+17,3%	-5,9%	113,96	+12,9%	-9,5%
∅ Motorway	129,37	133,89	133,96	+3,5%	+0,1%	130,90	+1,2%	-2,2%
∅ Overall	110,92	139,62	135,46	+22,1%	-3,0%	129,50	+16,7%	-7,2%

CO	HBEFA 3.2 / TREMOD v. 5.53 [g/km]	HBEFA 4.1 [g/km]	Simulation results RDE map, Real world VEH [g/km]	Deviation from HBEFA 3.2 / TREMOD v. 5.53	Deviation from HBEFA 4.1	Simulation results dynamometer map, Real world VEH [g/km]	Deviation from HBEFA 3.2 / TREMOD v. 5.53	Deviation from HBEFA 4.1
∅ Urban	1,01	0,38	0,79	-22,1%	+105,0%	0,71	-29,7%	+85,2%
∅ Rural	0,88	0,48	1,02	+16,4%	+111,9%	0,76	-13,4%	+57,6%
∅ Motorway	7,51	1,31	3,11	-58,6%	+137,1%	2,25	-70,1%	+71,5%
∅ Overall	1,60	0,53	1,15	-28,4%	+116,4%	0,89	-44,3%	+68,4%

NO <sub>x</sub>	HBEFA 3.2 / TREMOD v. 5.53 [g/km]	HBEFA 4.1 [g/km]	Simulation results RDE map, Real world VEH [g/km]	Deviation from HBEFA 3.2 / TREMOD v. 5.53	Deviation from HBEFA 4.1	Simulation results dynamometer map, Real world VEH [g/km]	Deviation from HBEFA 3.2 / TREMOD v. 5.53	Deviation from HBEFA 4.1
∅ Urban	0,054	0,058	0,155	+185,7%	+164,5%	0,137	+153,1%	+134,4%
∅ Rural	0,109	0,074	0,162	+48,8%	+115,8%	0,129	+18,5%	+71,8%
∅ Motorway	0,603	0,103	0,455	-24,6%	+341,0%	0,312	-48,3%	+202,1%
∅ Overall	0,139	0,071	0,189	+35,9%	+163,4%	0,151	+8,2%	+109,6%

<b>HC</b>	<b>HBEFA 3.2 / TREMOT v. 5.53 [g/km]</b>	<b>HBEFA 4.1 [g/km]</b>	<b>Simulation results RDE map, Real world VEH [g/km]</b>	<b>Deviation from HBEFA 3.2 / TREMOT v. 5.53</b>	<b>Deviation from HBEFA 4.1</b>	<b>Simulation results dynamometer map, Real world VEH [g/km]</b>	<b>Deviation from HBEFA 3.2 / TREMOT v. 5.53</b>	<b>Deviation from HBEFA 4.1</b>
<b>∅ Urban</b>	0,169	0,165	-	-	-	0,315	+86,8%	+90,7%
<b>∅ Rural</b>	0,115	0,157	-	-	-	0,266	+131,1%	+69,0%
<b>∅ Motorway</b>	0,284	0,065	-	-	-	0,332	+16,6%	+409,9%
<b>∅ Overall</b>	0,152	0,15	-	-	-	0,291	+91,2%	+92,8%

<b>CH<sub>4</sub></b>	<b>HBEFA 3.2 / TREMOT v. 5.53 [g/km]</b>	<b>HBEFA 4.1 [g/km]</b>	<b>Simulation results RDE map, Real world VEH [g/km]</b>	<b>Deviation from HBEFA 3.2 / TREMOD v. 5.53</b>	<b>Deviation from HBEFA 4.1</b>	<b>Simulation results dynamometer map, Real world VEH [g/km]</b>	<b>Deviation from HBEFA 3.2 / TREMOD v. 5.53</b>	<b>Deviation from HBEFA 4.1</b>
<b>∅ Urban</b>	0,014	0,049	-	-		0,022	+56%	-54,9%
<b>∅ Rural</b>	0,010	0,047	-	-		0,016	+67,3%	-65,3%
<b>∅ Motorway</b>	0,024	0,044	-	-		0,025	+1,5%	-44,3%
<b>∅ Overall</b>	0,013	0,047	-	-		0,019	+50,1%	-59,4%

## 7. TREMOD Motorcycle Emission Trend Scenario Calculation

The emission factors simulated with PHEM in chapter 6.4 are implemented in TREMOD and trend scenarios for the TREMOD vehicle segment “motorcycles, 4S, Euro 3, > 750 cm<sup>3</sup>, first registration year 2015” are calculated for the period 2015 – 2025 in this chapter. The calculations for the emission components CO<sub>2</sub>, CO, NO<sub>x</sub>, HC and CH<sub>4</sub> are based on the emission factors generated by on-board- and dynamometer measurements and the results are contrasted with the TREMOD baseline scenario, which includes emission factors from HBEFA 3.2. All trend scenario results are indicated for overall traffic and differentiated according to local area namely urban, rural and motorway. The vehicle fleet composition and the annual traffic data including the traffic distribution according to the traffic situation scheme are not changed. In Chapter 7.2, emission trend scenarios for certain non-regulated pollutant components are compiled based on average emission results gained from the FTIR measurement program in this study (see Chapter 5.3). This procedure is intended to make initial statements on the relevance of these pollutant components in Germany, of which some are classified as climate-relevant and partially harmful to human health. Based on cold-start emission data for CO- and HC-emissions determined in the measurement program combined with existing start / stop distribution data in TREMOD, the additional emission shares caused due to cold-starts are calculated and added to the hot emission scenario results. Thus, the relevance of cold-start surcharges to the total emissions in this vehicle segment should become clear. Furthermore, the distribution of cold-start shares according to local area is elaborated. Finally, within a detailed HC emission trend scenario, all relevant HC emission sources from motorcycles are taken into account, namely hot, cold-start- and evaporative emission data (chapter 7.4). On the one hand, the distribution of HC emission shares according to the underlying sources and, additionally, according to local area should become clear.

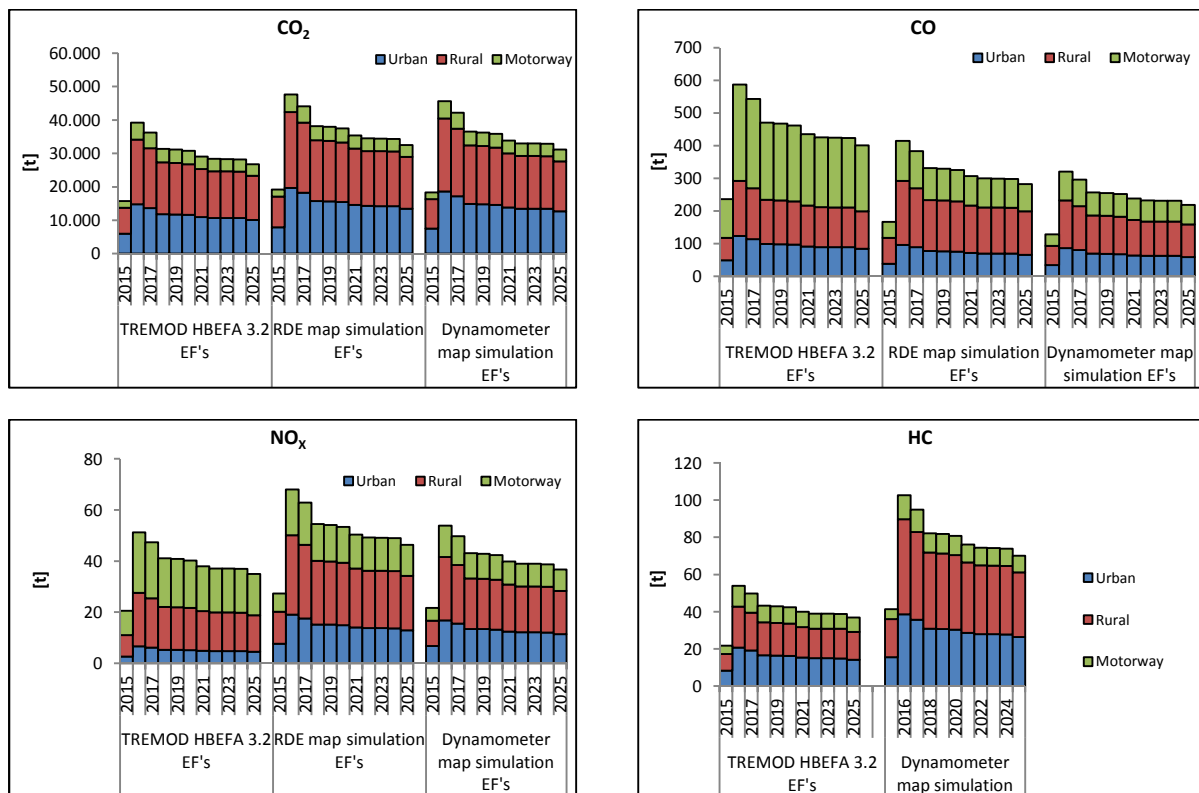
### 7.1. CO<sub>2</sub> and Regulated Emission Trend Scenario Results

Figure 7.1 demonstrates the TREMOD hot-emission trend scenario results for the emission components CO<sub>2</sub>, CO, NO<sub>x</sub> and HC in the period 2015 - 2025 for the TREMOD vehicle segment “motorcycles, 4S, Euro 3, > 750 cm<sup>3</sup>, first registration year 2015”; the TREMOD baseline scenario including the emission factors from HBEFA 3.2 (left) as well as the trend scenarios calculated based on the simulated on-board (RDE) emission factors (center) and the dynamometer emission factors (right). The results are differentiated according to local area. The deviations from the TREMOD baseline scenario results are listed in table 7.1.

It has to be considered here, that TREMOD averages the vehicle stock numbers of two subsequent years – e. g. 1. January 2015 (almost no vehicles of the vehicle segment concerned approved in the market) and 1. January 2016 (already a large number of vehicles approved and inside the German vehicle fleet) and thus the emission results in the scenario year 2015 are approximately half compared to the results of the following years. Thus, the number of registered vehicles with first registration year 2015 has its maximum value in 2016 and decreases according to the underlying TREMOD vehicle survival curves up to 2025 as vehicles leave the market. According to the mileage-age relation functions in TREMOD, vehicles show highest annual traffic within the first registration

---

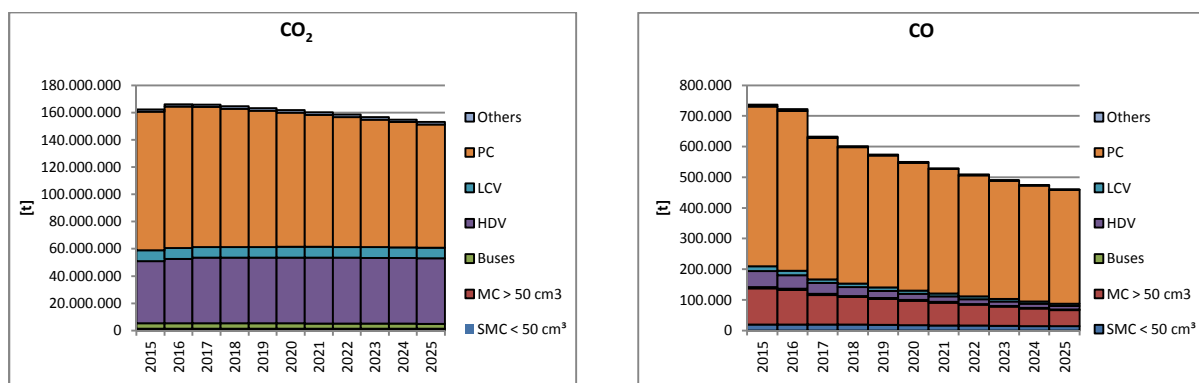
years. This means that vehicles approved in 2015 show highest annual traffic in 2015 and 2016 – then, the annual traffic decreases with increasing vehicle age up to 2025. The distribution of driving shares to the traffic situation scheme and to aggregated urban, rural and motorway level, however, remains the same for each year according to TREMOD. Additionally, the emission factors applied in the scenario calculations are the same for each year although one can assume that the emission behavior of a vehicle deteriorates with increasing age. However, deterioration factors for the individual exhaust gas components are not depicted in TREMOD in this vehicle category. In the case of CO<sub>2</sub>, deterioration effects are deemed to be less relevant as the fuel consumption changes only slightly over the life cycle of a motor vehicle, however, emission components that are significantly affected by the exhaust gas after-treatment system may be subject to aging effects to a higher extent. In other vehicle categories, this effect is partly taken into account by using vehicles with different odometer levels for the emission map and finally emission factor generation. Thus, the mean emission behavior over different stages of aging is mapped. Due to aforementioned aspects, the percentage change in emissions over the years is the same for all emission components, both, for the TREMOD baseline scenario and for the scenarios calculated with on-board- and the dynamometer emission factors – the change is only based on the decrease in traffic and due to the decrease in the vehicle stock over the years.



**Figure 7.1:** CO<sub>2</sub>, CO, NO<sub>x</sub> and HC-Emission trend scenario results for the TREMOD vehicle segment “motorcycles, 4S, Euro 3, > 750 cm<sup>3</sup>, first registration year 2015” for the period 2015 – 2025; TREMOD basic scenario (left) and TREMOD calculations with RDE (on-board) emission factors (center) and dynamometer emission factors (right).

The overall CO<sub>2</sub> emissions are approx. 22 % above the TREMOD baseline scenario results using the on-board CO<sub>2</sub> emission factors as input parameters; the dynamometer CO<sub>2</sub> emission factors lead to an increase of approx. 16 % compared to the TREMOD reference. Whereas the changes are rather pronounced for urban CO<sub>2</sub> emissions (+ 23 % calculated with on-board CO<sub>2</sub> emission factors and + 26 % by using the dynamometers CO<sub>2</sub> emission factors), there is almost no difference to the baseline scenario in motorway CO<sub>2</sub> emissions (+ 3 %). The overall decrease in CO<sub>2</sub> emissions from 2016 (highest CO<sub>2</sub> emission quantity in this vehicle segment) up to 2025 is approx. 31 % - this percentage decrease applies to all scenario variants. In the case of the CO emissions, the deviation of the simulation results based on on-board- and dynamometer CO emission factors to the TREMOD baseline scenario is higher pronounced compared to CO<sub>2</sub>. According to the significantly lower motorway CO emission factors generated with PHEM, the results of the total German CO emissions of the vehicle segment concerned are also significantly lower. The motorway CO emission scenario results calculated with on-board- and dynamometer CO emission factors are approx. 60 %, resp. 70 % lower than the TREMOD baseline scenario indicates. Concerning rural and urban CO emissions, the TREMOD simulation results based on on-board - and dynamometer CO emission factors lie in a range of approx. + 16 % to -29 % compared to the baseline scenario. With regard to the NO<sub>x</sub> emission development in Germany, the urban- and rural NO<sub>x</sub> emissions calculated with the simulated NO<sub>x</sub> emission factors are significantly higher pronounced than the TREMOD baseline scenario indicates (up to + 185 % for urban NO<sub>x</sub> emissions calculated with on-board NO<sub>x</sub> emission factors), whereas the motorway NO<sub>x</sub> shares are smaller contrasted to the TREMOD baseline scenario results (approx. - 24 % for the on-board NO<sub>x</sub> emission factors and - 48 % for the dynamometer NO<sub>x</sub> emission factors). The overall NO<sub>x</sub> emission scenario results simulated with the new NO<sub>x</sub> emission factors increase by + 36 % (on-board NO<sub>x</sub> emission factors) and + 8 % (dynamometer NO<sub>x</sub> emission factors) respectively. The overall HC emission results based on the dynamometer HC emission factors are approx. + 91 % higher compared to the baseline scenario. In particular, the urban and rural scenario results are significant above the results of the TREMOD reference, namely + 86 % for urban and + 131 % for rural traffic.

For comparison purposes, the overall CO<sub>2</sub>, CO, NO<sub>x</sub> and HC emission developments of the total German vehicle fleet in the same period in question are presented in figure 7.2. This includes all relevant vehicle categories that are reflected with TREMOD, namely passenger cars (PC), heavy-duty vehicles (HDV), Buses, light commercial vehicles (LCV), motorcycles (MC > 50 cm<sup>3</sup>), small motorcycles (SMC < 50 cm<sup>3</sup>) and other vehicle concepts.



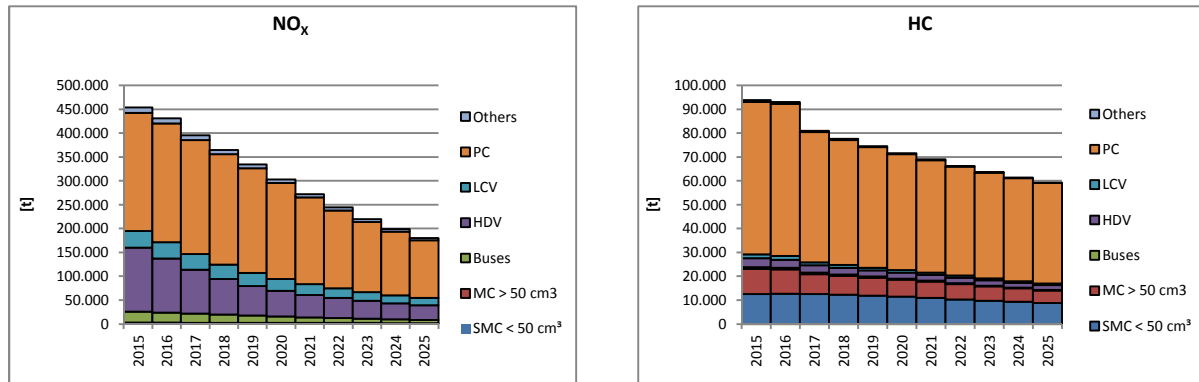


**Figure 7.2:** Overall CO<sub>2</sub>, CO, NO<sub>x</sub> and HC emissions of the German vehicle fleet for the period 2015 – 2025 according to TREMOD including all relevant vehicle categories.

The partly high emission level of powered two-wheelers is also reflected in the entire emission trend scenarios calculated with TREMOD. While the share of powered two-wheelers emissions to the total German road emissions for CO<sub>2</sub> and NO<sub>x</sub> is negligibly low (< 1 % in 2016), it represents a considerable proportion in the field of the pollutant components CO and HC (approx. 18 % and 24 %). The results of the scenario calculation for the total motorcycle segment are many times higher than the emission scenario results calculated for the vehicle segment “motorcycles, 4S, Euro 3, > 750 cm<sup>3</sup>, first registration year 2015” as presented in figure 7.1. While the entire motorcycle segment (MC > 50 cm<sup>3</sup>) in Germany consists of approx. 3,7 million vehicles in 2017 according to TREMOD, the vehicle segment considered in this study comprises approx. 28.000 vehicles in the same year.

The TREMOD scenario results demonstrate the sensitivity of the emission input data for the calculation process within TREMOD. Due to varying weighting factors for the individual traffic situations, changes in emission factors lead to partly significant deviations in the overall fleet emission results. One has to point out that the trend scenario calculations were carried out based on a single vehicle’s emission factor database that might not be representative for an entire vehicle fleet or a total TREMOD segment. So, additional emission measurement campaigns in this vehicle category may help to validate the emission factor database and thus also to improve the robustness of the fleet simulation with TREMOD. The HBEFA version 4.1 provides actual information in this context, as extensive emission measurements in this vehicle category – primarily real-world dynamometer measurements - were carried out for the emission factor generation. Besides an emission factor update, a revision of the annual traffic data linked with assumptions regarding the distribution of annual traffic shares according to the traffic situation scheme is necessary for valid simulation results in TREMOD. The implementation of deterioration functions of the exhaust gas after-treatment systems due to aging mechanisms and wear should be carried out in this vehicle category as well. Otherwise, average emission factors for different age stages and varying mileage levels for each vehicle segment should be introduced.

**Table 7.1:** Deviation of TREMOD trend scenario results with RDE EF's and dynamometer EF's compared to the basic TREMOD emission trend scenario results – differentiated according to local area and overall.

**Change in CO<sub>2</sub> emission shares according to local area (in relation to TREMOD basic scenario)**

	RDE map simulation	Dynamometer map simulation
Urban	+33%	+26%
Rural	+17%	+12%
Motorway	+3%	+1%
Overall	+22%	+16%

**Change in CO emission shares according to local area (in relation to TREMOD basic scenario)**

	RDE map simulation	Dynamometer map simulation
Urban	-22%	-29%
Rural	16%	-13%
Motorway	-58%	-70%
Overall	-29%	-45%

**Change in NO<sub>x</sub> emission shares according to local area (in relation to TREMOD basic scenario)**

	RDE map simulation	Dynamometer map simulation
Urban	+185%	+153%
Rural	+48%	+18%
Motorway	-24%	-48%
Overall	+36%	+8%

**Change in HC emission shares according to local area (in relation to TREMOD basic scenario)**

	RDE map simulation	Dynamometer map simulation
Urban	-	+86%
Rural	-	+131%
Motorway	-	+16%
Overall	-	+91%

### 7.2. Non-regulated Emission Trend Scenario Results

The following illustrations 7.3 show the hot-emission trend scenario results for the exhaust gas components CH<sub>4</sub> and C<sub>6</sub>H<sub>6</sub> for the vehicle segment concerned. Again, the results are differentiated according to local area and presented for the period 2015 - 2025. Since no PHEM simulations for the individual emission factors were carried out for C<sub>6</sub>H<sub>6</sub>, the TREMOD scenario calculations are conducted based on the average, aggregated emission measurement results from the measurement campaign in chapter 5.3. The aggregated C<sub>6</sub>H<sub>6</sub> emission results differentiated according to local area were multiplied by the aggregated annual traffic data for the individual years for the period in question. However, the CH<sub>4</sub> trend scenarios base on the simulated emission factors presented in chapter 6.4. Table 7.2 lists the deviation to the existing TREMOD baseline scenario.

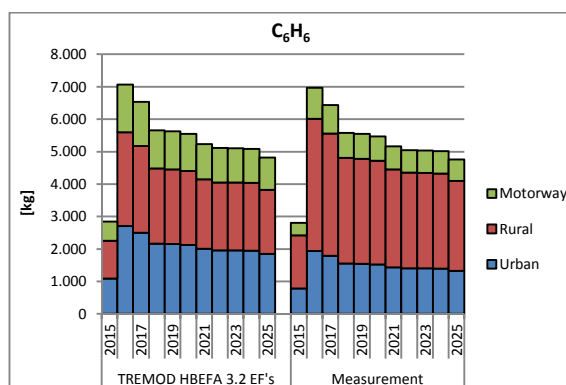
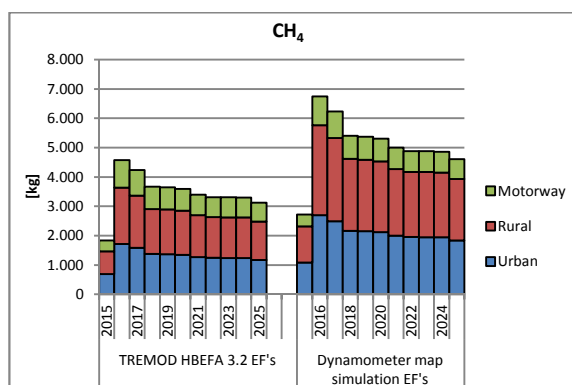


**Figure 7.3:** CH<sub>4</sub> and C<sub>6</sub>H<sub>6</sub> emission trend scenario results for the TREMOD segment “motorcycles, 4S, Euro 3, > 750 cm<sup>3</sup>, first registration year 2015” for the period 2015 – 2025; TREMOD basic scenario (left) and TREMOD calculations with simulated emission factors (CH<sub>4</sub>) and aggregated emission data derived from the dynamometer measurement program (C<sub>6</sub>H<sub>6</sub>).

The simulated CH<sub>4</sub> emission factors are partly higher than the emission factors stored in TREMOD 5.63 and HBEFA 3.2. – overall and aggregated to urban, rural and motorway. Accordingly, the TREMOD trend scenario results are also higher in the same way. Urban CH<sub>4</sub>-emission results show a difference to the baseline scenario results of approx. + 57 %, whereas the motorway CH<sub>4</sub>-emissions show only slight differences (+4,1 %) compared to the TREMOD reference. Overall, the total CH<sub>4</sub>-emissions increase on the basis of the simulated emission factors by approx. + 47 % compared to the existing database in TREMOD.

Concerning benzene emissions (C<sub>6</sub>H<sub>6</sub>), there is almost no change in absolute terms between the TREMOD baseline calculation and the trend scenario based on the FTIR measurement results; the difference is approx. –1,4 %. However, there is a clear trend towards higher rural C<sub>6</sub>H<sub>6</sub> emissions by using the emission datasets from the FTIR measurements in TREMOD. Compared to the baseline scenario, the rural C<sub>6</sub>H<sub>6</sub> emissions increase by approximately 40 %, while the urban- and motorway shares are decreasing by –28 %, respectively –34 % at the same time. The CH<sub>4</sub>- and C<sub>6</sub>H<sub>6</sub> emissions are approx. 10 % (total amount) of the regulated HC emissions as displayed in chapter 7.1.

**Table 7.2:** Deviation of TREMOD trend scenario results for CH<sub>4</sub> and C<sub>6</sub>H<sub>6</sub> calculated with emission factors from the PHEM simulation (CH<sub>4</sub>) and data from the FTIR measurement program (C<sub>6</sub>H<sub>6</sub>) compared to the basic TREMOD scenario results – differentiated according to local area and overall.

Change in CH <sub>4</sub> emission differentiated to local area (in relation to TREMOD basic scenario)		Change in C <sub>6</sub> H <sub>6</sub> emissions differentiated to local area (in relation to TREMOD basic scenario)	
	Dynamometer map simulation		Measurement
Urban	+ 57 %	Urban	- 28 %
Rural	+ 60 %	Rural	+ 40 %
Motorway	+ 4,1 %	Motorway	- 34 %
Overall	+ 47 %	Overall	- 1,4 %

At this point, the entire German methane- and benzene emissions from the road traffic sector are presented for comparison purposes, see figure 7.4.

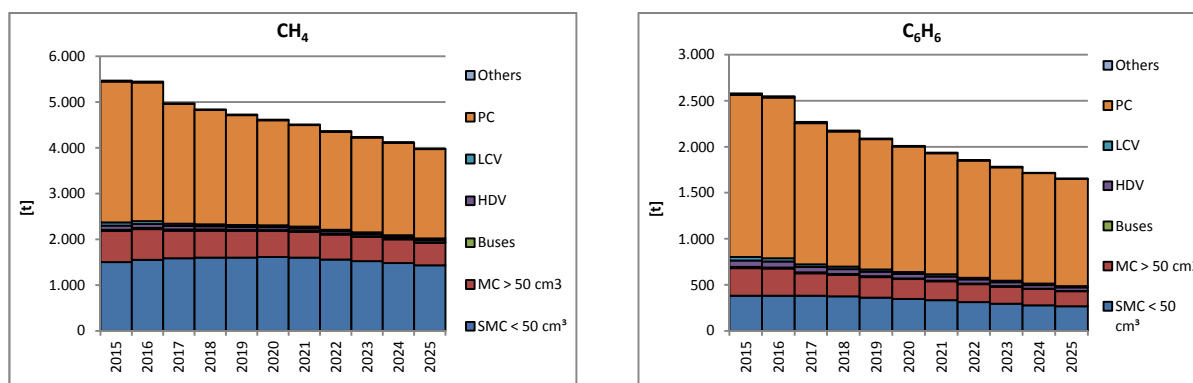


**Figure 7.4:** Overall CH<sub>4</sub> and C<sub>6</sub>H<sub>6</sub> emissions of the German vehicle fleet for the period 2015 – 2025 according to TREMOD including all relevant vehicle categories.

It turns out that the share of CH<sub>4</sub> and C<sub>6</sub>H<sub>6</sub> emissions from powered two-wheelers to the total road traffic emissions in Germany is partly remarkable – the share of powered two-wheelers CH<sub>4</sub> emissions to the total German CH<sub>4</sub> emissions in approx. 39 % in 2016; C<sub>6</sub>H<sub>6</sub> emissions from powered two-wheelers make up approx. 26 % to the total German C<sub>6</sub>H<sub>6</sub> emissions in the road traffic sector in 2016.

For the non-regulated emission components acetylene (C<sub>2</sub>H<sub>2</sub>), butadiene (C<sub>4</sub>H<sub>6</sub>), ethane (C<sub>2</sub>H<sub>6</sub>) and formaldehyde (HCHO), there are currently no emission data sets for powered two-wheelers in TREMOD or HBEFA 3.2 implemented. Therefore, the following TREMOD calculations represent a first estimation for the development of these components caused by motorcycles in Germany. The results are again based on the average emission results from the FTIR measurement program. Figure 7.5 shows the TREMOD trend scenario results for the period 2015 - 2025 in Germany for the TREMOD vehicle segment concerned differentiated according to local area and overall.

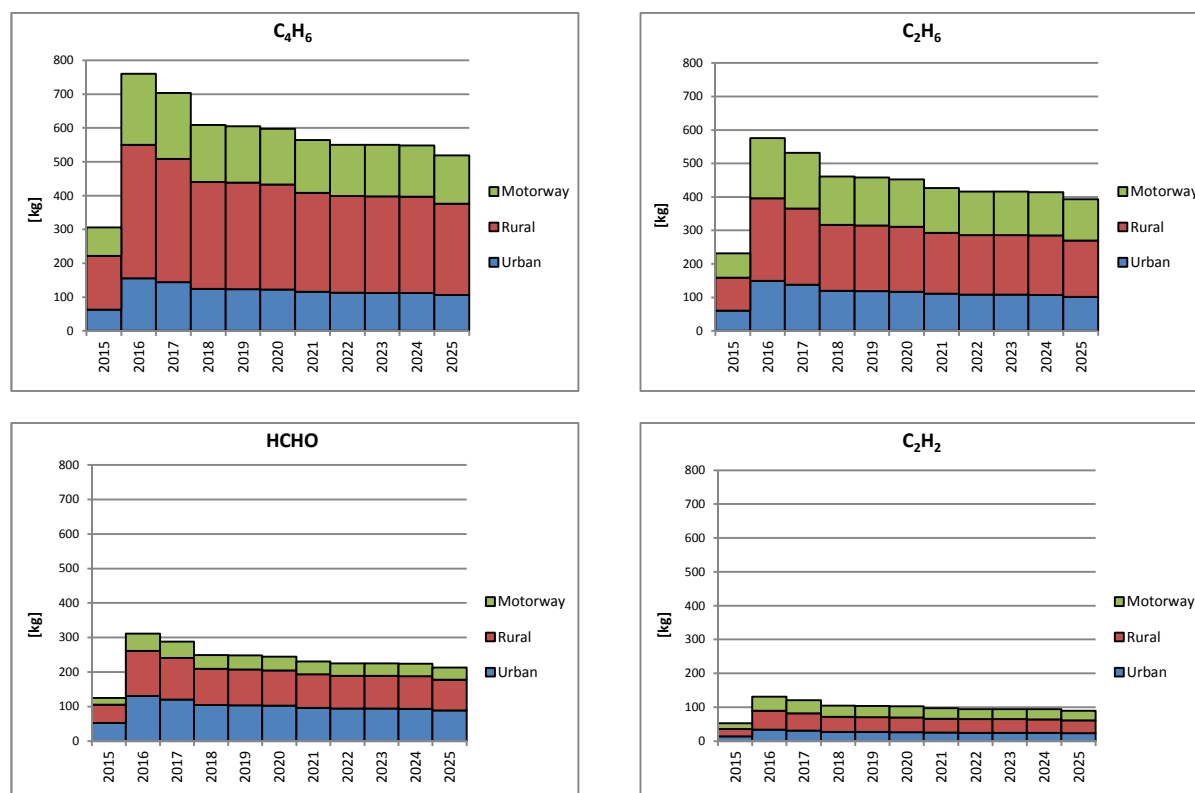


**Figure 7.5:** C<sub>2</sub>H<sub>2</sub>, C<sub>4</sub>H<sub>6</sub>, C<sub>2</sub>H<sub>6</sub> and HCHO emission trend scenario results for the TREMOD vehicle segment “motorcycles, 4S, Euro 3, > 750 cm<sup>3</sup>, first registration year 2015” for the period 2015 – 2025 based on aggregated emission data derived from the dynamometer measurement program.

The C<sub>2</sub>H<sub>2</sub> emissions in Germany in 2016 caused by the motorcycle segment concerned are approx. 130 kg in total. By 2025, this value will drop to around 89 kg. About 43 % of the total C<sub>2</sub>H<sub>2</sub> emissions can be allocated to rural traffic. The C<sub>4</sub>H<sub>6</sub> emissions decrease from approx. 760 kg in 2016 to approx. 510 kg in 2025 and the C<sub>2</sub>H<sub>6</sub> emissions from approx. 575 kg to approx. 390 kg in the same period of question. Both emission components show increased shares of rural emissions with 52 % (C<sub>4</sub>H<sub>6</sub>) respectively 43 % (C<sub>2</sub>H<sub>6</sub>). HCHO emissions decrease from approx. 310 kg (2016) to 212 kg (2025). HCHO shows higher urban shares of approx. 42 % in relation to the previously mentioned

components. In general, one can state out that the emissions results calculated here amount approx. 1 % of the regulated HC emissions calculated in chapter 7.1. So, these unregulated hydrocarbon fractions represent only a very small proportion to the total HC exhaust gas emissions in this vehicle segment, however, some of this components show considerable health-endangering properties and they are mainly emitted in urban and rural areas.

### **7.3. Cold-start Surcharges – Baseline Trend Scenario Results**

The emission measurement program indicates that a considerable share of the CO and HC emissions occurs during the warm-up phase of the engine. Within this phase, the CO and HC emission rates are partly much higher compared to the emission rates measured in warm engine operation mode. Until now, the additional cold-start surcharges are not reflected in TREMOD (version 5.63) for the vehicle category of powered two-wheelers. Thus, based on the measured cold-start emissions in this study, an estimation of the additional cold-start surcharges for HC and CO emissions for the TREMOD vehicle segment “motorcycles, 4S, Euro 3, > 750 cm<sup>3</sup>, first registration year 2015” is carried out. It is intended to provide a first assessment of the relevance of cold-start emission shares in this vehicle category. The calculation process of cold-start emission shares requires the cold-start surcharges per engine start and the number of engine starts of the vehicle segment concerned.

Based on annual traffic data of the vehicle segment concerned and information on the average trip distance, the number of start / stop operations can be calculated. The average trip length is approximately 14,4 km aggregated over all Euro 3 motorcycles with a first registration year between 2006 – 2016 according to TREMOD. This value is assumed to be constant over the years in the trend scenario considered. The number of start / stop operations can be calculated by dividing the annual traffic by the average trip length. Figure 7.6 shows the number of start / stop operations for the vehicle segment concerned up to the year 2025. This value correlates with the annual traffic in this vehicle segment, since the average trip distance does not change over the years. Taking into account the number of vehicles of the vehicle segment “motorcycles, 4S, Euro 3, > 750 cm<sup>3</sup>, first registration year 2015” (approx. 28.000 vehicles in 2015), this results in a value of approx. 345 start / stops per vehicle per year. One can assume that a large share of the driven distance is attributable to the summer months in this vehicle category. Furthermore, one can assume that not every start represents a “full” cold-start, instead, vehicles are also partially started with slightly warm engine. Here, the emission behavior is not as bad as with a “totally” cold engine. However, it is difficult to estimate in what frequency which type of cold-start occurs – reliable information is not available in this context. Thus, the calculations in the following paragraphs are therefore based on simplifications and own assumptions.

---

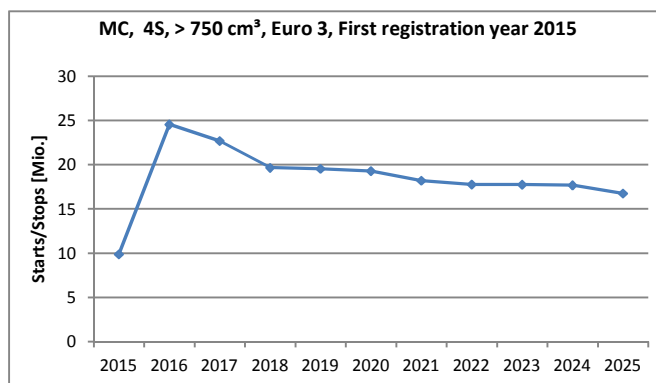


**Figure 7.6:** Start/Stop distribution of the TREMOD vehicle segment “motorcycles, 4S, > 750 cm<sup>3</sup>, Euro 3, first registration year 2015” in the period 2015 – 2025.

The results from the emission measurement program (chapter 5) were taken to derive the required information on additional HC and CO emissions after engine starts. For this purpose, the average kilometer-related HC and CO emission values within the first two kilometers after cold-start were determined taking into account all individual measurements - on-board trips and dynamometer measurements. Within a distance of two kilometers, a "normal" emission level of CO and HC emissions was reached in all individual measurements. Finally, a HC and CO cold-start surcharge value weighted over all measurements was calculated. Table 7.3 shows the aggregated, CO and HC cold-start values derived from the measurement program.

**Table 7.3:** Aggregated CO and HC emission cold-start surcharge derived from the on-board- and dynamometer measurement program.

Ave. CO and HC emission cold-start surcharge [g/start]	
Component	[g/start]
CO	15,5
HC	2,2

The above-mentioned CO and HC emission values (table 7.3), were multiplied by the number of starts / stops to obtain the additional cold-start emission shares of the vehicle segment concerned. It is assumed here that almost all cold-start emissions are emitted in urban areas - vehicles are primarily parked in residential areas and near private homes - more detailed information in this context respective relevant data sets were not available in this scenario calculation. Figures 7.7 show the development of CO and HC emissions for the vehicle segment “motorcycles, 4S, > 750 cm<sup>3</sup>, Euro 3, first registration year 2015” for the period 2015 - 2025, including the cold-start emission shares.

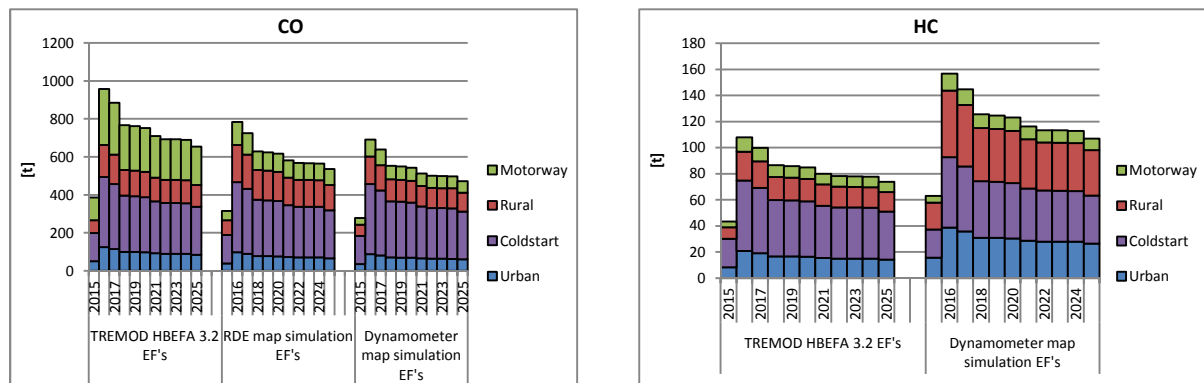


**Figure 7.7:** CO and HC emission trend scenarios for the TREMOD vehicle segment “motorcycles, 4S, > 750 cm<sup>3</sup>, Euro 3, first registration year 2015” taking into account cold-start surcharges – calculations carried out with baseline TREMOD / HBEFA emission factors and RDE EF’s and dynamometer EF’s derived from the PHEM simulations.

It turns out that the CO and HC cold-start surcharges represent a significant share within the total CO and HC emissions in this vehicle segment. CO cold-start surcharges represent approximately 38 % of the total CO emissions in the TREMOD baseline scenario, approx. 47 % in the trend scenario calculated with the on-board emission factors and up to 53 % in the trend scenario, which is based on the emission factors gained from the dynamometer emission measurements. Provided, that all cold-starts take place in urban areas, the urban CO share in the TREMOD baseline scenario increases to approx. 51 %; up to 59 % in the trend scenario calculated with the on-board emission factors and up to 66 % in the dynamometer emission factor trend scenario.

In the HC emission baseline trend scenario the proportion of cold-start surcharges is almost 50 %. Within the TREMOD trend scenario in which the dynamometer emission factors were implemented, cold-start surcharges are approx. 34 %. Similarly to CO cold-start surcharges, the total urban HC emission share increases correspondingly, if all HC cold-start surcharges are attributed to the urban HC emissions: up to 69 % in the TREMOD baseline scenario and 59 % in the trend scenario calculated with the dynamometers emission factors. However, as already mentioned, these calculations are partly a simplification. Not every cold-start can be seen as a full cold-start, and not every engine start takes place in urban areas.

Overall, it turns out that the additional CO and HC cold-start emissions are of crucial importance in the motorcycle segment and a mere consideration of hot emissions is not sufficient. In addition, the predominant shares of HC and CO cold-start surcharges are deemed to be emitted in urban areas, which directly affects air quality in residential regions. Further investigations on cold-start emissions in this vehicle category are required in order to improve the reliability of the TREMOD calculations. Therefore, more detailed information on the start / stop distribution according to local area and concerning the number of start / stop operations as well as effects of ambient temperatures and parking time before a engine start are necessary.

#### 7.4. Hydrocarbon Trend Scenario including Cold-start- and Evaporative Emission data

In addition to the cold-start surcharges, the effect of evaporative emissions on the total HC emissions of the considered vehicle segment “motorcycles, 4S, > 750 cm<sup>3</sup>, Euro 3, first registration year 2015” was investigated in an additional TREMOD scenario. The reference is the trend scenario based on the HC emission factors from the dynamometer measurement program. As described in chapter 4.2.4 the data sets on evaporation emissions of powered two-wheelers were adopted from COPERT to HBEFA 3.2. These data sets include information on running losses – each differentiated according to local area – diurnal losses and hot soak emissions, see table 7.4.

**Table 7.4:** Evaporative emission factors for the vehicle segment “motorcycles, 4S, > 750 cm<sup>3</sup>, Euro 3, first registration year 2015” according to HBEFA 3.2.

Evaporative Emissions factors (HBEFA 3.2)		
Running losses Urban	0,089	g/km
Running losses Rural	0,033	g7km
Running losses Motorway	0,024	g/km
Diurnal losses	0,399	g/Veh*day
Hot soak emissions	0,756	g/stop

The total amount of running-loss emissions is obtained by multiplying the local-area-specific running-loss emission factors in g / km by the corresponding driving distance indicated by TREMOD. Diurnal losses of the entire vehicle segment are calculated for each year of the calculation period considered by multiplying the diurnal loss emission factor (given in g / Veh.\*day) by 365 and by the vehicle stock of the respective year. Hot soak emissions finally are calculated by multiplying the number of stops per year times the hot soak emission factor indicated in g / stop. The evaporative emission results are added to the HC trend scenario calculated with the dynamometer emission factors. The TREMOD trend scenario results are presented in figure 7.8 a). Figure 7.8 b) shows as an example the emission shares of all HC emission types for the year 2018.

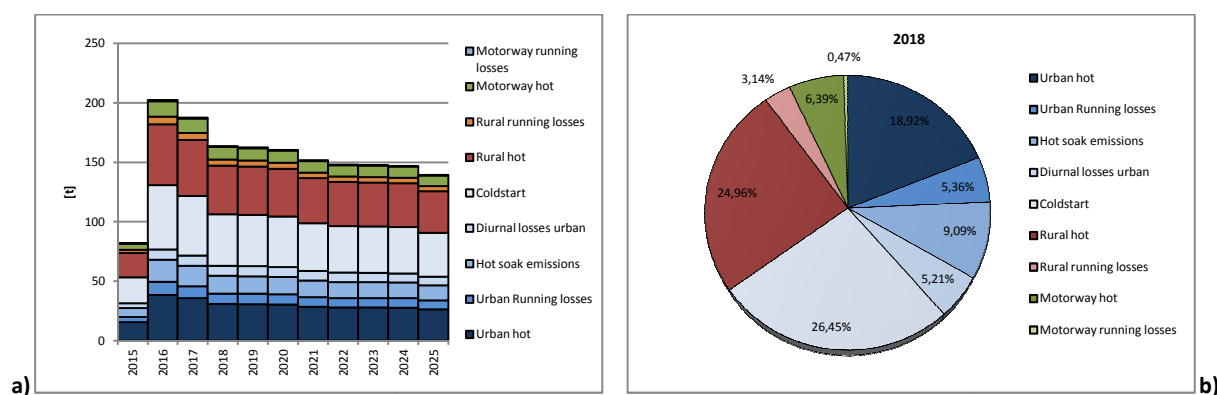


**Figure 7.8:** a) HC-emission trend scenario results for the TREMOD vehicle segment “motorcycles, 4S, > 750 cm<sup>3</sup>, Euro 3, first registration year 2015” including cold-start- and evaporative emissions for the period 2015 -2025; b) HC emission shares differentiated according to different emission sources for the year 2018.

In addition to the hot and cold-start HC emissions, there is a further increase in HC emissions by approx. 23 % for the reference years taking into account all sources of HC evaporative emissions. As no deterioration effects are indicated for evaporative emission factors, the amount of evaporative HC emissions in this vehicle layer is the same for every scenario year – however, it is expected that due to aging effects of fuel carrying components the evaporative emissions may increase at least partially over time. In this scenario calculation it is assumed that the hot soak- and the diurnal losses are attributed only to urban HC emissions (vehicles are primarily parked on private grounds respective in residential areas and the engines are also switched off here). Certainly, parts of the diurnal and hot soak emission shares may also occur outside urban areas (e. g. workplace, further destinations); however, this share cannot be further quantified here. For detailed information in this context, further driving investigations regarding the user profiles of motorcycle owners are required in order to substantiate the estimations made in the calculations here. Based on the detailed analysis made for the year 2018 (figure 7.8 b)), it turns out that approx. 65 % of all HC emissions can be attributed to urban areas.

Since no limit values for evaporative emissions were prescribed until the introduction of Euro 4/5 by Regulation EU 168/2013, total evaporative emissions in the powered two-wheeler segment are sometimes above average. In addition, it is difficult to gain valid information on running-loss emissions, as vehicles need to be tested regarding the outlet of HC emission fumes while driving. Therefore, specified emission test facilities (drivable SHED chambers) are required; however, running losses are not regulated legislatively. So, there are only few testing institutions on the market that offer such detailed emission measurement procedures. However, the trend scenario calculations carried out here provide an initial estimation concerning the overall HC emission amounts and distributions in this vehicle segment.

---

## 8. Summary and Outlook

Reliable information on vehicle-specific emissions in the road traffic sector is an essential basis for the description of environmental impacts and developments. On the one hand, the preparation of political measures requires robust information on the real-world emission behavior of different vehicle categories in high resolution; on the other hand, pollutant and greenhouse gas emission inventories have to be updated continuously with correct emission information to fulfill international reporting obligations.

In this context, powered two-wheelers represent - in some cases - a significant source of pollutant emissions, which have been investigated partly insufficiently contrasted with other motor vehicle categories. Powered two-wheelers represent only a small share in the German vehicle fleet linked with marginal annual traffic, however, this vehicle category shows partly disproportionately high emission shares. Particularly, the CO and HC emission behavior in urban areas can be assumed to be disproportionately high. In addition, the share of cold-start emissions and fuel evaporation in this vehicle category can be specified as above average compared to other vehicle categories, which further worsens powered two-wheelers emission balance. The assessment of the real-world emission behavior of motor vehicles requires intensive exhaust gas measurements, either under real-driving conditions on the road or by dynamometer measurements in real world-test cycles. Whereas exhaust gas emission measurements via mobile measurement technology already apply in the case of certification purposes in the field of commercial- and passenger cars, powered two-wheelers are not a subject to such regulations so far.

The motivation of this doctoral thesis was derived from above-mentioned issues, namely to assess mobile emission measurement technology in the motorcycle segment on the one hand, and to get a better understanding of motorcycle emission behavior under real driving conditions. In this context, real-world emission measurements on a representative motorcycle were carried out – both, by using mobile exhaust-gas measurement technology on the road and by investigating the same test vehicle on an exhaust-gas dynamometer test bench. For this purpose, extensive test drives in Graz city and its surroundings were performed by using a commercial PEMS system. Furthermore, dynamometer measurements on a two-wheeler test bench in the test facilities of Graz University of Technology were conducted. On-board test drives were made on RDE-compliant routes and, additionally, on mountainous road sections with the intention to simulate sporty motorcycle driving. In this context, it was examined to what extent the mobile measurement equipment affects the driving dynamics of motorcycles and what it necessitates in future measurement campaigns concerning the usability of mobile emission data. The evaluation of the on-board measurement data was carried out in accordance with the RDE-legislation evaluation scheme adopted from the passenger car sector.

Driving dynamic investigations revealed that driving with a PEMS system installed on a conventional motorcycle is partly limited in lower speed ranges (urban traffic < 60 km / h) due to the payload and the overhanging design of the test vehicle configuration and not least due to driving safety aspects. Comparisons with motorcycle traffic situations as implemented in TREMOD revealed that the relevant dynamic parameter RPA (relative positive acceleration) was partly significantly lower in low speed ranges during the on-board tests. The starting procedure with a PEMS systems installed on a motorcycle seems to be rather challenging - in higher speed ranges, however, the influence of the

---

measurement system on the driving dynamics decreased continuously, not least due to increasing longitudinal stability of the test vehicle. Based on these findings, one can say, that PEMS systems in motorcycle applications are primarily recommended in heavy and powerful machines, as the influence on the driving dynamic is deemed to be less pronounced contrasted with light motorcycles.

The emission results from the measurement campaign were analyzed differentiated according to local area, namely to urban, rural and motorway traffic and, in addition, cold-start emission shares and hot emissions were indicated separately. The measured emission data on the road showed partly a higher level opposed to the dynamometer measurements, which certainly can be attributed to the additional measurement setup linked with uncommonly high driving resistances and due to driving shares on mountainous road sections. Within the chassis dynamometer test program, however, the test vehicle showed lower emission rates as the driving resistance settings were correspondingly lower compared to the on-board tests. Particularly, the CO and HC cold-start emission results were partly significantly more pronounced than the hot emission measurement results. Furthermore, information on the emissions of non-regulated exhaust gas components were generated and evaluated by using a FTIR-analyzer. Here, relevant concentrations were recorded for methane (CH<sub>4</sub>) and benzene (C<sub>6</sub>H<sub>6</sub>) emissions (approx. 20 mg / km) - further unregulated emission components C<sub>2</sub>H<sub>2</sub>, C<sub>2</sub>H<sub>6</sub>, C<sub>4</sub>H<sub>6</sub> and HCHO showed concentrations of < 5 mg / km, which lies partly within the measurement tolerance of a FTIR-analyzer.

The emission measurement data were implemented in the simulation model PHEM and emission maps for the exhaust gas components CO<sub>2</sub>, CO, NO<sub>x</sub> and HC were generated – both, for on-board and dynamometer emission measurement data. Since no second-by-second engine power signal was available during the on-board tests, the emission maps were generated by using generic CO<sub>2</sub> emission maps - this method is already applied in the field of passenger car emission factor generation in the context of HBEFA. In general, the emission maps generated based on the on-board measurement data are characterized by an adequate engine map coverage over wide engine load areas – during the on-board tests, almost all relevant engine load points were covered. The emission maps created on the basis of the dynamometer measurements, however, show map areas in which no emission signal during the measurement was available, as these engine load points were not driven through due to general limitations of dynamometer measurements in this vehicle segment, among others, slipping between dynamometer roll and motorcycle tires in strong acceleration phases.

The robustness of the emission maps was investigated by re-simulating the test drives with PHEM – both, the on-board and the dynamometer tests. The re-simulations showed satisfactory results for both emission map variants depending on the exhaust gas components. Within a parameter variation the influence of the most relevant driving resistance parameters on the emission simulations with PHEM was investigated. In particular, a correct adjustment of the air resistance coefficient and the vehicle frontal area affects the simulation results in PHEM decisively. Emission factor simulation purposes for inventorying tools like TREMOD have to reflect typical real-world motorcycling on the road. Therefore, a real-world motorcycle vehicle configuration was defined based on assumptions derived from the measurement programs and literature information. This vehicle configuration was used to calculate emission factors in the structure of the German emission inventory model TREMOD with PHEM for all relevant motorcycle traffic situations. The simulation results were contrasted with the existing emission factor data base from HBEFA 3.2 and HBEFA 4.1 for the vehicle segment

---

concerned. The emission factor simulation results show partly remarkable deviations from the baseline TREMOD emission factors depending on the emission component concerned and according to a local area differentiation.

Finally, emission trend scenarios for the emission components CO<sub>2</sub>, CO, NO<sub>x</sub>, HC and CH<sub>4</sub> for the TREMOD vehicle segment “motorcycles, 4S, > 750 cm<sup>3</sup>, Euro 3, first registration year 2015” were calculated with TREMOD up to the year 2025 by using the simulated emission factors gained from the PHEM simulations. The TREMOD trend scenario results were contrasted with the baseline scenario results using emission factors from HBEFA version 3.2. The other input parameters in TREMOD such as vehicle fleet and annual traffic data were adopted. The TREMOD trend scenarios show partly significant variations contrasted with the baseline scenarios depending on the emission component – particularly with regard to CO and HC emissions. Remarkable shifts in terms of local-area-specific emissions are also recognizable. Besides legislative regulated pollutant components, TREMOD trend scenarios were calculated for certain non-regulated pollutant components such as C<sub>6</sub>H<sub>6</sub>, C<sub>2</sub>H<sub>2</sub>, C<sub>2</sub>H<sub>6</sub>, C<sub>4</sub>H<sub>6</sub> and HCHO for the first time with TREMOD. The nationwide amount is in the range of a few tons (C<sub>6</sub>H<sub>6</sub>) respectively a few hundred kilograms in the case of the other non-regulated pollutant components concerned. Based on cold-start emission information gained from the measurement program, an exemplary trend scenario in TREMOD was calculated for the additional HC and CO surcharges. As a result, one can say that the additional share of cold-start emissions can reach up to 40 % of total CO and 50 % of total HC emissions in this vehicle segment. In this context, the major share of cold-start emissions can be attributed to urban areas. Taking into account evaporative HC emission fractions one can say that approx. 65 % of total HC emissions in this vehicle category are deemed to occur in urban areas according to TREMOD. This issue was investigated by calculating hot, cold-start and evaporative HC emissions in a separate comprehensive emission trend scenario.

## Outlook

The work carried out in this doctoral thesis provides initial fundamentals for the application of mobile emission measurement technology in the motorcycle segment and the usability of mobile emission data sets within emission inventorying models like TREMOD. However, the findings in this work have to be considered partly under differing aspects.

All measurements within this study were performed with the same individual test vehicle. This may not be representative for an entire vehicle fleet, but it provides initial indications of the emission behavior of a certain vehicle segment with a specific engine and vehicle technology. Possible deteriorations or damages to the vehicle itself and, in particular, of the exhaust gas after-treatment systems cannot be safely excluded. Hence, it is necessary to validate the findings from this study by measuring additional motorcycles with different engine / exhaust gas mitigation technologies on the road by using mobile measurement technology and under laboratory testing conditions. The assembling of a PEMS system on a motorcycle represents an innovation, which is necessary for further testing on different suitable vehicle types. In this context, common standards in the field of mounting a PEMS system on a motorcycle have to be established to generate comparable results.

Driving with on-board measurement devices does not represent typical motorcycling - the loading and the composition of the measurement equipment produces unrealistically high driving

---

resistances, which was reflected in the on-board emission level of the test vehicle in this study. Depending on the vehicle type and motorization, this influence is deemed to be different. It is expected that the impact of the additional equipment on the driving dynamics and the exhaust gas emissions decreases with increasing vehicle weight and engine power. In the course of further emission measurements of motorcycles under real driving conditions, it is always necessary to quantify the influence of the measurement technology on the driving dynamics and finally the emission results for every vehicle type. This is essential to obtain reliable information on the real-world emission behavior of a specific vehicle type. In the context of driving resistance parameters for PHEM simulations, coast-down tests for the determination of real-world driving resistance data for different motorcycle configurations (among others, varying vehicle designs, changing drivers position and clothing) are recommended in order to enhance the simulation settings in PHEM even more.

Based on additional on-board emission data, it is possible to create vehicle segment-specific emission maps with PHEM for all relevant vehicle segments as applied within emission inventorying models like TREMOD. The emission maps can be weighted in accordance with official registration numbers of the vehicle fleet for every nation and model considered. In this way, reliable emission factors can be derived not only for one specific vehicle type, but also for entire vehicle fleets representing similar vehicle technologies. Hereby, it is assumed that the robustness and the volume of the emission database in TREMOD in the motorcycle segment would be increased significantly. In addition to the emission factor database, the correct assignment of traffic shares to vehicle specific segments is of substantial importance for the quality of emission trend scenario calculations in TREMOD. It is recommended to revise the traffic data assignments for motorcycles in TREMOD as it is based on partly outdated data sets and old assumptions. For this purpose, coordinated driving performance investigations, vehicle owners surveys or high-resolution traffic data measurements on national or international level seem to be appropriate.

---

**IV Literature**

- [1.1] Stohl, A.: **Intercontinental Transport of air pollution – The handbook of environmental chemistry.** Berlin, Heidelberg, 2004.
- [1.2] **Transport Emission Model; Version 5.63 B**, 31.01.2016. Developed by: ifeu – Institut für Energie- und Umweltforschung Heidelberg GmbH, Im Weiher 10 69121, Heidelberg, Germany. Copyright by: UBA – Umweltbundesamt Germany, D-06813 Dessau, Germany.
- [1.3] L'Association des constructeurs européens de motocycles (ACEM). **Circulating Parc figures (European Union) – Circulating Parc up to 2014.** Official website of ACEM. <http://www.acem.eu/market-data> (queried on 03/03/2017).
- [1.4] Clairotte, M., Adam, T. W., Chirico, R., Giechaskiel, B., Manfredi, U., Elsasser, M., Sklorz, M., DeCarlo, P. F., Heringa, M. F., Zimmermann, R., Martini, G., Krasenbrink, A., Vicet, A., Tournié, E., Prévot, A. S. H., Astorga, C.: **Online characterization of regulated and unregulated gaseous and particulate exhaust emissions from two-stroke mopeds: A chemometric approach.** Analytica Chimica Acta, Volume 717, 2012.
- [1.5] Cornelis, E., De Vlieger, I., Int Panis, L.: **Emissions of Mopeds and Motorcycles in Belgium.** Urban Transport VIII. Vito, Flemish Institute for Technological Research. Belgium, 2002.
- [1.6] Buckeridge, D. L., Glazier, R., Harvey, B. J., Escobar, M., Amrhein, C., Frank, J.: **Effect of Motor Vehicle Emissions on Respiratory Health in an Urban Area.** Environmental Health Perspectives, Volume 110, Number 3, March 2002.
- [1.7] Chen, G., Wan, X., Yang, G., Zou, X.: **Traffic-related air pollution and lung cancer: A meta-analysis.** Thoracic cancer (6), 2015.
- [1.8] Brunekreef, B., Beelen, R., Hoek, G., Schouten, L., Bausch-Goldbohm, S., Fischer, P., Armstrong, B., Hughes, E., Jerret, M., van den Brandt, P.: **Effects of Long-Term Exposure to Traffic-Related Air Pollution on Respiratory and Cardiovascular Mortality in the Netherlands: The NLCS-AIR Study.** HEI Research Report 139, Health Effects Institute, Boston, MA. 2009.
- [1.9] Latham, S., Kollamthodi, S., Boulter, P. G., Nelson, P. M., Hickman, A. J.: **Assessment of primary NO<sub>2</sub> emissions, hydrocarbon speciation and particulate sizing on range of road vehicles.** Project report PR/SE/353/2001.
- [1.10] United Nations. **Kyoto Protocol to the United Nations Framework Convention on Climate Change.** 1998.
- [1.11] European Commission. **Directive 2001/81/EC of the European Parliament and of the Council of 23 October 2001 on national emission ceilings for certain atmospheric pollutants.** Official Journal of the European Communities, L 309/22, 2001.
-

- [1.12] Hausberger, S., Rexeis, M., Zallinger, M., Luz, R.: **Emission factors from the Model PHEM for the HBEFA Version 3**. Report Nr. I-20/2009 Haus-Em 33/08/679 from 07.12.2009.
- [1.13] Knörr, W., Heidt, C., Schacht, A.: **Aktualisierung „Daten- und Rechenmodell: Energieverbrauch und Schadstoffemissionen des motorisierten Verkehrs in Deutschland 1960 – 2030“ (TREMODO, Version 5.3) für die Emissionsberichtserstattung 2013 (Berichtsperiode 1990 – 2011)**. Heidelberg, 30.09.2012.
- [1.14] Gkatzoflias, D., Kouridis, C., Ntziachristos, L., Samaras, Z.: **COPERT 4 - Computer programme to calculate emissions from road transport - User manual (version 9.0)**. February 2012.
- [1.15] Heijne, V., Ligterink, N., Stelwagen, U.: **2016 Emission factors for diesel Euro-6 passenger cars, light commercial vehicles and Euro-VI trucks**. TNO Report, TNO 2016 R10304v2, 7 March 2016.
- [2.1] Dünnebeil, F., Höpfner, U., Lambrecht, U., Reuter, C.: **Motorrad-Umwelt-Liste. Analyse der umweltrelevanten Eigenschaften von Motorrädern. Wissenschaftlicher Grundlagenbericht**. Endbericht vom 31. Oktober 2004. Gefördert vom Umweltbundesamt. Heidelberg, Oktober 2004.
- [2.2] Stoffregen, J.: **Motorradtechnik. Grundlagen und Konzepte von Motor, Antrieb und Fahrwerk. 8.**, vollständig überarbeitete und ergänzte Auflage. ATZ/MTZ-Fachbuch. Olching, Germany. 2012.
- [2.3] Grigoratos, T.; Martini, G.: **Non exhaust traffic related emissions. Brake and tyre wear PM. Report EUR 26648 EN**. European Commission. Joint Research Centre. Institute of Energy and Transport. 2014.
- [2.4] **Informal document GRB-66-15:** (European Commission) Study on Euro 5 sound level limits of L-category vehicles (66th GRB meeting, 4-6 September 2017, agenda item 10).
- [2.5] **<https://www.neander-motors.com/motoren/kraftrad/>** (queried on 15/11/2018)
- [2.6] Cherry, C.: **Electric Two-Wheelers in China: Promise, Progress and Potential**. ACCESS Magazine. ACCESS 37, Fall 2010. **<http://www.accessmagazine.org/fall-2010/electric-two-wheelers-china-promise-progress-potential/>** (queried on 10/06/2018)
- [2.7] Schmidt, H.: **Der Abgaskrieg. Gegen die Verteufelung des Diesels. Die Spuren einer verhängnisvollen Entwicklung. Literatur – Review**. Neuauflage aktualisiert und umfangreich ergänzt. Germany, 2017.
- [2.8] Sinha, K.C.; Labi, S. **Transportation Decision Making: Principles of Project Evaluation and Programming**. Published by John Wiley & Sons, Inc., Hoboken, New Jersey, 2007.
-

- [2.9] Roberts, A., Brooks, R., Shipway, P.: **Internal combustion engine cold-start efficiency: A review of the problem, causes and potential solutions.** Energy Conversion and Management. Volume 82, June 2014.
- [2.10] Fallah, Saber: **Electric and Hybrid Vehicles - Technologies, Modeling and Control: A Mechatronic Approach.** University of Surrey. April, 2014.
- [2.11] European Industrial Gases Association. **Physiologische Gefahren durch Kohlendioxid (CO<sub>2</sub>) "Nicht nur erstickend"**. Erstellt von Safety Advisory Council. Übersetzt von IGV – Industriegaseverband e.V. Safety Information, Sicherheitsinformation 24/11/D.
- [2.12] Forster, P., V. Ramaswamy, P. Artaxo, T. Berntsen, R. Betts, D.W. Fahey, J. Haywood, J. Lean, D.C. Lowe, G. Myhre, J. Nganga, R. Prinn, G. Raga, M. Schulz and R. Van Dorland, 2007: **Changes in Atmospheric Constituents and in Radiative Forcing.** In: *Climate Change 2007: The Physical Science Basis. Contribution of Working Group I to the Fourth Assessment Report of the Intergovernmental Panel on Climate Change* [Solomon, S., D. Qin, M. Manning, Z. Chen, M. Marquis, K.B. Averyt, M.Tignor and H.L. Miller (eds.)]. Cambridge University Press, Cambridge, United Kingdom and New York, NY, USA.
- [2.13] Khalil, M.A.K.: **Atmospheric Methane: Sources, Sinks, and Role in Global Change.** Proceedings of the NATO Research Advanced Workshop on the Atmospheric Methane Cycle: Sources, Sinks, Distributions and Role in Global Change, held at Mt Hood near Portland, OR, USA, October 7-11, 1991.
- [2.14] [http://www.chemie.de/lexikon/Kohlenstoffmonoxid.html#\\_ref-CEVIK-2006-INTJCLINPRACT\\_0/](http://www.chemie.de/lexikon/Kohlenstoffmonoxid.html#_ref-CEVIK-2006-INTJCLINPRACT_0/) (queried on 12/11/2018)
- [2.15] Olivier, J., Bloos, J., Berdowski, J., Visschedijk, A., Bouwman, A.: **A 1990 global emission inventory of anthropogenic sources of carbon monoxide on 1° x 1° developed in the framework of EDGAR/GEIA.** Chemosphere - Global Change Science Volume 1, Issues 1–3, August 1999, Pages 1-17.
- [2.16] Atkinson, R., Arey, J.: **Atmospheric degradation of volatile organic compounds.** Chemical Review, 2003 (103): 4605 – 4638, 2003.
- [2.17] US Department of Health and Human Services: **Report on Carcinogens, twelfth edition.** U.S. Department of Health and Human Services, Public Health Services, National Toxicology Program. 2001.
- [2.18] Sportisse, B.: **Fundamentals in Air Pollution: From Processes to Modelling.** Springer, 2010.
- [2.19] Xing, Y., Xu, Y., Shi, M., Lian, Y.: **The impact of PM 2.5 on the human respiratory system.** Journal of Thoracic Diseases. 2016 Jan; 8(1): E69–E74.
- [2.20] Kittelson, D. B.: **Engines and nanoparticles: a review.** Journal of Aerosol Science, 29(56): 575-588, 1998.
-

- [2.21] Martini, G., Manfredi, U., Rocha, M., Marotta, A.: **Review of the European Test Procedure for Evaporative Emissions: Main Issues and Proposed Solutions**. JRC Scientific and Policy Reports, Final Report. European Commission, Joint Research Centre, Institute for Energy and Transport , 2012.
- [2.22] Kolke, R.: **Berechnung der Verdunstungsemissionen von motorisierten Zweirädern (MZR) - Basisemissionsfaktoren für TREMOD**. Umweltbundesamt. Dokument Nummer: I 3.2-52 213/0. 10.12.2002
- [2.23] ARAL Aktiengesellschaft , official homepage.  
<http://www.aral.de/de/forschung/kraftstoffe/ottokraftstoffe/eigenschaften.html> (queried on 05/04/2017).
- [2.24] **ASTM D323 - 15a. Standard Test Method for Vapor Pressure of Petroleum Products (Reid Method)**. 2015.
- [2.25] DIN EN 13016-1:2007-11. **Liquid petroleum products - Vapour pressure - Part 1: Determination of air saturated vapour pressure (ASVP) and calculated dry vapour pressure equivalent (DVPE); German version EN 13016-1:2007**. 2007.
- [2.26] European Commission. **Directive 2009/30/EC of the European Parliament and of the Council of 23 April 2009 amending Directive 98/70/EC as regards the specification of petrol, diesel and gas-oil and introducing a mechanism to monitor and reduce greenhouse gas emissions and amending Council Directive 1999/32/EC as regards the specification of fuel used by inland waterway vessels and repealing Directive 93/12/EEC**. Official Journal of the European Union, L 140/88, 2009.
- [2.27] European Commission. **Directive 2003/30/EC of the European Parliament and of the Council of 8 May 2003 on the promotion of the use of biofuels or other renewable fuels for transport**. Official Journal of the European Union, L 123/42, 2003.
- [2.28] Landmann, L. C.: **Evaluating Resting Loss and Diurnal Evaporative Emissions Using RTD Test**. Mobile6 Model Development Stakeholder Review Document, Document Number M6.RDT.001, U. S. EPA, 1997.
- [2.29] Committee on Vehicle Emission Inspection and Maintenance Programs, Board on Environmental Studies and Toxicology, Transportation Research Board, National Research Council: **Evaluating Vehicle Emissions Inspection and Maintenance Programs. 2001**.
- [2.30] Obermeier, A., Friedrich, R., John, C., Voß, A.: **Zeitlicher Verlauf und räumliche Verteilung der Emissionen von flüchtigen organischen Verbindungen und Kohlenmonoxid in Baden-Württemberg**. Forschungsbericht KfK-PEF 78, Institut für Energiewirtschaft und Rationelle Energieanwendung (IER), Universität Stuttgart, 1991.
- [2.31] Lambrecht, U., Helms, H., Kullmer, K., Knörr, W.: **Entwicklung eines Modells zur Berechnung der Luftschadstoffemissionen und des Kraftstoffverbrauchs von**
-

- Verbrennungsmotoren in mobilen Geräten und Maschinen.** Im Auftrag des Umweltbundesamtes, UFOPLAN Nr. 299 45 113, Heidelberg, 2004.
- [2.32] European Commission. **Directive 2009/126/EC of the European Parliament and the Council of 21 October 2009 on Stage II petrol vapour recovery during refuelling of motor vehicles at service stations.** Official Journal of the European Union, L285/36, 2009.
- [2.33] Kennedy, P., Gadd, J.: **Preliminary examination of trace elements in tyres, brake pads, and road bitumen in New Zealand.** Prepared for Ministry of Transport, New Zealand, Infrastructure Auckland; 2003.
- [2.34] Abu-Allaban, M., Gillies J. A., Gertler, A. W., Clayton, R., Proffitt, D.: **Tailpipe, resuspended road dust, and brake-wear emission factors from on-road vehicles.** Atmospheric Environment, 37, 5283-5293. 2003.
- [2.35] **Working Party on Pollution and Energy (GRPE). Particle Measurement Programme (PMP).** <https://wiki.unece.org/pages/viewpage.action?pageId=2523173> (queried on 01/03/2017)
- [3.1] European Commission. **Regulation (EU) No 168/2013 of the European Parliament and of the council of 15 January 2013 on the approval and market surveillance of two- or three-wheel vehicles and quadricycles.** Official Journal of the European Union, L 60/52, 2013.
- [3.2] European Commission. **Directive 97/24/EC of the European Parliament and of the Council of 17 June 1997 on certain components and characteristics of two or three-wheel motor vehicles.** Official Journal of the European Communities, 1997.
- [3.3] European Commission. **Directive 2002/51/EC of the European Parliament and of the Council of 19 July 2002 on the reduction of the level of pollutant emissions from two- and three-wheel motor vehicles and amending Directive 97/24/EC.** Official Journal of the European Communities, L 252/20, 2002.
- [3.4] United Nations. **Addendum 46 to the 1958 Agreement concerning the adoption of uniform conditions of approval and reciprocal recognition of approval for motor vehicle equipment and parts. Regulation No. 47. Uniform Provisions concerning the type approval of Mopeds equipped with a positive ignition engine with regard to the emission of gaseous pollutants by the engine, Annex 4.** 1981.
- [3.5] United Nations. **Addendum 39 to the 1958 Agreement concerning the adoption of uniform conditions of approval and reciprocal recognition of approval for motor vehicle equipment and parts. Regulation No. 40. Uniform Provisions concerning the type approval of motor cycles equipped with a positive ignition engine with regard to the emission of gaseous pollutants by the engine, Annex 4.** 1979.
- [3.6] European Commission. **Commission Directive 2006/72/EC of 18 August 2006 amending for the purposes of adapting to technical progress Directive 97/24/EC of the European Parliament and of the Council on certain components and**
-

- characteristics of two or three-wheel motor vehicles.** Official Journal of the European Union, L 227/43, 2006.
- [3.7] United Nations. **Global technical regulation No. 2. Measurement procedure for two-wheeled motorcycles equipped with a positive or compression ignition engine with regard to the emission of gaseous pollutants, CO<sub>2</sub> emissions and fuel consumption.** 2005.
- [3.8] European Commission. **Commission delegated Regulation (EU) No 134/2014 of 16 December 2013 supplementing Regulation (EU) No 168/2013 of the European Parliament and of the Council with regard to environmental and propulsion unit performance requirements and amending Annex V thereof.** Official Journal of the European Union, L 53/1, 2013.
- [4.1] European Commission. **Directive 2001/81/EC of the European Parliament and of the Council of 23 October 2001.** Official Journal of the European Communities, L309/22, 27.11.2001.
- [4.2] United Nations. **Kyoto Protocol to the United Nations Framework Convention on climate change.** 1998.
- [4.3] [http://ermesgroup.eu/web/system/files/filedepot/11/ERMES\\_presentation\\_Dec2013.pdf](http://ermesgroup.eu/web/system/files/filedepot/11/ERMES_presentation_Dec2013.pdf) (queried on 14/08/2018).
- [4.4] Hausberger, S., Schwingshackl, M.: **Update der Emissionsprognose Verkehr Österreich bis 2030.** Bericht Nr. Inst-03/11/ Haus Em 09/10-679 vom 28.03.2011, Graz, 2011.
- [4.5] Keller, M., de Haan, P., Knörr, W., Hausberger, S., Steven, H.: **Handbuch Emissionsfaktoren des Straßenverkehrs 2.1 – Dokumentation.** Bern/Heidelberg/Graz/Essen. 18. August 2004.
- [4.6] Knörr, W., Heidt, C., Schacht, A.: **Aktualisierung "Daten- und Rechenmodell: Energieverbrauch und Schadstoffemissionen des motorisierten Verkehrs in Deutschland 1960-2030" (TREMODO, Version 5.3) für die Emissionsberichtserstattung 2013 (Berichtsperiode 1990-2011).** Heidelberg, 30.09.2012.
- [4.7] Ntziachristos, L., Gkatzoflias, D., Kouridis, C., Samaras Z.: **COPERT: A European Road Transport Emission Inventory Model.** Proceedings of the 4th International ICSC Symposium Thessaloniki, Greece, May 28-29, 2009. Chapter from book "Information Technologies in Environmental Engineering" (pp.491-504).
- [4.8] [http://ermes-group.eu/web/leading\\_EU\\_models](http://ermes-group.eu/web/leading_EU_models) (queried on 01/08/2018).
- [4.9] Smit, R., Smokers, R., Rabe, E.: **A new modelling approach for road traffic emissions: VERSIT+.** Delft, 2007.
- [4.10] Koukkari, H., Nors, M.: **Life Cycle Assessment of Products and Technologies.** LCA Symposium. VTT, Espoo, Finland, 6. October 2009.
-

- [4.11] Hausberger, S., Dippold, M., Hiesmayr, J., Stadlhofer, W., Zinner, C.: **Entwicklung eines Modells zur Generierung von Emissionsfaktoren für motorisierte Zweiräder aus Abgasmessungen**. Endbericht zum Projekt: FE 84.0521/2015. Erstellt im Auftrag der Bundesanstalt für Straßenwesen. Bergisch Gladbach, 2017.
- [4.12] KA Sensors Ltd. **Engineering Document KA008P-EN. RWT - Rear Wheel Torque Transducer**.  
<http://www.kasensors.com/sites/default/files/downloads/%28KA008PEN%29%20RWT%20Application%20data.pdf> (queried on 09/08/2018)
- [4.13] Hausberger, S., Matzer, C.: **Update of Emission Factors for EURO 4, EURO 5 and EURO 6 Diesel Passenger Cars for the HBEFA Version 3.3**. Final Report. Report No. I-09/17/ CM EM 16/26/679 from 01.06.2017.
- [4.14] Matzer, C.; Hausberger, S.; Lipp, S.; Rexeis, M.: **New Approach for Systematic use of PEMS Data in Emission Simulation**. Journal of Earth Sciences and Geotechnical Engineering, vol. 7, no.1, 2017, 33-50 ISSN: 1792-9040 (print), 1792-9660 (online) Scienpress Ltd, 2017
- [4.15] Hill N., Windisch E., Hausberger S., Matzer C., Skinner I., et.al. (2015): **Improving understanding of technology and costs for CO<sub>2</sub> reductions from cars and LCVs in the period to 2030 and development of cost curves**. Service Request 4 to LDV Emissions Framework Contract; Final Report for DG Climate Action. Ref. CLIMA.C.2/FRA/2012/0006; Ricardo AEA, U.
- [4.16] Lu, M., De Bock, J.: **Sustainable Logistics and Supply Chain**. Innovations and Integral Approaches. Springer International Publishing Switzerland 2016.
- [4.17] Keller, M., Wüthrich, P., Notter, B.: **HBEFA - Handbook emission factors for road transport 3.1 / 3.2/ 3.3**. Quick reference. Bern, April 24, 2017.
- [4.18] **Handbook Emission Factors for Road Transport**. HBEFA Expert Version. V. 3.2
- [4.19] Steven, H.: **Update der Emissionsfaktoren für Motorräder**. RWTÜV Fahrzeug GmbH. Im Rahmen des UBA-Vorhabens Nr. F+E 298 43 100/02 (alt 205 06 100/02). Im Auftrag von INFRAS, Bern. 08. 12. 2003.
- [4.20] Knörr, W., Heidt, C., Gores, S. (Öko Institut), Bergk, F., 2016. **Aktualisierung „Daten- und Rechenmodell: Energieverbrauch und Schadstoffemissionen des motorisierten Verkehrs in Deutschland 1960-2035“ (TREMODO) für die Emissionsberichterstattung 2016**. (Berichtsperiode 1990-2014), Annex. Ifeu-Institut für Energie- und Umweltforschung Heidelberg GmbH. Im Auftrag des Umweltbundesamtes. Projektnummer 54329. Endbericht. 31.01.2016.
- [4.21] Umweltbundesamt. **1. Auflage 2012 „Daten zum Verkehr“**. Ausgabe 2012. Umweltbundesamt, Dessau, Oktober 2012.
- [4.22] Piasecki, C.: **Estimation of possible braking energy recovery from electric vehicles - Investigation on the basis of driving dynamic- and traffic situation analysis in**
-

- Germany.** Proceedings of 7th Transport Research Arena TRA 2018, April 16-19, 2018, Vienna, Austria.
- [4.23] Auf Der Maur, A., Strassburg, S., Knörr, W., Heidt, C., Wüthrich, P.: **Revision der Emissionsmodellierung für leichte Nutzfahrzeuge. Bedarfsanalyse auf Basis einer Vorstudie.** Berichte der Bundesanstalt für Straßenwesen. Fahrzeugtechnik. Heft 122. Bergisch Gladbach, Februar 2018.
- [4.24] Bergk, F., Heidt, C., Knörr, W. (IFEU) Keller, M. (INFRAS AG). **Erweiterung der Software TREMOD um zukünftige Fahrzeugkonzepte, Antriebe und Kraftstoffe. Endbericht.** Im Auftrag der Bundesanstalt für Straßenwesen (BASt). 30.09.2014.
- [4.25] Fitschen, A., Nordmann, H.: **Verkehrsentwicklung auf Bundesfernstraßen 2014.** Bundesanstalt für Straßenwesen, Unterreihe V "Verkehrstechnik", Heft V 278, Bergisch Gladbach, Oktober 2016.
- [4.26] **Richtlinien für die Straßenverkehrszählung im Jahre 2015 auf den Bundesfernstraßen.** Bundesministerium für Verkehr und digitale Infrastruktur, Referat StB 11.
- [4.27] Bäumer, M., Hautzinger, H., Pfeiffer, M., Stock, W., Lenz, B., Kuhnimhof, T., Köhler, K.: **Fahrleistungserhebung 2014 – Inlandsfahrleistung und Unfallrisiko.** Berichte der Bundesanstalt für Straßenwesen, Unterreihe V „Verkehrstechnik“ Heft V 291, Bergisch Gladbach, August 2017.
- [4.28] Kalinowska, D., Kloas, J., Kuhfeld, H., Kunert, U.: **Aktualisierung und Weiterentwicklung der Berechnungsmodelle für die Fahrleistungen von Kraftfahrzeugen und für das Aufkommen und für die Verkehrsleistungen im Personenverkehr (MIV).** Gutachten. Im Auftrag des Bundesministeriums für Verkehr, Bau- und Wohnungswesen. Endbericht. Berlin, April 2005.
- [4.29] Bundesamt für Güterverkehr: **Marktbeobachtung Güterverkehr.** Jahresbericht 2013. Köln, Juni 2014.
- [4.30] Palm, I., Regniet, G., Schmidt, G., Heusch-Boesefeldt (1996): **Ermittlung der Pkw- und Nfz-Jahresfahrleistungen 1993 auf allen Straßen in der Bundesrepublik Deutschland.** Im Auftrag des Bundesministeriums für Verkehr, Aachen.
- [4.31] Ntziachristos, L., Samaras, Z.: **COPERT III Computer programme to calculate emissions from road transport. Methodology and emission factors (Version 2.1).** Technical report No 49. November 2000. With contributions from: Eggleston, S., Gorißen, N., Hassel, D., Hickman A.-J., Joumard, R., Rijkeboer, R., White, L., Zierock, K.-H.
- [4.32] <https://www.emisia.com/utilities/copert/> (queried on 13/01/2019).
- [4.33] Gkatzoflias, D., Kouridis, C., Ntziachristos, L., Samaras, Z.: **COPERT 4 – Computer programme to calculate emissions from road transport. User manual (version 9.0).** February 2012.
-

- [5.1] Hiesmayr, J.: **Experimental Investigation and Simulation of Gaseous Emissions and Fuel Consumption in Real World Driving Scenarios for Two-Wheeler-Applications**. Doctoral Thesis. Graz University of Technology. 2019.
- [5.2] European Commission. **Commission Regulation (EU) No 2016/646 of 20 April 2016 amending Regulation (EC) No 692/2008 as regards emissions from light passenger and commercial vehicles (Euro 6)**. Official Journal of the European Union. L109/1. 2016.
- [5.3] AVL List GmbH. AVL M.O.V.E PEMS iS for LDV Real Driving Emissions Regulation. [https://www.avl.com/documents/10138/1986409/09\\_AVL+M.O.V.E+PEMS+iS+FOR+LDV.pdf](https://www.avl.com/documents/10138/1986409/09_AVL+M.O.V.E+PEMS+iS+FOR+LDV.pdf) (queried on 14/08/2018).
- [5.4] AVL List GmbH. AVL M.O.V.E EFM Exhaust Flow Meter. <https://www.avl.com/documents/10138/3902841/AVL+M.O.V.E+EFM+Fact+Sheet.pdf> (queried on 14/08/2018).
- [5.5] Wanker, R.: AVL List GmbH. **RDE-Validierung und Typzulassung mit AVL M.O.V.E**. <https://www.avl.com/documents/1982862/4664597/03+Dr.+Wanker++RDE+Validierung+und+Typzulassung+mit+AVL+M.O.V.pdf> (queried on 14/08/2018).
- [5.6] AVL List GmbH: AVL M.O.V.E. System Control: [https://www.avl.com/vehicle-emission-certification/-/asset\\_publisher/gYjUpY19vEA8/content/avl-m-o-v-e-system-control](https://www.avl.com/vehicle-emission-certification/-/asset_publisher/gYjUpY19vEA8/content/avl-m-o-v-e-system-control) (queried on 14/08/2018).
- [5.7] European Commission. **Commission Regulation (EU) 2016/427 of 10 March 2016 amending Regulation (EC) No 692/2008 as regards emissions from light passenger and commercial vehicles (Euro 6)**. Official Journal of the European Union, L 82/1, 2016.
- [5.8] Bernhard Gaul Web-Programmierung: <http://www.bernhard-gaul.de/gpxviewer/gpxviewer.php> (queried on 27/09/2018).
- [5.9] <http://www.openstreetmap.org/copyright/en> (queried on 27/09/2018).
- [5.10] <https://opendatacommons.org/licenses/odbl/> (queried on 27/09/2018).
- [5.11] <https://creativecommons.org/licenses/by-sa/2.0/> (queried on 27/09/2018).
- [5.12] [http://maplorer.com/view\\_gpx\\_3D.html](http://maplorer.com/view_gpx_3D.html) (queried on 27/09/2018).
- [5.13] Steven, H.: **Worldwide Harmonised Motorcycle Emissions Certification Procedure**. Draft Technical Report. UN/ECE-WP 29 – GRPE. WMTC Working Group. Informal document No. 9 (45th GRPE, 13-17 January 2003, agenda item 3.) 28. December 2002.
- [5.14] European Commission. **Directive 2009/30/EC of the European Parliament and of the Council of 23 April 2009 amending Directive 98/70/EC as regards the specification of petrol, diesel and gas-oil and introducing a mechanism to monitor and reduce**
-

**greenhouse gas emissions and amending Council Directive 1999/32/EC as regards the specification of fuel used by inland waterway vessels and repealing Directive 93/12/EEC.** Official Journal of the European Union, L140/88, 2009.

- [5.15] IAG Industrie Automatisierungsgesellschaft m.b.H. [http://www.iag.at/versa06-FTIR-AnalyseSystem.html?file=files/iag/divisions/pt/downloads/messanlagen/IAG\\_Datenblatt\\_versa06\\_DE.pdf](http://www.iag.at/versa06-FTIR-AnalyseSystem.html?file=files/iag/divisions/pt/downloads/messanlagen/IAG_Datenblatt_versa06_DE.pdf) (queried on 20/08/2018).
- [6.1] United Nations Economic Commission for Europe. **Global technical regulation No. 2 – Measurement procedure for two-wheeled motorcycles equipped with an positive or compression ignition engine with regard to the emissions of gaseous pollutants, CO<sub>2</sub> emissions and fuel consumption.** Established in the Global Registry on 22 June 2005. United Nations. Annex 3. Classification of equivalent inertia and running resistance.
-

**V** List of Figures

- Figure 1.1:** Annual traffic shares of relevant road vehicle categories in Germany according to local area in 2017 according to TREMOD.
- Figure 1.2:** European powered two-wheelers market – vehicle fleet development within the EU and its most relevant sales markets, 2002 – 2014
- Figure 1.3:** **a)** Development of the total urban hydrocarbon emissions from the road traffic sector in Germany differentiated according to vehicle category – powered-two-wheelers hydrocarbon emission share **b):** Proportionate urban annual traffic by vehicle categories in 2017.
- Figure 2.1:** Exhaust gas composition of modern petrol engines equipped with manifold injection.
- Figure 2.2:** Effects of air-/fuel ratio variations on petrol engine emission rates.
- Figure 2.3:** Powered two-wheelers hydrocarbon emissions in Germany differentiated according to operational- vs. evaporative emissions; evaporative emission share.
- Figure 2.4:** Powered two-wheelers evaporative emissions differentiated according to local area – motorcycles and mopeds.
- Figure 3.1:** Motorcycle tailpipe emission limits according to emission standard Euro 1-5, vehicle specifications and underlying test procedures.
- Figure 3.2:** Sequence of evaporative test procedure according to Regulation (EU) No 134/2014
- Figure 4.1:** Distribution of road traffic emission calculation models for the national emission reporting obligations of greenhouse gases and air pollutants in Europe.
- Figure 4.2:** Schematic structure of the PHEM model
- Figure 4.3:** Fuel consumption map (left) and NO<sub>x</sub>-emission map (right) for diesel passenger cars (Euro 5) generated with PHEM.
- Figure 4.4:** Second-by-second engine power calculation scheme based on generic CO<sub>2</sub> emission maps.
- Figure 4.5:** Resistance forces affecting a moving motorcycle.
- Figure 4.6:** Differentiation criteria in the motorcycle segment in HBEFA.
- Figure 4.7:** Traffic situation scheme according to HBEFA.
- Figure 4.8:** Motorcycle CO emission factors for different emission standards according to HBEFA 3.2.
- Figure 4.9:** Schematic structure and function of TREMOD for the road traffic sector.
- Figure 4.10:** Traffic differentiation scheme for motorcycles in TREMOD.
- Figure 4.11:** Worldwide distribution of the COPERT model and number of users by country.
- Figure 5.1:** Experimental setup of the PEMS device on the test vehicle.
-

- Figure 5.2:** Comparison of measured GPS-altitude data and topography data for the “Arzberg”-Route.
- Figure 5.3:** Route profiles “Arzberg” (top), “Ries” (middle) and „Gaberl” (button): maps including 3d-model, altitude profiles and road gradient characteristics.
- Figure 5.4:** Cumulative speed frequency distribution of the on-board trips with- and without Gaberl-trip, traffic weighted TREMOD TS and WMTC – all trips / cycles including stop phases.
- Figure 5.5:** Average vehicle acceleration values over average vehicle speed without stops according to urban, rural and motorway speed classes and overall – on-board trips in total and excluding the “Gaberl”-trip.
- Figure 5.6:** **a)** Mean RPA values of individual TREMOD motorcycle traffic situations, WMTC and on-board measurement trips over average cycle speed without stops; **b)** aggregated RPA values according to urban, rural, motorway and overall speed classes for TREMOD motorcycle traffic situations (traffic-weighted), WMTC and on-board measurement trips (with and without “Gaberl”-trip) over average cycle speed without stops.
- Figure 5.7:** Example of a motorcycle traffic situation with a high urban RPA value: “Rural/Motorway/120/Saturated”.
- Figure 5.8:** Kilometer-related emission results of the on-board trips for CO<sub>2</sub>, CO, NO<sub>x</sub>, NO, NO<sub>2</sub> differentiated according to RDE speed classes urban, rural, motorway and overall and differentiated according to hot- and cold-start emissions.
- Figure 5.9:** Second-by-second- and cumulative CO-emissions recorded for the “Arzberg 1”-trip.
- Figure 5.10:** Test cycles applied in the dynamometer emission measurement program.
- Figure 5.11:** Kilometer-related emission results of the chassis dynamometer test program for CO<sub>2</sub>, CO, NO<sub>x</sub>, and HC according to RDE speed classes urban, rural, motorway and overall and differentiated to hot- and cold-start emissions.
- Figure 5.12:** Kilometer-related emission results of the FTIR-measurements for CH<sub>4</sub>, C<sub>6</sub>H<sub>6</sub>, C<sub>4</sub>H<sub>6</sub>, C<sub>2</sub>H<sub>2</sub>, C<sub>2</sub>H<sub>6</sub>, HCHO averaged over all valid test runs according to RDE speed classes urban, rural, motorway and overall and differentiated to hot- and cold-start emissions.
- Figure 6.1:** Emission maps generated with emission data from the on-board measurement program – CO<sub>2</sub>, CO, NO<sub>x</sub>.
- Figure 6.2:** Emission maps generated with emission data from the dynamometer measurement program – CO<sub>2</sub>, CO, NO<sub>x</sub>, HC, CH<sub>4</sub>.
- Figure 6.3:** Speed-acceleration distribution of dynamometer driving cycles (blue) and on-board trips (red) from the test vehicle of the measurement program – WMTC (green) indicated for comparison purposes. a) Individual acceleration values over vehicle speed b) aggregated to acceleration classes.
- Figure 6.4:** Second-by-second and cumulative engine speed – measurement vs. PHEM simulation; a) dynamometer measurements, b) on-board measurements.
-

- Figure 6.5:** Second-by-second and cumulative dynamometer emission measurement- and PHEM simulation results of lined-up dynamometer tests based on emission maps generated from the dynamometer measurement program.
- Figure 6.6:** Deviation between simulated and measured CO emissions related to cycle engine power in RDC1 cycle.
- Figure 6.7:** Duration and RPA values of the individual TREMOD motorcycle traffic situations.
- Figure 6.8:** Second-by-second and cumulative on-board measurement results and PHEM simulation results based on emission maps generated from the on-board measurement program.
- Figure 6.9:** Deviation of the simulated cumulated emission results (CO<sub>2</sub>, CO and NO<sub>x</sub>) of the on-board trips by variation of relevant driving resistance parameters in PHEM.
- Figure 6.10:** Cumulative PHEM simulation results for the on-board measurement trips based on on-board- and dynamometer emission maps for different vehicle configurations; comparison of measurement results.
- Figure 6.11:** Cumulative simulation results for dynamometer measurements based on on-board and dynamometer emission maps for different vehicle configurations; comparison to measurement results.
- Figure 6.12:** Comparison between the individual TREMOD 5.53 / HBEFA 3.2 and HBEFA 4.1 motorcycle emission factors for the vehicle segment “motorcycles, 4S, Euro 3, > 750 cm<sup>3</sup>” and the PHEM simulation results for the emission components CO<sub>2</sub>, CO, NO<sub>x</sub>, HC and CH<sub>4</sub> – simulation results with RDE (on-board) emission maps and dynamometer emission maps. Left column: individual emissions factors; right column: aggregated emission factors according to urban, rural, and motorway speed classes and overall.
- Figure 7.1:** CO<sub>2</sub>, CO, NO<sub>x</sub> and HC-Emission trend scenario results for the TREMOD vehicle segment “motorcycles, 4S, Euro 3, > 750 cm<sup>3</sup>, first registration year 2015” for the period 2015 – 2025; TREMOD basic scenario (left) and TREMOD calculations with RDE (on-board) emission factors (center) and dynamometer emission factors (right).
- Figure 7.2:** Overall CO<sub>2</sub>, CO, NO<sub>x</sub> and HC emissions of the German vehicle fleet for the period 2015 – 2025 according to TREMOD including all relevant vehicle categories.
- Figure 7.3:** CH<sub>4</sub> and C<sub>6</sub>H<sub>6</sub> emission trend scenario results for the TREMOD segment “motorcycles, 4S, Euro 3, > 750 cm<sup>3</sup>, first registration year 2015” for the period 2015 – 2025; TREMOD basic scenario (left) and TREMOD calculations with simulated emission factors (CH<sub>4</sub>) and aggregated emission data derived from the dynamometer measurement program (C<sub>6</sub>H<sub>6</sub>).
- Figure 7.4:** Overall CH<sub>4</sub> and C<sub>6</sub>H<sub>6</sub> emissions of the German vehicle fleet for the period 2015 – 2025 according to TREMOD including all relevant vehicle categories.
- Figure 7.5:** C<sub>2</sub>H<sub>2</sub>, C<sub>4</sub>H<sub>6</sub>, C<sub>2</sub>H<sub>6</sub> and HCHO-emission trend scenario results for the TREMOD vehicle segment “motorcycles, 4S, Euro 3, > 750 cm<sup>3</sup>, first registration year 2015” for the period 2015 – 2025 based on aggregated emission data derived from the dynamometer measurement program.
-

- 
- Figure 7.6:** Start/Stop distribution of the TREMOD vehicle segment “motorcycles, 4S, > 750 cm<sup>3</sup>, Euro 3, first registration year 2015” in the period 2015 – 2025.
- Figure 7.7:** CO and HC emission trend scenarios for the TREMOD vehicle segment “motorcycles, 4S, > 750 cm<sup>3</sup>, Euro 3, first registration year 2015” taking into account cold-start surcharges – calculations carried out with baseline TREMOD / HBEFA emission factors and RDE EF’s and dynamometer EF’s derived from the PHEM simulations.
- Figure 7.8:** **a)** HC emission trend scenario results for the TREMOD vehicle segment “motorcycles, 4S, > 750 cm<sup>3</sup>, Euro 3, first registration year 2015” including cold-start- and evaporative emissions for the period 2015 -2025; **b)** HC emission shares differentiated according to different emission sources for the year 2018.
-

**VI List of Tables**

- Table 3.1:** Vehicle classification criteria according to Regulation (EU) No 168/2013. Common classification criteria and supplemented sub-classification criteria. Top: all L-category vehicles (L1e – L7e); bottom: two-wheeled motorcycles (L3e).
- Table 4.1:** Definition of traffic conditions in TREMOD and HBEFA – Levels of services.
- Table 5.1:** Technical specifications of the test vehicle.
- Table 5.2:** Relevant test route parameters.
- Table 5.3:** Relevant cycle- / trip parameter of onboard trips – with and without “Gaberl”-trip traffic weighted TREMOD TS and WMTC.
- Table 5.4:** Average vehicle speed without stops and aggregated positive acceleration values of the on-board trips – with and without “Gaberl” share – compared to traffic weighted TREMOD motorcycle traffic situations (TS) and WMTC; differentiated according to local level and overall; all percentage deviations are related to the TREMOD TS.
- Table 5.5:** Mean RPA values of the on-board trips (with and without “Gaberl” share) compared to the TREMOD motorcycle traffic situations and WMTC; differentiated according to local level and overall; all percentage deviations are related to the TREMOD traffic situations.
- Table 5.6:** Kilometer-related emission results of the on-board trips differentiated according to RDE speed classes urban, rural, motorway and overall and differentiated to warm- and cold-start emissions.
- Table 5.7:** Technical specifications of IVT two-wheeler test bench.
- Table 5.8:** Kilometer-related emission results of the chassis dynamometer test program for regulated emission components and CO<sub>2</sub> differentiated to RDE speed classes urban, rural, motorway and overall and according to hot- and cold-start emissions.
- Table 5.9:** Kilometer-related emission results of the chassis dynamometer test program for unregulated emission components differentiated to RDE speed classes urban, rural, motorway and overall and according to hot- and cold-start emissions.
- Table 6.1:** Driving resistance data of the test vehicle for the dynamometer measurement re-simulation in PHEM.
- Table 6.2:** Deviation between the cumulative dynamometer emission measurement results and the PHEM simulation results of lined-up dynamometer tests based on emission maps generated from the dynamometer measurement program.
- Table 6.3:** Driving resistance data for on-board trip re-simulations in PHEM.
- Table 6.4:** Deviation between the cumulative on-board emission measurement results and the PHEM simulation results of lined-up on-board trips based on emission maps generated from the on-board measurement program.
- Table 6.5:** Different test vehicle configurations in comparison; on-board, dynamometer- and real-world test vehicle configuration.
-

- 
- Table 6.6:** Deviations between the on-board trip re-simulation results and the emission measurement results for the real-world vehicle configuration; simulation based on on-board and dynamometer emission maps.
- Table 6.7:** Deviation between the dynamometer measurement re-simulation results and the emission measurement results for the real-world vehicle configuration; simulation based on on-board and dynamometer emission maps.
- Table 6.8:** Deviation between the individual- and aggregated TREMOD / HBEFA motorcycle emission factors for the vehicle layer concerned “motorcycles, 4S, Euro 3, > 750 cm<sup>3</sup>” and the PHEM simulation results for emission components CO<sub>2</sub>, CO, NO<sub>x</sub>, HC and CH<sub>4</sub> – simulation with on-board- and dynamometer emission maps.
- Table 7.1:** Deviation of TREMOD trend scenario results with RDE EF’s and dynamometer EF’s compared to the basic TREMOD emission trend scenario results – differentiated according to local area and overall.
- Table 7.2:** Deviation of TREMOD trend scenario results for CH<sub>4</sub> and C<sub>6</sub>H<sub>6</sub> calculated with emission factors from the PHEM simulation (CH<sub>4</sub>) and data from the FTIR measurement program (C<sub>6</sub>H<sub>6</sub>) compared to the basic TREMOD scenario results – differentiated according to local area and overall.
- Table 7.3:** Aggregated CO and HC emission cold-start surcharge derived from the on-board- and dynamometer measurement program.
- Table 7.4:** Evaporative emission factors for the vehicle segment “motorcycles, 4S, > 750 cm<sup>3</sup>, Euro 3, first registration year 2015” according to HBEFA 3.2.
-